The Institute of Paper Science and Technology

Atlanta, Georgia

Doctor's Dissertation

An Investigation of Some Factors Affecting the Corrosion of Carbon Steel Boiler Tube Material Exposed to Simulated Kraft Smelt

Gregory S. Kulas

July, 1989

AN INVESTIGATION OF SOME FACTORS AFFECTING THE CORROSION OF CARBON STEEL BOILER TUBE MATERIAL EXPOSED TO SIMULATED KRAFT SMELT

A Thesis Submitted by

Gregory S. Kulas

B.S. 1983, University of Wisconsin-Stevens Point

M.S. 1985, Lawrence University

in partial fulfillment of the requirements
of The Institute of Paper Science and Technology
for the degree of Doctor of Philosophy
Atlanta, Georgia

July, 1989

ABSTRACT

Carbon steel waterwall tubes in kraft recovery boilers are subject to corrosion rates of 0.5-1.5 mm/yr when the metal temperature is 300-350°C. The corrosion products have been reported to be iron sulfides.

In this work, the corrosion of carbon steel boiler tube material by a frozen smelt layer was studied. The experiments were performed with an air-cooled probe which was submerged in a molten smelt, forming a frozen smelt layer on a corrosion coupon. The heat flux through the corrosion coupon was representative of recovery furnace waterwall tube heat fluxes, and the metal temperature was maintained at 320-350°C, which is in the range of metal temperatures in which waterwall tube corrosion occurs.

When the boiler tube material was exposed to a frozen smelt layer containing sodium sulfide, sulfate, carbonate, and a small amount of sulfite, only iron oxide corrosion products (Fe_2O_3 and Fe_3O_4) were formed. Thus, these smelt components are not directly responsible for sulfidation corrosion. The iron oxide corrosion product layer was adherent to the metal surface, and was protective against continued corrosion. The long term corrosion rate extrapolated from the experimental data was less than 0.1 mm/yr when the metal temperature was 320-350°C.

When the boiler tube material was exposed to a frozen smelt layer containing 0.5-1.0% polysulfide sulfur in addition to sulfide, sulfate, carbonate, and sulfite, iron sulfide ($Fe_{1-x}S$) corrosion product was formed. With a metal temperature of 330-350°C, the average corrosion rate for the first 12 hours of exposure was 1.6 mm/yr, three times the initial corrosion rate when the smelt did not contain polysulfide. The rate of corrosion after

about 24 hours of exposure was similar to that for exposure to smelt without polysulfide sulfur, less than 0.1 mm/yr. The limitation on the corrosion reaction at longer times was not defined.

These results suggest that corrosion by frozen smelt containing polysulfide could occur at the rates observed in recovery boilers, 0.5-1.5 mm/yr. Continued corrosion at this rate would require renewal of the corrosive condition, which most likely depends on the removal and reformation of the frozen smelt layer.

TABLE OF CONTENTS

LIST OF FIGURES

LIST OF TABLES

INTRODUCTION

The recovery boiler is a key element in the kraft recovery process. It has two primary functions: to recover the cooking chemicals used to produce pulp, and to produce energy and process steam. In the recovery boiler a mixture of dissolved organics and spent pulping chemicals, called black liquor, is burned. The organic fraction of the black liquor is oxidized, and the inorganics are reduced in the char bed to regenerate the pulping chemicals.

The corrosion of carbon steel waterwall tubes in kraft recovery boilers is a significant problem. Carbon steel waterwall tubes can suffer severe corrosion in localized areas. The area of most severe corrosion in the lower furnace is at the level of the primary air ports.

Bowers[1] in 1984 conducted a survey of 48 recovery boilers with carbon steel waterwall tubes. It was reported that in one third of the boilers, corrosion had proceeded to the point where replacement of at least a portion of the waterwall tubes was required in less than 10 years of service. This illustrates the magnitude of the waterwall tube corrosion problem.

The corrosion of waterwall tubes has serious consequences. If the corrosion proceeds to the point where a leak develops in the tube wall, water may enter the furnace cavity, and the possibility of a smelt-water explosion exists. Even if the corrosion is detected prior to the development of a tube leak, as is usually the case, the cost of repairing or replacing the corroded tube or tubes is quite high. In addition to the cost of the repair, the costs

associated with the downtime required for inspection and for repairing corrosion damage can be substantial.

Three common methods of waterwall tube corrosion protection have been employed over the past thirty years. These are studded tubes, composite tubes, and thermal spray coatings.

Carbon steel tubes can be protected by studs, which provide corrosion protection by holding a thick frozen smelt layer on the tube surface. However, the studs are exposed to much higher temperatures than the tube surface, and are therefore subject to severe corrosion, so that frequent replacement of studs is required.

Composite tubes were first used in recovery boilers in the early 1970's. Composite tubes consist of an outer layer of stainless steel, which provides corrosion protection, and an inner layer of carbon steel. The inner layer is carbon steel because stainless steel in contact with the boiler water is susceptible to stress corrosion cracking. Composite tubes provide good protection against the type of corrosion which occurs on carbon steel waterwall tubes. However, composite tubes are subject to other minor corrosion problems, such as corrosion near air ports, and cracking near smelt spouts. In addition, composite tubes are expensive in comparison to carbon steel tubes.

Corrosion protection can also be achieved by spraying a protective coating of a corrosion resistant material on the surface of the waterwall tubes. These coatings, called thermal spray coatings or plasma spray coatings, can provide good protection, but only for limited periods of time. The major problem with spray coatings is that the effectiveness of the coating

is dependent on the preparation of the metal surface prior to application of the coating and on the technique used to apply the coating.

The methods of corrosion protection currently available are not completely effective. An understanding of the factors responsible for waterwall tube corrosion could lead to the development of more effective means of corrosion protection. Thus, this study was undertaken to investigate the effect of the composition of the frozen smelt layer on the corrosion of carbon steel boiler tube material. A better understanding of the conditions which cause the corrosion of waterwall tubes may lead to more effective methods of preventing corrosion damage.

LITERATURE REVIEW

LOWER FURNACE CONDITIONS

The fireside of the lower furnace of a kraft recovery boiler is exposed to very high temperatures and a complex chemical environment. The fuel for the boiler is kraft black liquor, which contains dissolved organics, Na_2CO_3, Na_2SO_4, NaOH, Na_2S, $Na_2S_2O_3$, and minor constituents such as NaCl, potassium salts, and transition metal ions.[2] The black liquor also contains 20-40% water. Black liquor is sprayed into the lower furnace, where it undergoes drying and pyrolysis of the organic fraction as it falls toward the furnace hearth. The remaining char contains 5-10% carbon in addition to the inorganic salts. In the char bed, the carbon is oxidized to CO and CO_2, and Na_2SO_4 is reduced to Na_2S. The inorganic salts melt and flow out of the boiler through smelt spouts.

The combustion is contained within a completely water-cooled furnace. The waterwall tubes in the lower furnace can be exposed to three different phases - lower furnace gases, molten smelt, and frozen smelt.

The major constituents of the lower furnace gases are N_2, H_2O, H_2, O_2, CO, and CO_2.[3-5] Smaller quantities of H_2S and SO_2 are also present.[3-5] The composition of the gas in the lower furnace is quite variable. Stelling and Vegeby[3] reported great variation in lower furnace gas composition between different boilers and within the same boiler as a function of time. They presented lower furnace gas compositions for several boilers. The gas analyses are shown in Table 1. These boilers were found to have significant

quantities of H_2, O_2, CO, and CO_2, and lesser amounts of H_2S and SO_2. Plumley et al.[4] also presented gas analyses from several boilers. Their analyses are shown in Table 2.

Table 1. Gas Compositions from the Lower Furnace of Kraft Recovery Boilers[3]

Species	Volume % Minimum	Maximum
H_2	0	21
O_2	1	17
CO	0	23
CO_2	6	19
H_2S	0.001	5
SO_2	0.0001	5

Table 2. Gas Compositions from the Lower Furnace of Kraft Recovery Boilers[4]

Species	Volume % Boiler A	Boiler B	Boiler C
CO_2	8.5	14.5	13.5
CO	-	0.1	6.2
O_2	10.7	4.1	2.7
H_2S	0.22	0.38	0.45
SO_2	0.07	0.08	0.018

The major smelt components are Na_2S, Na_2SO_4, and Na_2CO_3.[2,3] The minimum melting point of a mixture of these three components is 715°C.[6] Minor smelt constituents, such as potassium and chloride, lower the smelt melting point.[7-10] A eutectic melting point of 525°C has been reported[7] for a smelt containing chloride and potassium.

The tube surface temperature is dependent on the heat flux through the tube wall, the boiling heat transfer coefficient for the boiling water, the amount of scaling on the waterside of the tube, and the boiler operating pressure. The average heat absorption rate on the waterwalls is 126 kW/m^2 (40,000 $Btu/hr-ft^2$).[4] In the lower regions of the furnace, from the surface of the smelt to 0.3-0.6 m above the primary air ports, the heat transfer rate is much higher, and may reach 189 kW/m^2 (60,000 $Btu/hr-ft^2$).[4] For tubes which are clean on the waterside, such heat fluxes result in tube surface temperatures between 250-350°C.[4,11,12] In addition to influencing the metal temperature, the heat flux is related to the thickness of the frozen smelt layer. A higher heat flux results in a thinner frozen smelt layer.

The smelt melting point is considerably above the surface temperature of the waterwall tubes. Thus, molten smelt can not exist in stable contact with the tube metal. It has been observed that the waterwall tubes in the lower furnace are covered with a layer of frozen smelt[12-15], with a thin layer of molten smelt flowing down the outside of the frozen layer.[13] Tallent and Plumley[13] have reported that the frozen smelt layer is separated from the tube surface by a thin layer of irregularly spaced porous material, which they claim is probably dried black liquor. The frozen layer occasionally falls off of the tube surface.[13-15] Visual observation of the tube surfaces has shown that the smelt layer is reestablished within 30 seconds of being removed.[4]

During these brief periods before the smelt layer is reestablished, the tube surface may be exposed to either molten smelt, corrosive gases, or both.

In summary, waterwall tubes are primarily covered with a frozen smelt layer, with only occasional, brief exposure to molten smelt or furnace gases. The temperature of the tube surface is normally in the range of 250-350°C. Waterside scaling may cause this temperature to increase significantly. The heat flux through the tubes in the lower furnace is about 126 kW/m^2, but may reach 189 kW/m^2 in some areas.

CORROSION OCCURRENCE

Carbon steel waterwall tubes are observed to experience severe corrosion attack in the regions near the primary air ports. Tallent and Plumley[13] reported in 1969 that severe corrosion, up to 0.75 mm/yr, was observed in a narrow band below the primary air ports of Combustion Engineering boilers. Moskal[14] in 1985 observed a corrosion rate of 1.25 mm/yr at the smelt spout level in a similar CE boiler. Moskal also reported that in Babcock and Wilcox recovery boilers, the zone of greatest corrosion is between and immediately above the primary air ports. Moberg[9] performed field tests in which various types of protective coatings were tested in a carbon steel boiler. In addition, composite tubes with 18Cr-8Ni stainless steel were installed in a portion of the lower furnace. Over a 4 year test period, carbon steel was found to corrode at a rate of 0.55 mm/yr, and the composite tube at 0.065 mm/yr.

Bowers[1] calculated that based on the minimum wall thickness required by code, the maximum allowable corrosion rate for a 15-20 year tube life is

0.2 mm/yr. The corrosion rates reported above exceed this by at least a factor of 2. Bowers[1] also reported the service life of 48 boilers in the results of a recovery boiler survey. The reported service of tubes in the lower furnace was less than 10 years for 17 of 48 boilers. Another 13 boilers had tube service lives of 11-15 years. These results indicate that the corrosion of lower furnace waterwall tubes is a very significant problem.

It has been reported that in areas where severe waterwall tube corrosion was found, there was a hard black corrosion product tightly bonded to the surface of the tube.[13] X-ray diffraction analysis of this product showed that it was predominantly ferrous sulfide (FeS).

The corrosion of carbon steel tubes has been observed to have a strong temperature dependence. Prior to 1960, recovery boilers were operated at low pressure, and corrosion problems were attributable to waterside scaling. As boiler operating pressures increased, the tube metal temperatures also increased, and corrosion problems became more frequent. General experience has been that carbon steel boiler waterwall tubes suffer very little corrosion below 315°C, but accelerated corrosion occurs above this temperature. However, very little experimental data are available in the literature to substantiate this.

Plumley *et al.*[4] present some corrosion measurements made with two different types of probes inserted into operating recovery furnaces. The data obtained with a probe which protruded into the furnace cavity at the primary air port level showed the corrosion rate increased by a factor of 5 when the metal temperature was increased from 260°C to 430°C. The data obtained with the other probe, mounted vertically in the plane of the furnace wall at the primary air port level, also showed an increase in the corrosion rate with

temperature. The corrosion rate at 400°C was four times the corrosion rate at 345°C. However, the corrosion data at 345°C and the data at 400°C were obtained in different 1000 hr. test periods, so there is no assurance that the operating conditions during the two tests were the same.

PREVIOUS RECOVERY BOILER CORROSION RESEARCH

The conditions inside the lower furnace of a recovery boiler are very complex and also very transient. This makes simulation of these conditions difficult. Researchers have simulated various aspects of the lower furnace environment in order to obtain information about lower furnace corrosion.

This discussion will be broken into several sections, each pertaining to corrosion studies dealing with a different aspect of the recovery furnace environment. These sections describe the following:

- the corrosion due to furnace gas components
- the corrosion due to molten smelt
- the corrosion due to frozen smelt
- the corrosion due to interactions between the furnace gases and frozen smelt

Exposure to simulated recovery furnace gases

Between 1964 and 1972, research was carried out in Finland and Sweden which investigated the effect of simulated furnace gas on the corrosion of various steels.[3,9,10,16-18] Stelling and Vegeby[3] in 1969 reported on the first phase of this project, which was the investigation of the effect of different components of recovery furnace gas on the corrosion of carbon steel

boiler tube material.

The tests were carried out in electrically heated glass tube ovens.[3] The metal coupons were made from carbon steel tubes. The components which were studied were N_2, H_2O, H_2, O_2, H_2S, SO_2, CO, and CO_2. The corrosion coupon and the gas were at the same temperature, which was varied between 290°C and 450°C.

The influence of the various gas components on the corrosion rate was determined by systematically varying the gas composition. H_2S and O_2 were found to have the biggest effect on the rate of attack. With a H_2S content of 0.1%, and O_2 contents ranging from 0-0.5%, a maximum rate of corrosion was observed when the molar ratio of H_2S to O_2 was approximately 1:1. Lower corrosion rates were observed if the ratio was either higher or lower. When the gas composition was 0.1% H_2S, 0.1% O_2, 10% H_2, balance N_2, the average corrosion rate in a 4 hour exposure at 410°C was 13.6 mm/yr. The addition of SO_2, CO, and CO_2 had no significant effect on the corrosion rate. The effect of H_2 in the gas was to increase the metal weight loss. For gas composed of 0.1% H_2S, 0.1% O_2, varying H_2, and balance N_2, at 330°C, the addition of 10% H_2 increased the corrosion rate to 4.0 mm/yr in a 4 hour test, compared to 1.3 mm/yr when the gas contained no H_2. The effect of 25% H_2O added to the gas was to shift the maximum corrosion to a H_2S:O_2 ratio of 2:1, and to lower the maximum corrosion by a factor of two.

A maximum rate of corrosion at approximately a 1:1 H_2S:O_2 ratio was observed for temperatures ranging from 290-450°C. The maximum was more evident at higher temperatures. The maximum corrosion at 410°C was a factor of eight greater than the maximum corrosion at 290°C.

The composition of the corrosion products formed during these experiments was determined by x-ray diffraction. The corrosion product was FeS when the $H_2S:O_2$ ratio was 1:1 or greater, and Fe_3O_4 when the ratio was less than 1:5. At the intermediate $H_2S:O_2$ ratios, mixtures of FeS, FeS_2, and Fe_3O_4 were observed. The addition of 25% H_2O to gas containing 0.1% H_2S and 0.1% O_2, which reduced the corrosion rate, changed the corrosion product composition from iron sulfides to a mixture of iron sulfides and oxides.

The rate of corrosion was investigated as a function of time for a 1:1 ratio of $H_2S:O_2$, and was observed to be a linear function of time over 24 hours. This showed that the corrosion products, iron sulfides, provided no protection against continued corrosion. When the $H_2S:O_2$ ratio was less than 1:1, the corrosion rate was a parabolic function of time, indicating that the corrosion products, which contained a mixture of sulfides and oxides, provided protection against continued corrosion.

The corrosion rate was investigated as a function of temperature for a $H_2S:O_2$ ratio of 2:1, which resulted in FeS corrosion products. The corrosion rate increased sharply with temperature, from 1.4 mm/yr at 350°C to 10.9 mm/yr at 450°C in 4 hour tests. The activation energy was calculated to be 20 kcal/mole. This is equal to the activation energy of iron diffusion through iron sulfide, which is reported to be 20-23 kcal/mole[19,20], suggesting that the limiting step in this corrosion process is the diffusion of iron ions through the FeS layer. The formation of iron sulfide does not occur at the metal surface, but at the outer surface of the FeS layer.

Stelling and Vegeby[3] also investigated the formation of sulfur vapor in gas containing H_2S and O_2 at 370°C. They reported that the sulfur concentration in the gas was highest, 50 ppm, at a 1:1 ratio of $H_2S:O_2$. The

curve showing metal weight loss as a function of the $H_2S:O_2$ ratio and the curve showing sulfur generation as a function of the $H_2S:O_2$ ratio had similar shapes, with each having a maximum at a 1:1 ratio. This is not consistent with the stoichiometry of the H_2S-O_2 reaction:

$$H_2S + 1/2\ O_2 \Longrightarrow H_2O + S \qquad \text{(rxn. 1)}$$

Based on this reaction, a maximum S production would be expected at a 2:1 ratio of $H_2S:O_2$. This suggests that the corrosion observed in H_2S-O_2 gas may be due to sulfur which is formed by interaction between H_2S and O_2, but that the reaction is more complex than reaction 1.

In the second phase of this work, workers at the Swedish Corrosion Institute[9,17] exposed a carbon steel, a 13Cr steel, and an 18Cr-8Ni steel to gas composed of 0.1% H_2S-0.1% O_2-2.0% H_2O-10% H_2-balance N_2. at 400°C. The tests were performed in a horizontal tube oven, with a gas flow of 7 cm/s. Each material was exposed for three different periods of time - 2, 24, and 242 hours. The weight loss of carbon steel coupons was 4 mg/cm^2 in the 4 hr test (10.9 mm/yr), and 54 mg/cm^2 in the 242 hr test (2.4 mm/yr). The long term corrosion rates shown in Table 3 were obtained.

Table 3. Corrosion rates for exposure to standard gas at 400°C for 242 hours[3]

Carbon steel	- 2.4 mm/yr
13Cr steel	- 1.4 mm/yr
18Cr-8Ni steel	- 0.09 mm/yr

The corrosion product on the carbon steel consisted of 2 distinct layers. The inner layer was compact, while the outer layer was porous. The product contained 95% FeS and 5% Fe_3O_4 after the 242 hr test.

Additional tests were performed at the Swedish Corrosion Institute[10] using the same gas, but in a vertical tube oven, with a gas flow of 5 cm/sec. Carbon steel was corroded at a rate of 18.8 mm/yr in a 4 hr test at 400°C.

In Finland[9,21], 31 different grades of steel were exposed to the test conditions described above. The objective of the tests was to determine the suitability of different grades of steel for use in recovery boiler waterwall tubes. It was assumed that exposure to these test conditions was representative of exposure to recovery furnace conditions. The results of these tests showed that steel containing more than 13% Cr was ten times more resistant to corrosion by gas containing H_2S and O_2 than carbon steel. These tests were performed in a vertical tube oven, with a gas velocity of 2 cm/s. The rate of corrosion of carbon steel was 12.7 mm/yr in a 6 hour exposure.

Ahlers[22] recently exposed carbon steel to gas composed of 1% H_2S, 1% O_2, 2% H_2O, 10% CO_2, and balance N_2 at 300°C and 400°C. In 5 hour tests, the rate of corrosion was 1.5 mm/yr at 300°C and 2.4 mm/yr at 400°C.

The results of all of these experiments are summarized in Table 4. The results of short term tests are all fairly comparable, with the exception of the results of Ahlers.[22] The major experimental difference between the work of Ahlers and the others was that Ahlers did not include H_2 in the gas. Stelling and Vegeby[3] showed, as discussed earlier, that the addition of 10% H_2 to gas containing equimolar H_2S and O_2 increased the rate of corrosion of carbon steel by a factor of three.

Table 4. Summary of corrosion rates of carbon steel exposed to simulated furnace gas

	Temperature (°C)	Time (hr)	Weight Loss (mg/cm^2)	Corrosion Rate (mg/cm^2-hr)	(mm/yr)	Ref
Stelling and Vegeby[a]	330	4	1.5	0.37	4.0	3
	410	4	5.0	1.25	13.6	3
Finnish[b]	400	6	7.0	1.2	13.1	21
SCI[c]	400	4	3.5	0.9	9.6	9,17
	400	242	54	0.2	2.4	9,17
SCI[d]	400	4	6.9	1.7	18.7	9,17
Ahlers[e]	300	5	0.7	0.14	1.5	22
	400	5	1.1	0.22	2.4	22

[a] 0.1% H_2S, 0.1% O_2, 10% H_2, balance N_2, gas velocity 20-30 cm/sec

[b] 0.1% H_2S, 0.1% O_2, 2.0% H_2O, 10% H_2, balance N_2, gas velocity 2 cm/sec

[c] 0.1% H_2S, 0.1% O_2, 2.0% H_2O, 10% H_2, balance N_2, gas velocity 7 cm/sec, horizontal oven

[d] 0.1% H_2S, 0.1% O_2, 2.0% H_2O, 10% H_2, balance N_2, gas velocity 5 cm/sec, vertical oven

[e] 1.0% H_2S, 1.0% O_2, 2.0% H_2O, 10% CO_2, balance N_2, gas velocity 0.12 cm/sec, horizontal oven

All of these corrosion rates, with the exception of those obtained by Ahlers[22], exceed the observed recovery boiler waterwall tube corrosion rates of 0.5-1.25 mm/yr. The objective of many of these gas phase investigations was to develop a corrosion test which would accurately predict recovery furnace performance. This test was used to rank the predicted performance of different materials, and was successfully used in selecting corrosion resistant materials for composite tubes. The gas test provides a good accelerated test for predicting the corrosion behavior of different materials in the lower furnace of a recovery boiler.

However, the gas test provides little information regarding the furnace conditions which lead to waterwall tube corrosion. The waterwall tubes are covered with a layer of frozen smelt, which prevents direct contact between the gas and the metal. In addition, the standard gas composition was not chosen to be representative of lower furnace conditions, but rather was chosen because it resulted in a high rate of corrosion of carbon steel. In the lower furnace, the $H_2S:O_2$ ratio is likely to be quite variable, and would be expected to be considerably lower than 1:1.

Plumley et al.[4] exposed carbon steel coupons directly to furnace gases. The gases were removed from the operating floor level of a recovery boiler. A vacuum was used to pull the furnace gases through a port in the furnace wall and through a tubular furnace containing the carbon steel sample at 375°C. The corrosion rate was 0.42 mm/yr in a 40 hour exposure. This corrosion rate is an order of magnitude lower than the corrosion rates reported when simulated furnace gases were used. This suggests that the simulated furnace gas mixture used by many of the investigators is more corrosive than actual recovery furnace gases.

Exposure to Molten smelt

The waterwall tubes of a kraft recovery boiler have surface temperatures of 250-350°C under normal operating conditions.[4,11,12] These temperatures may increase if upset conditions, such as waterside scaling, occur.

The composition of the smelt in contact with the tube surface is mainly Na_2CO_3, Na_2S, and Na_2SO_4.[3,4,11] The minimum melting point of a mixture

of these species is 715°C.[6] Minor constituents, such as potassium and chloride, may lower the melting point of the smelt as low as 525°C.[7-10] Polysulfides (Na_2S_2, Na_2S_4, and Na_2S_5) also may lower the smelt melting point. Na_2S_2 melts at 482°C, Na_2S_4 at 294°C, and Na_2S_5 melts at 265°C.[23] A smelt mixture containing 4% polysulfide sulfur has been reported to have a lowest melting point of 442°C.[18]

The lowest smelt melting point is at least 100°C above the normal tube surface temperature. Thus, it is not possible for molten smelt to exist in stable contact with the tube metal.

When the frozen layer spalls off of the tube surface, molten smelt may contact the tube surface prior to the formation of a new frozen smelt layer. Workers at the Swedish Corrosion Institute[10] studied the corrosion which occurred during the formation of a frozen smelt layer. They dipped uncooled metal samples, initially at 400°C, into a molten smelt for less than 0.5 sec to form a frozen smelt layer. They found that the metal temperature increased to 500°C during the dipping, and the sample weight loss due to the dipping was 0.1 mg/cm^2 (0.0001 mm).

There have been a limited number of experiments performed with metal coupons exposed directly to molten smelt.[3,11] Stelling and Vegeby[3] exposed carbon steel coupons to molten smelt composed of Na_2CO_3 and Na_2S at 850°C. The exact smelt composition was not reported. They also exposed carbon steel to the same smelt with 4% Na_2SO_4 added. The corrosion rate in 1 minute exposures was 650 mm/yr with the carbonate-sulfide melt, and 2150 mm/yr with 4% Na_2SO_4 added, showing that molten sulfate is corrosive toward carbon steel.

Stelling and Vegeby[3] also exposed carbon steel to molten carbonate

with different amounts of Na_2SO_4 added. The corrosion rate in 2 minute exposures was dependent on the sulfate content of the melt. The rate of corrosion with smelt containing 3% Na_2SO_4 was 1730 mm/yr, 13 times the rate of corrosion of 130 mm/yr with pure carbonate melt.

Thiosulfate added to molten carbonate resulted in corrosion similar to that seen with sulfate. This would be expected, since thiosulfate reacts in molten carbonate to form sulfate and sulfide:[24]

$$Na_2S_2O_3 + Na_2CO_3 \Longrightarrow Na_2S + Na_2SO_4 + CO_2 \qquad \text{(rxn. 2)}$$

When NaOH was added to carbonate, the corrosion rate was the same as for pure carbonate, with a rate of 100 mm/yr in 2 minute exposures. Stelling and Vegeby[3] also exposed carbon steel to a molten kraft smelt for 1 minute, and the corrosion rate was 26,200 mm/yr, which is an order of magnitude higher than the corrosion found with the other smelts. The kraft smelt was reported to have a high sulfate content of about 15%, compared with a maximum of 4% Na_2SO_4 in the simulated smelts. This high sulfate content is likely responsible for the severe corrosion in the molten kraft smelt.

Poturaj[11] investigated the corrosion of a carbon steel and 5 alloyed steels to stagnant and flowing smelt at 757°C. One smelt was composed of 61.5% Na_2CO_3, 5% K_2CO_3, 29.2% Na_2S, 3.9% Na_2SO_4, and 0.4% NaCl. The other smelt was the same, except 4% NaOH was used, and only 57.5% Na_2CO_3.

Poturaj[11] exposed only one carbon steel coupon to each smelt under stagnant conditions, and another under flowing conditions. The carbon steel corrosion rate during a 5 hour exposure to stagnant smelt was 198 mm/yr for the smelt without NaOH, and 140 mm/yr for the smelt containing NaOH. Five hour exposures to flowing smelt resulted in corrosion rates of 408 mm/yr and

447 mm/yr for the smelts containing 0 and 4% NaOH, respectively. The corrosion product was a thick layer consisting of iron sulfides.

The results of the experiments in which carbon steel was exposed to molten smelt are summarized in Table 5.

Table 5. Summary of corrosion rates of carbon steel exposed to molten smelt

	Temperature (°C)	Time (min)	Weight Loss (mg/cm^2)	Corrosion Rate (mg/cm^2-hr)	(mm/yr)	
Stelling and Vegeby[3]	850	1	3.3	198	2150	a
	850	2	5.3	159	1730	b
	850	1	40	2400	26200	c
Poturaj[11]	747	300	91	18.2	198	d
	747	300	187	37.4	408	e

[a] Na_2CO_3-Na_2S-4% Na_2SO_4

[b] 97% Na_2CO_3-3% Na_2SO_4

[c] kraft smelt

[d] stagnant 61.5% Na_2CO_3, 5% K_2CO_3, 29.2% Na_2S, 3.9% Na_2SO_4, and 0.4% NaCl

[e] flowing 61.5% Na_2CO_3, 5% K_2CO_3, 29.2% Na_2S, 3.9% Na_2SO_4, and 0.4% NaCl

The corrosion rates of carbon steel in molten smelt are quite severe. They are several orders of magnitude larger than the maximum rate of corrosion of recovery boiler tubes. However, molten smelt will not exist in stable contact with recovery boiler waterwall tubes.

Exposure to Frozen Smelt

The corrosiveness of frozen smelt has been investigated by covering metal coupons with either smelt powder or with a frozen smelt layer, and then

placing the covered coupon in a nitrogen atmosphere, so that the observed corrosion is due only to the frozen smelt. Frozen smelt layers have been established by dipping a sample into a molten smelt pool for a short period of time, by submerging an air-cooled probe in a molten smelt pool, or by pouring molten smelt over the sample and allowing it to freeze.

Frozen Smelt Layer

Kaibara et al.[25] poured molten smelt with a sulfidity of 21% over metal coupons, and cooled it to temperatures ranging from 300-400°C in nitrogen. Carbon steel, 9Cr steel, 18Cr steel, and 18Cr-8Ni steel coupons covered with frozen smelt were placed in a furnace under nitrogen for 200 and 600 hours. The corrosion rates during 600 hr exposures were 0.018 mm/yr at 300°C and 0.091 mm/yr at 400°C for carbon steel. The weight losses for 9Cr steel were similar. For the other two steels, the corrosion rate was less than 0.009 mm/yr in the 600 hour tests.

Workers at the Swedish Corrosion Institute[10] established frozen smelt layers on metal coupons by dipping them into a molten smelt pool. Four dippings of less than 0.5 sec each resulted in frozen smelt layers 1-1.5 mm thick. The molten smelt composition was 40% Na_2S, 30% Na_2CO_3, and 30% Na_2SO_4. The covered coupons were placed in a nitrogen atmosphere at 400°C for 4 hours. The weight loss due to the dipping procedure was 0.29 mg/cm^2, and the weight loss due to the four hour exposure was 1 mg/cm^2 (2.7 mm/yr) for carbon steel. This indicated that short term tests such as this were unacceptable, since 30% of the corrosion was due to the molten smelt.

Plumley et al.[4] and Kaibara et al.[25] placed air-cooled probes in

molten smelt in a nitrogen atmosphere. When the air-cooled probe was submerged in the molten smelt, a frozen smelt layer formed on the probe. Plumley et al.[4] used molten smelt composed of sodium carbonate and 16-30% sodium sulfide. The rate of corrosion was not dependent on the sulfide content of the melt. The corrosion rate increased with temperature, ranging from 0.15-0.30 mm/yr at 260°C to 0.58-1.16 mm/yr at 370°C during 75 hour exposures.

Kaibara et al.[25] used smelts ranging in sulfidity from 20 to 70%. Carbon steel at 250°C sustained corrosion of 1.1-2.2 mm/yr in 10 hour exposures, while at 350°C, the rate of corrosion was 3.3-5.5 mm/yr. The effect of the Na_2S content of the smelt on the corrosion was not significant.

The corrosion of carbon steel by frozen smelt is summarized in Table 6.

The experiments performed with air-cooled probes resulted in higher corrosion rates than the other experiments. The corrosion rates in the experiments of Kaibara, et al.[25], where molten smelt was poured over the sample and allowed to cool, were 100 times lower than the rates of corrosion in the air-cooled probe experiments. The corrosion rate obtained by the Swedish Corrosion Institute[10] when an uncooled sample was dipped into molten smelt for a short period of time to form a frozen layer was 2.7 mm/yr at 400°C, compared to rates of 11.7 mm/yr at 370°C[4] and 5.5 mm/yr at 350°C[25] when air-cooled probes were dipped in molten smelt. These results suggest that in the experiments performed with air-cooled probes, either corrosive species diffuse from the molten smelt through the frozen smelt layer to the metal surface, or the temperature gradient in the frozen smelt layer may enhance the rate of corrosion.

Table 6. Summary of corrosion rates of carbon steel exposed to frozen smelt in a nitrogen atmosphere

	Temperature (°C)	Time (hr)	Weight Loss (mg/cm^2)	Corrosion Rate (mg/cm^2-hr)	(mm/yr)	Ref
Kaibara[a] et al.	300	200	0.6	0.003	0.033	25
	400	200	2.0	0.010	0.11	25
	300	600	1.0	0.0017	0.018	25
	400	600	5.0	0.0083	0.091	25
SCI[b]	400	4	1.0	0.25	2.7	10
Plumley[c] et al.	260	7.5	2.0	0.27	2.9	4
	370	7.5	8.0	1.07	11.7	4
Kaibara[d] et al.	250	10	2.0	0.2	2.2	25
	350	10	5.0	0.5	5.5	25

[a] 21% sulfidity smelt, molten smelt poured over samples and frozen

[b] 40% Na_2S, 30% Na_2CO_3, and 30% Na_2SO_4, frozen layer established by dipping

[c] 16-30% Na_2S-Na_2CO_3, frozen layer established with air-cooled probe

[d] 20-70% sulfidity smelt, frozen layer established with air-cooled probe

In summary, the experiments where the frozen layer was established by dipping a sample into a molten smelt pool resulted in corrosion rates of 2.2-11.7 mm/yr in short term tests. A corrosion rate of 0.2 mm/yr is considered the maximum allowable in a recovery boiler. Since the waterwall tubes in the lower furnace of a recovery boiler are covered by a frozen smelt layer, these results suggest that the frozen smelt layer composition may be a significant factor in waterwall tube corrosion.

Smelt Powder

Other workers have studied the corrosion of boiler tube material buried in smelt powder. Plumley et al.[4] systematically investigated the effects of 6 different smelt components and mixtures of them during 1 week exposures at 370°C. The results of Plumley's experiments are summarized in Table 7.

Table 7. Corrosion of carbon steel exposed to smelt powder at 370°C for 1 week in nitrogen atmosphere[4]

Smelt	Wt loss (mg/cm^2)	Corrosion rate (mg/cm^2-hr)	mm/yr
Bare metal	1.4	0.0083	0.09
Na_2CO_3	1.7	0.010	0.11
Na_2SO_4	1.4	0.0083	0.09
Na_2S	1.4	0.0083	0.09
Na_2S_x	1.9	0.011	0.12
$Na_2S_2O_3$	21.2	0.13	1.38
Na_2SO_3	1.4	0.0083	0.09
10% Na_2S-90% Na_2CO_3	2.0	0.012	0.13
10% Na_2S-90% Na_2SO_4	3.7	0.022	0.24
10% Na_2SO_4-90% Na_2CO_3	2.2	0.013	0.14
25% Na_2S-25% Na_2SO_4-50%Na_2CO_3	3.3	0.020	0.21

The only individual smelt component which resulted in significantly greater weight loss than exposure of the bare metal to nitrogen was sodium thiosulfate. The corrosion due to thiosulfate was ten times the weight loss due to the other smelt components. This result can be explained by the fact that thiosulfate is not stable at 370°C. In the experiments with thiosulfate, sulfur was deposited in the reaction tube, suggesting that thiosulfate decomposed, forming elemental sulfur. Tallent and Plumley[13] suggest that thiosulfate thermally decomposes according to:

$$Na_2S_2O_3 \Longrightarrow Na_2SO_3 + S \qquad \text{(rxn. 3)}$$

According to Kubelka and Votoupal[26], thiosulfate begins to decompose at 225°C:

$$4\ Na_2S_2O_3 \Longrightarrow 3\ Na_2SO_4 + Na_2S_5 \qquad \text{(rxn. 4)}$$

Na_2S_5 will decompose to lower polysulfides (Na_2S_4 and Na_2S_2), releasing elemental sulfur.[26] Either of these mechanisms of thiosulfate decomposition explains the formation of elemental sulfur, which was observed in the experiments. Elemental sulfur at 370°C is molten, and will attack carbon steel.[13]

The exposure of carbon steel directly to polysulfide (Na_2S_x) powder resulted in a very low corrosion rate. The composition of the polysulfide was not reported. The low rate of corrosion suggests that the polysulfide released much less sulfur than was released in the thiosulfate experiments. Since both Na_2S_4 and Na_2S_5 decompose, releasing sulfur, at temperatures less than 370°C[26], it seems likely that the composition of this polysulfide was Na_2S_x with $x = 2$ or less. Na_2S_2 is stable up to its melting point of 482°C. A sulfur vapor pressure would be associated with Na_2S_2 at 370°C, but this would be small in comparison to the amount of sulfur released by the

decomposition of thiosulfate in the experiments discussed above. The rate of corrosion in the thiosulfate experiments is much higher than in the polysulfide experiments because the amount of sulfur released by thiosulfate decomposition is much higher than the amount of sulfur vapor associated with the polysulfide, and the sulfur is responsible for the corrosion.

Two smelt mixtures resulted in increased corrosion, about 2 to 3 times that occurring on bare metal.[4] These were the mixtures containing both sulfide and sulfate. The mixtures of sulfide and carbonate, and sulfate and carbonate were not corrosive toward carbon steel.

Crowe[27] buried carbon steel coupons in smelt composed of 12% Na_2SO_4-8% Na_2S-80% Na_2CO_3, and placed them in nitrogen atmosphere for 2 weeks. At 300°C, the weight loss was 0.15 mg/cm^2 (0.005 mm/yr), and at 400°C it was 0.30 mg/cm^2 (0.010 mm/yr).

Kaibara et al.[25] exposed coupons to smelt powder with sulfidity ranging from 22-80% in nitrogen at 300°C. The smelt sulfidity had no effect on the corrosion rate during 200 hour exposures. The rate of corrosion was about 0.05 mm/yr. The results of Crowe[27] and Kaibara et al.[25] are shown in Table 8.

Table 8. Corrosion of carbon steel exposed to smelt powder in nitrogen atmosphere

	Temperature (°C)	Time (hr)	Weight Loss (mg/cm^2)	Corrosion Rate (mg/cm^2-hr)	(mm/yr)	Ref
Crowe[a]	300	340	0.15	0.0004	0.005	27
	400	340	0.30	0.0009	0.010	27
Kaibara et al.[b]	300	200	1.0	0.005	0.05	25

[a] 12% Na_2SO_4-8% Na_2S-80% Na_2CO_3

[b] 22% smelt sulfidity

Plumley et al.[4] reported an unusually large weight loss, 1.4 mg/cm^2, due to exposure of the bare coupon to nitrogen. The reason for this was not reported. Since nitrogen is not corrosive, this weight loss must be attributed either to the corrosion product removal procedure, or to oxygen contacting the coupon. Oxygen could enter the system either with the nitrogen or through a leak in the reaction chamber. This weight loss must be considered when comparing the magnitude of their weight losses to Crowe's results. The results of Crowe[27] and Plumley et al.[4] are similar in magnitude, if this is taken into account. If this 1.4 mg/cm^2 of weight loss which occurs with coupons exposed to nitrogen is subtracted from the weight loss in the other experiments, the corrosion rate due to 25% Na_2S-25% Na_2SO_4-50% Na_2CO_3 smelt powder is 0.039 mm/yr at 370°C, compared with the 0.010 mm/yr at 400°C reported by Crowe for a similar smelt.

The corrosion rates reported for exposure to smelt powder are about 100 times lower than the corrosion rates reported for exposure to a frozen smelt layer formed on an air-cooled probe. There are two major differences

between these two types of experiment. First, the smelt is in a different state in the two types of tests. Smelt powder may affect the metal differently than a continuous smelt layer. The brief period of exposure of the sample to molten smelt as the frozen smelt layer is forming may significantly affect the results of the test. This exposure to molten smelt will remove the thin layer of oxide which forms on all samples exposed to air. In the smelt powder tests, this thin oxide layer is not removed, and it may act as a protective layer.

The second possible difference between the two types of test is that in the experiments with the air-cooled probe, a temperature gradient was established in the frozen smelt. The smelt powder tests were isothermal. A temperature gradient in the smelt may enhance the rate of corrosion by enhancing the transport of corrosive species to the metal surface.

The experiments done at the Swedish Corrosion Institute[10] in which a frozen smelt layer was formed by dipping a sample into molten smelt for a short period of time were isothermal, and resulted in high rates of corrosion compared to smelt powder experiments. This suggests that the most significant difference between the frozen layer tests and the smelt powder tests is the initial exposure to molten smelt.

Effect of Gas-Smelt Interactions

A number of investigators have performed experiments which focused on the interactions between the gases which exist in the lower furnace and the components of the frozen smelt layer, and the effect of these interactions on the corrosion of carbon steel boiler tube material.

The experiments can be divided into two categories - those performed with smelt powder, and those in which frozen smelt layers were formed on the metal surface.

Smelt Powder Tests

Plumley et al.[4] investigated the effect of a number of different salts and salt combinations on the corrosion of carbon steel in 370°C air. In addition, the effect of Na_2S in CO_2, and SO_2 were investigated. The results of these tests are shown in Table 9.

Table 9. Corrosion of carbon steel buried in smelt powder and exposed to gas at 370°C for 1 week[4]

Smelt	Wt loss (mg/cm^2)	Corrosion rate (mg/cm^2-hr)	mm/yr
Exposure in air			
Bare metal	1.6	0.0092	0.10
Na_2CO_3	1.9	0.011	0.12
Na_2SO_4	1.2	0.0074	0.08
Na_2S	6.4	0.038	0.41
Na_2S_x	3.4	0.020	0.22
$Na_2S_2O_3$	7.0	0.041	0.45
Na_2SO_3	3.1	0.018	0.20
10% Na_2S-90% Na_2CO_3	2.5	0.015	0.16
10% Na_2S-90% Na_2SO_4	3.3	0.019	0.21
10% Na_2SO_4-90% Na_2CO_3	2.2	0.013	0.14
25% Na_2S-25% Na_2SO_4-50%Na_2CO_3	1.9	0.011	0.12
Exposure in CO_2			
Bare metal	1.5	0.009	0.10
Na_2S	57.0	0.340	3.70
Exposure in SO_2			
Bare metal	9.5	0.056	0.61
Na_2S	26.0	0.155	1.69

Several salt combinations were no more corrosive in air than they were in N_2 (Table 7), indicating that the air was not interacting with the smelt in any way which affected the corrosion reactions. These salts included Na_2CO_3, Na_2SO_4, 10% Na_2S-90% Na_2SO_4, 10% Na_2S-90% Na_2CO_3, and 25% Na_2S-25% Na_2SO_4-50% Na_2CO_3.

Thiosulfate in air was only one third as corrosive as thiosulfate in nitrogen.[4] In nitrogen, thiosulfate decomposed, releasing elemental sulfur, according to Reaction 3 or 4. When air was added to the system, the elemental sulfur was oxidized, and did not corrode the metal as much as in the exposure under nitrogen.

With Na_2SO_3, an air atmosphere doubled the corrosion rate compared with that in a N_2 atmosphere, from 0.09 mm/yr to 0.20 mm/yr in 1 week exposures. Similarly, with Na_2S_x, the rate of corrosion increased from 0.12 mm/yr in nitrogen to 0.22 mm/yr in air. Apparently the oxidation of these species in air results in species which are corrosive to carbon steel.

The interactions of air, CO_2, and SO_2 with Na_2S significantly increased the corrosion over that which occurred with either Na_2S or the gases alone.[4] The most corrosive combination was Na_2S and CO_2. The corrosion rate in a one week test with this combination was 3.7 mm/yr, compared to 0.1 mm/yr for direct exposure of the sample to either the smelt powder or the gas alone. For Na_2S in combination with air, the rate of corrosion was 0.4 mm/yr, and for Na_2S in combination with SO_2, the corrosion rate was 1.7 mm/yr.

In the tests with Na_2S in combination with either air, CO_2, or SO_2, it was reported that sulfur was deposited in the cooler sections of the reaction tube. This suggests that these gases interact with Na_2S to form

elemental sulfur, and that the elemental sulfur is responsible for the increased corrosion.

Tallent and Plumley[13] suggested that the reaction between sodium sulfide and air is:

$$2\ Na_2S + 2\ O_2 \Longrightarrow Na_2S_2O_3 + Na_2O \qquad \text{(rxn. 5)}$$

$$Na_2S_2O_3 \Longrightarrow Na_2SO_3 + S \qquad \text{(rxn. 6)}$$

Tallent and Plumley[13] suggested that the Na_2S-air interaction may be important in recovery boiler corrosion, since the most severe corrosion occurs near the primary air ports, where the Na_2S content of the wall deposits is high, and the O_2 supply is high.

The Na_2S-CO_2 reaction may also be significant, as large concentrations of CO_2 can exist in the lower furnace.[3-5] Tallent and Plumley[13] suggest that the reaction between CO_2 and Na_2S is:

$$Na_2S + 2\ CO_2 \Longrightarrow Na_2CO_3 + S + CO \qquad \text{(rxn. 7)}$$

Smaller concentrations of SO_2 exist in the lower furnace[3-5], but the effect of the SO_2-Na_2S interaction may also be important.

Kaibara et al.[25] exposed samples buried in smelt powder with different sulfide contents to gases containing a mixture of 15% CO_2-0.5% SO_2-5% O_2-balance N_2. These gas components are the same species which interacted with Na_2S in the experiments of Plumley et al.[4] Kaibara et al.[25] found that this gas mixture increased the corrosion of carbon steel buried in smelt powder. For example, with a 20% sulfidity smelt, this gas mixture increased the corrosion rate in a 200 hour exposure at 300°C to 0.2 mm/yr, compared to 0.05 mm/yr with the same smelt in nitrogen. With a smelt powder containing no

sulfide, this gas mixture had no effect on the corrosion rate, indicating that the increased weight loss was due to interaction between Na_2S and the CO_2-SO_2-O_2 mixture.

Kaibara et al.[25] found that H_2S and H_2O added to the 15% CO_2-0.5% SO_2-5% O_2 mixture had less significant effects on the corrosion rate. Addition of 20% H_2O had no effect on the weight loss. Addition of 0.5% H_2S increased the corrosion by only 0.02 mm/yr in a 200 hour exposure.

Plumley et al.[4] performed tests in which recovery furnace gases, taken from the operating floor level, were passed over carbon steel coupons buried in Na_2S, in $Na_2S_2O_3$, and also over bare metal coupons at 375°C. A vacuum was used to pull furnace gases through a port in the furnace wall, and through a tube furnace containing the corrosion coupons. In 40 hour tests, the rate of corrosion of the bare metal coupons was 0.4 mm/yr. The rate of corrosion of the coupons buried in thiosulfate was 0.3 mm/yr, and the rate of attack of the coupons buried in Na_2S was 1.9 mm/yr. These results show that the furnace gases interacted with Na_2S to corrode the metal at a rate 5 times greater than the rate in the gas.

Plumley et al.[4] and Kaibara et al.[25] both found a linear relationship between the Na_2S content of the smelt and the rate of corrosion due to exposure to gases. Plumley et al.[4] found that the corrosion increased from 0.12 mm/yr with pure carbonate in air to 0.28 mm/yr with 50% Na_2S-50% Na_2CO_3 in air during 1 week tests. Kaibara et al.[25] similarly found that the corrosion increased from 0.05 mm/yr with no Na_2S in the smelt to 0.5 mm/yr with 75% Na_2S in the smelt during 200 hour exposures to 15% CO_2-0.5% SO_2-5% O_2-balance N_2.

Kaibara et al.[25] found a strong temperature dependence in their experiments. Increasing the temperature from 250°C to 350°C increased the weight loss in a 24 hour test by a factor of 10 for a smelt with 20% sulfidity. This is the temperature range in which recovery boiler corrosion is reported to increase rapidly with temperature.[4]

Stelling and Vegeby[3] performed similar experiments. Corrosion coupons were buried in several different smelt powders, and exposed to 370°C gas containing 0.1% H_2S, 0.09% O_2, 10% H_2, 3.5% H_2O, and the balance N_2. Coupons buried in smelt powder containing 10% and 20% Na_2SO_4 added to Na_2CO_3 corroded at the same rate as coupons buried in pure carbonate. The rate of corrosion in each of these tests was 0.9 mm/yr in a 24 hour exposure. These tests show that the gas does not interact with sodium sulfate to form corrosive species.

When Na_2S was added to carbonate, the corrosion increased.[3] With 25% Na_2S added to carbonate, the corrosion was 1.3 mm/yr in a 24 hour exposure, compared to 0.9 mm/yr with pure carbonate. With 40% Na_2S added to carbonate, the rate of corrosion was 2.3 mm/yr in a 24 hour exposure. When bare carbon steel was exposed to the same gas composition, 0.1% H_2S, 0.09% O_2, 10% H_2, 3.5% H_2O, and the balance N_2, at 370°C, the corrosion rate was 4.2 mm/yr in a 24 hour exposure. Thus, although the gas-smelt powder combination is more corrosive when the smelt contains Na_2S, the rate of corrosion is still only one half of that for metal exposed directly to the gas.

When 10% CO_2 was added to the gas, the corrosion increased to 3.6 mm/yr in a 24 hour test.[3] Unfortunately, the smelt composition for this test was not reported. The authors explained this increased corrosion by claiming

that the CO_2 reacted with Na_2S to generate H_2S, which is the corrosive species.

Ahlers[22] has recently performed powdered smelt tests using smelt composed of 80% Na_2CO_3, 12% Na_2SO_4, and 8% Na_2S. The gas composition was 1% H_2S, 1% O_2, 2% H_2O, 10% CO_2, and balance N_2. Tests were also performed using bare metal exposed to this same gas composition. The corrosion rates obtained when coupons were buried in the smelt powder were 2.8-4.4 mm/yr at 300°C and 5.0-7.0 mm/yr at 400°C for 5 hour exposures. These weight losses are twice the weight losses measured with exposure of the metal directly to the gas. The gas-smelt interaction accelerates the corrosion over that which occurs in either smelt powder or gas alone.

Stelling and Vegeby[3] and Ahlers[22] observed different effects of smelt and gas in combination. Stelling and Vegeby reported that the smelt powder was protective, so that the corrosion rate was lower when the sample was covered with smelt powder than when it was exposed directly to the gas. This is because the carbonate in the smelt powder absorbed the corrosive gas species, H_2S, making the gas less corrosive. Ahlers[22] reported that the gas reacted with the smelt powder to become more corrosive, so that the corrosion rate was higher when the sample was covered with smelt powder than when it was exposed directly to the gas. This is because the gas used by Ahlers contained 10% CO_2 in addition to H_2S and O_2. Plumley *et al.*[4], Kaibara *et al.*[25], and Stelling and Vegeby[3] have reported that CO_2 reacts with Na_2S to generate corrosive species, H_2S or elemental sulfur. Thus, the difference between the results of Stelling and Vegeby[3] and Ahlers[22] is explained by the presence of CO_2 in the gas used by Ahlers.

The results of all the tests in which coupons were buried in smelt powder and exposed to gas are summarized in Table 10.

The experiments in which corrosion samples were buried in smelt powder and exposed to gas were performed using a wide variety of smelt powder and gas compositions, and a wide range of exposure times. However, the corrosion rates were all within an order of magnitude. The two experiments which resulted in the lowest corrosion rates were the test by Plumley et al.[4] in which Na_2S was exposed to air, and the test by Kaibara et al.[25] in which smelt with a sulfidity of 20% was exposed to gas containing 15% CO_2, 0.5% SO_2, 5% O_2. These two tests resulted in corrosion rates an order of magnitude lower than the other tests. The common factor in these two tests is the high oxygen content in the gas phase. Plumley et al.[4] used air, which is 21% O_2, and Kaibara et al.[25] used 5% O_2. None of the other tests used more than 1% O_2, with the possible exception of Plumley et al.'s[4] test with furnace gases of unknown composition.

Table 10. Summary of corrosion rates of carbon steel buried in smelt powder and exposed to gas

	Temperature (°C)	Time (hr)	Weight Loss (mg/cm^2)	Corrosion Rate (mg/cm^2-hr)	(mm/yr)
Plumley, et al.[4]					
Na_2S	370	168	1.4	0.008	0.09
CO_2	370	168	1.6	0.009	0.10
Na_2S-CO_2	370	168	57	0.34	3.7
Air	370	168	1.6	0.009	0.10
Na_2S-Air	370	168	6	0.036	0.40
SO_2	370	168	9.6	0.057	0.62
Na_2S-SO_2	370	168	26	0.15	1.6
Kaibara, et al.[25]					
Smelt[a]	300	200	1	0.005	0.05
Smelt-gas[b]	300	200	4	0.02	0.2
Plumley, et al.[4]					
Furnace gas	375	40	1.3	0.033	0.36
Na_2S-furnace gas	375	40	6.8	0.17	1.9
Stelling and Vegeby[3]					
Gas[c]	370	24	9.3	0.39	4.2
Smelt-gas[d]	370	24	2.9	0.12	1.3
Ahlers[22]					
Gas[e]	300	5	0.7	0.14	1.5
Smelt-gas[f]	300	5	1.7	0.34	3.7
Gas[e]	400	5	1.1	0.22	2.4
Smelt-gas[f]	400	5	2.8	0.56	6.1

[a] 20% sulfidity smelt

[b] 20% sulfidity smelt, 15% CO_2-0.5% SO_2-5% O_2-balance N_2

[c] 0.1% H_2S-0.09% O_2-10% H_2-3.5% H_2O-balance N_2

[d] 25% Na_2S-75% Na_2CO_3, 0.1% H_2S-0.09% O_2-10% H_2-3.5% H_2O-balance N_2

[e] 1% H_2S-1% O_2-2% H_2O-10% CO_2-balance N_2

[f] 80% Na_2CO_3-12% Na_2SO_4-8% Na_2S, 1% H_2S-1% O_2-2% H_2O-10% CO_2-balance N_2

The effect of the interaction between smelt powder and some of the gas species known to exist in the recovery furnace, is to increase the corrosivity of the smelt. In all the experiments shown in Table 10, except Stelling and Vegeby's[3], the interaction of gases with the smelt powder resulted in greater corrosion than if the sample was exposed directly to gas of the same composition. This suggests that some components of the gas interact with the components of the smelt powder to form species which are more corrosive to the metal than the gas. The corrosive smelt species formed by smelt powder-gas interactions were not identified. Plumley et al.[4] reported finding condensed sulfur in their reaction chamber, suggesting that the gas had reacted with the smelt to form elemental sulfur. The smelt composition after exposure to the gas was not determined in any of the experiments.

In Stelling and Vegeby's experiments[3], the smelt powder provided corrosion protection from the gas. The corrosion rate was 1.3 mm/yr when the coupon was buried in smelt powder, compared to 4.2 mm/yr when the bare coupon was exposed to gas of the same composition. This is because the only reactive component in the gas used by Stelling and Vegeby[3] was H_2S, which was absorbed by the carbonate in the smelt powder. The gas did not contain CO_2, which has been shown to react with smelt to increase corrosion.

Frozen Smelt Layer Tests

Stelling and Vegeby[3] examined the corrosion of carbon steel coupons covered with a layer of frozen smelt and exposed to corrosive gases. The frozen smelt layer was established by dipping the sample into a molten smelt

composed of Na_2CO_3 and Na_2S for 60 sec. The molten smelt composition and the thickness of the frozen smelt layer were not reported. The sample covered with the frozen smelt layer was exposed to gas composed of 0.1% H_2S, 0.1% O_2, 10% H_2, balance N_2 for 4 hours. The corrosion rate was 1.2 mm/yr when the gas temperature was 300°C, and 5.8 mm/yr when the gas temperature was 400°C. These corrosion rates were about one half the rates for bare metal exposed directly to gas of the same composition, showing that the frozen smelt layer protected the metal from the corrosive gases.

Swedish workers[9,10,18] also investigated the corrosion of carbon steel covered with a thin layer of frozen smelt and exposed to high temperature gases. The frozen smelt layers in these experiments were established by dipping the sample into a molten salt pool composed of 40% Na_2S, 30% Na_2SO_4, 30% Na_2CO_3 for less than 0.5 sec., and then removing the sample from the melt and placing it in 400°C gas. The gas contained 0.1% H_2S, 0.1% O_2, 10% H_2, balance N_2. The sample was dipped back into the molten smelt three times, for less than 0.5 sec. each, after 1, 2, and 3 hours of exposure to the gas. Dipping the sample into the molten smelt four times resulted in a smelt layer thickness of 1-1.5 mm. The corrosion rate was 3.3 mm/yr. This compares to 18.8 mm/yr for direct exposure of the metal sample to gas of the same composition, and 2.7 mm/yr for exposure of the metal sample covered with a frozen smelt layer of the same composition to nitrogen. The frozen smelt layer protected the metal from the corrosive gas in these experiments.

These tests were extended to longer times, and the protective effect of the frozen smelt layer was lost.[9,18] The weight loss with the same smelt and gas composition was 40 mg/cm^2 in a 24 hour test. Increasing the test

length by a factor of 6 resulted in 33 times the weight loss. The corrosion in this test was about the same as for direct exposure to the gas.

The composition of the frozen smelt layer after the 24 hour exposure to the gas was determined, and it was found that the gas had reacted with the frozen smelt layer to generate 6% polysulfide sulfur in the frozen smelt layer.[9,18] The authors attributed the increased corrosion to the polysulfide.

The results of the experiments where metal samples covered with a layer of frozen smelt were exposed to high temperature gas are summarized in Table 11.

Table 11. Summary of corrosion rates of carbon steel covered with a frozen smelt layer and exposed to gas

	Temperature (°C)	Time (hr)	Weight Loss (mg/cm^2)	Corrosion Rate (mg/cm^2-hr)	(mm/yr)
Stelling and Vegeby[3]					
Gas[a]	410	4	5.0	1.25	13.6
Gas-Smelt[b]	400	4	2.1	0.54	5.8
Moberg[9]					
Gas[c]	400	4	6.9	1.7	18.8
Gas-Smelt[d]	400	4	1.2	0.3	3.3
Gas-Smelt[d]	400	24	40	1.7	18.2

[a] 0.1% H_2S-0.1% O_2-10% H_2-balance N_2

[b] Na_2CO_3-Na_2S, 0.1% H_2S-0.1% O_2-10% H_2-balance N_2

[c] 0.1% H_2S-0.1% O_2-2% H_2O-10% H_2-balance N_2

[d] 40% Na_2S-30% Na_2SO_4-30% Na_2CO_3, 0.1% H_2S-0.1% O_2-10% H_2-balance N_2

Summary of Previous Work

There are a number of possible conditions which may lead to accelerated recovery furnace corrosion. The work reviewed above included the investigation of a number of different conditions which might simulate recovery furnace conditions. The results of each type of test are presented in Table 12.

Table 12. Summary of corrosion rates observed in recovery boiler research experiments

Maximum allowable furnace corrosion[1]	0.2 mm/yr
Maximum observed furnace corrosion	0.5-1.5 mm/yr
Gas tests	1.5-18.7 mm/yr
Molten smelt tests	200-26,200 mm/yr
Frozen smelt in N_2	0.02-11.7 mm/yr
Smelt powder in N_2	0.01-0.24 mm/yr
Smelt powder/gas	0.2-6.1 mm/yr
Frozen smelt/gas	1.2-18.2 mm/yr

The corrosion rates observed when carbon steel is exposed to simulated furnace gas are in general higher than the maximum corrosion rates seen in recovery boilers. The corrosion rates observed when carbon steel is exposed directly to molten smelt are several orders of magnitude higher than the maximum corrosion rates seen in the lower furnace of recovery boilers. However, the waterwall tubes in the lower furnace of a kraft recovery boiler are covered with a layer of frozen smelt, which prevents direct contact between either the furnace gases or the molten smelt and the tube surface.

The tests in which metal samples were exposed to smelt powder resulted in corrosion rates which are acceptable in recovery boilers. However, this type of test may not represent actual furnace conditions. Tests performed with metal samples exposed to frozen smelt layers resulted in

corrosion rates 100 times higher than those observed in powdered smelt tests.

The tests in which the carbon steel was covered with a layer of frozen smelt most closely simulated the conditions which the waterwall tube sees. The waterwall tubes are covered with a layer of frozen smelt, except for brief periods when the frozen layer falls off and reforms.

Previous frozen smelt layer tests have been limited. Some of these tests have resulted in very high corrosion rates, up to 11.7 mm/yr, indicating that the frozen smelt layer covering the tube may be corrosive to carbon steel. The effect of the smelt composition on the corrosiveness of the frozen smelt layer has not been investigated.

The tests in which samples were covered with frozen smelt, either smelt powder or a frozen layer, and then exposed to a simulated furnace gas mixture, have shown that the simulated furnace gases will react with the frozen smelt to generate smelt species which are corrosive toward carbon steel. In the recovery furnace, molten smelt is observed flowing down the outside of the frozen smelt layer. This prevents direct contact between the frozen smelt layer and the furnace gases. However, furnace gases can interact with the molten smelt flowing down the furnace wall to form corrosive species. Corrosive species generated by gas-molten smelt interactions can either be captured in the frozen smelt layer when it forms or can diffuse from the molten smelt into the frozen smelt layer. The effect of the minor smelt species generated in these gas-smelt interactions on the corrosion of carbon steel has not been investigated. This type of smelt/gas interaction may have a very important effect on recovery furnace waterwall tube corrosion.

Previous studies have suggested that elemental sulfur or polysulfide

is the cause of high rates of corrosion of carbon steel. The results of Stelling and Vegeby[3] suggested that the corrosion occurring in H_2S-O_2 mixtures was the result of gas reaction which formed sulfur vapor. In smelt powder tests[4,13], gas-smelt powder combinations which caused high corrosion rates also caused the formation of elemental sulfur, suggesting that elemental sulfur was responsible for the corrosion. In addition, when a frozen smelt layer was exposed to gas containing H_2S and O_2, the frozen layer reacted with the gas to form 6% polysulfide in the frozen smelt[9,18], and the corrosion rate was high, suggesting that the polysulfide caused the high rate of corrosion.

In summary, the exposure of carbon steel to frozen smelt has resulted in substantial corrosion in previous laboratory experiments. The effect of the smelt composition on the corrosiveness of the frozen smelt has not been determined. In addition, corrosive smelt species are generated when simulated furnace gas interacts with frozen smelt. The effect of these interactions on the smelt composition, and on the corrosiveness of the smelt, has not been determined. This thesis will address these two aspects of the corrosion of waterwall tubes in kraft recovery furnaces.

OBJECTIVES

The objectives of this work are to

1. Construct an experimental apparatus to investigate the corrosion of carbon steel boiler tube material covered by a layer of frozen smelt under heat transfer conditions, when the metal temperature is 315-370°C (600-700°F). The apparatus will simulate typical conditions which recovery furnace waterwall tubes are exposed to. The tube surface temperature, the thickness of the frozen smelt layer, and the heat flux through the tube wall will be representative of recovery furnace waterwall conditions.

2. Determine the rate of corrosion as a function of time and the composition of the corrosion product when carbon steel boiler tube material at 320-350°C is covered with a frozen smelt layer containing sodium sulfide, sodium sulfate, and sodium carbonate. These are the major constituents of the frozen smelt layer on the waterwall tubes of recovery boilers.

3. Iron sulfide corrosion products have been identified in areas of accelerated corrosion in recovery boilers. Previous studies have suggested that elemental sulfur is responsible for the formation of iron sulfide corrosion products when carbon steel is exposed to smelt powders. Elemental sulfur in molten smelt containing sulfide exists in the form of polysulfide. An objective of this work is to determine the rate of corrosion as a function of time and to determine the composition of the corrosion product when carbon steel boiler tube material at 330-350°C is covered with a frozen smelt layer

containing sodium sulfide, sodium sulfate, sodium carbonate, and sodium polysulfide.

4. Fit previously developed corrosion models, such as the parabolic model and the logarithmic model, to the experimental corrosion rate vs. time data obtained with smelt containing just sodium sulfide, sodium sulfate, and sodium carbonate, and also to the data obtained with smelt containing polysulfide. The shape of the corrosion rate curve will be used to identify the limiting step in the corrosion reaction.

5. Determine whether the shape of the corrosion rate vs. time curve for corrosion of carbon steel by frozen smelt containing polysulfide is described by a model based on the limiting step of the corrosion mechanism being transport of sulfur to the surface of the corrosion product layer. This will provide additional information regarding the rate limiting step in this corrosion process.

6. Relate the results of this work to the problem of kraft recovery furnace waterwall corrosion. Specifically, identify which components of the frozen smelt layer corrode carbon steel to form iron sulfide. Compare the rates of corrosion measured experimentally to the rates of corrosion observed in recovery furnaces, to determine if the rates of recovery boiler corrosion can be explained by frozen smelt corrosion.

EXPERIMENTAL

EXPERIMENTAL APPROACH

The objective of this work is to identify the components of frozen smelt which are corrosive to carbon steel boiler tube material under heat transfer conditions. The corrosion rate data was collected with an air-cooled probe submerged in a molten smelt pool. A cooled probe was used because it allowed for the establishment of a temperature gradient through the frozen smelt layer and for continuous contact between the molten smelt and the frozen smelt layer. Air was chosen as the cooling medium because it is readily available and because there is no concern about an explosive reaction with the molten smelt should a leak develop in the probe.

When the air-cooled probe is submerged in a molten smelt pool, a frozen smelt layer is formed over the cooled metal sample, with molten smelt covering the outside of the frozen smelt layer. The frozen smelt layer covering the sample simulates the conditions in the lower portion of a recovery furnace, where the waterwall tubes are covered with a frozen smelt layer, with molten smelt flowing down the outside of the frozen layer.

In addition, with the air-cooled probe used in this work, the thickness of the frozen smelt layer formed on the sample and the heat flux through the sample are representative of recovery boiler lower furnace waterwall conditions. Thus, the experimental conditions are a very good simulation of the conditions which exist in the lower furnace of a recovery boiler.

Previous studies[4,25] using air-cooled probes have yielded no information about the identity of the smelt components which lead to the formation of iron sulfide corrosion products. This is because the experiments were performed by covering the cooled probe with a frozen smelt layer composed of only sodium carbonate and sodium sulfide. In these studies, the sodium sulfide content of the melt was varied, and this was found to have no effect on the rate of corrosion. The corrosion products were not identified. The effect of minor smelt components, such as excess sulfur, on the rate of corrosion by frozen smelt and on the corrosion product composition was not investigated. This study investigated the effect of excess sulfur in the frozen smelt layer on both the rate of corrosion and the identity of the corrosion product.

In this work, corrosion rate vs. time curves were developed for two smelt compositions at one temperature. The initial smelt was prepared using 15% sodium sulfide, 15% sodium sulfate, and 70% sodium carbonate. These are the major components of the frozen smelt layers in the lower furnace of recovery boilers, and this is a representative composition. The second smelt was prepared with a the same components, but also contained 0.5-1.0% excess sulfur, which existed in the smelt as polysulfide (Na_2S_x). This smelt composition was studied because previous corrosion studies with gases and also with gases and smelt powder in combination have suggested that elemental sulfur is involved in the formation of iron sulfide on carbon steel.

The setpoint temperature for the experiments was 650°F, which is 343°C. Actually, the experimental temperatures ranged from 320-350°C for the experiments with sulfide, sulfate, and carbonate, and 330-350°C for the experiments with smelt containing polysulfide. These temperatures are at the

upper end of the range of recovery furnace waterwall tube surface temperatures, and represent the conditions under which corrosion of carbon steel tube material is reported. It was not possible to obtain metal temperatures lower than this with this experimental system.

In order to define the corrosion mechanism for a smelt composition at a given temperature, the identity of the corrosion product and the shape of the corrosion weight loss vs. exposure time curve were determined. Since the corrosion rate under a frozen smelt layer could not be monitored continuously, a series of corrosion tests of different lengths of time were performed to develop a corrosion rate curve. The exposures ranged in length from 15 minutes to 100 hours. For each exposure the weight loss due to corrosion was measured, providing one point for the weight loss vs. exposure time curve. The corrosion product was identified by x-ray diffraction.

FROZEN SMELT LAYER EXPERIMENTS

The frozen smelt layer experiments were performed with an air-cooled probe. A cooled probe was used in this work to establish a temperature gradient in the frozen smelt layer and to maintain continuous contact between the molten smelt and the frozen smelt layer. An air-cooled probe submerged in a molten smelt pool will form a frozen smelt layer over the cooled metal sample, with molten smelt covering the outside of the frozen smelt layer. This frozen smelt layer covering the sample simulates the conditions in the lower portion of a recovery furnace, where the waterwall tubes are covered with a frozen smelt layer, with molten smelt flowing down the outside of the frozen layer.[4]

The air-cooled probe has two functions. The first is to act as a sample holder, to suspend the sample in the molten smelt pool. The second is to maintain the exposed surface of the corrosion coupon at a temperature approximating that of recovery boiler waterwall tubes (260-370°C).

Experimental Apparatus

The experimental system is illustrated in Fig. 1. An air-cooled corrosion probe was submerged in a molten salt pool. The molten salt was contained in a high purity aluminum oxide (alumina) crucible, with an inside diameter of 16.5 cm, and a depth of 35.6 cm. The crucible was contained in a stainless steel retort, which was hung inside a tubular furnace with an inside diameter of 21 cm. The retort cover had two openings. One was used as an entry for either a gas purge tube or an alumina thermocouple sheath, and the other was for the corrosion probe. Either opening could be closed when not in use.

The probe is illustrated in Fig. 2. It was constructed of two concentric stainless steel tubes. The outer tube was the sample holder, and the inner tube was the supply tube for cooling air. The cooling air flowed down the inside of the inner tube, and then back up through the annulus between the inner and outer tube. The outer surface of the probe, with the exception of the corrosion coupon, was protected from the molten salt by an alumina sheath.

The cooling air supply system also is illustrated in Fig. 2. The air was supplied by a compressor at 412 kPa, and is reduced to 205 kPa by a pressure regulator. The air flow rate was controlled by a manually adjusted

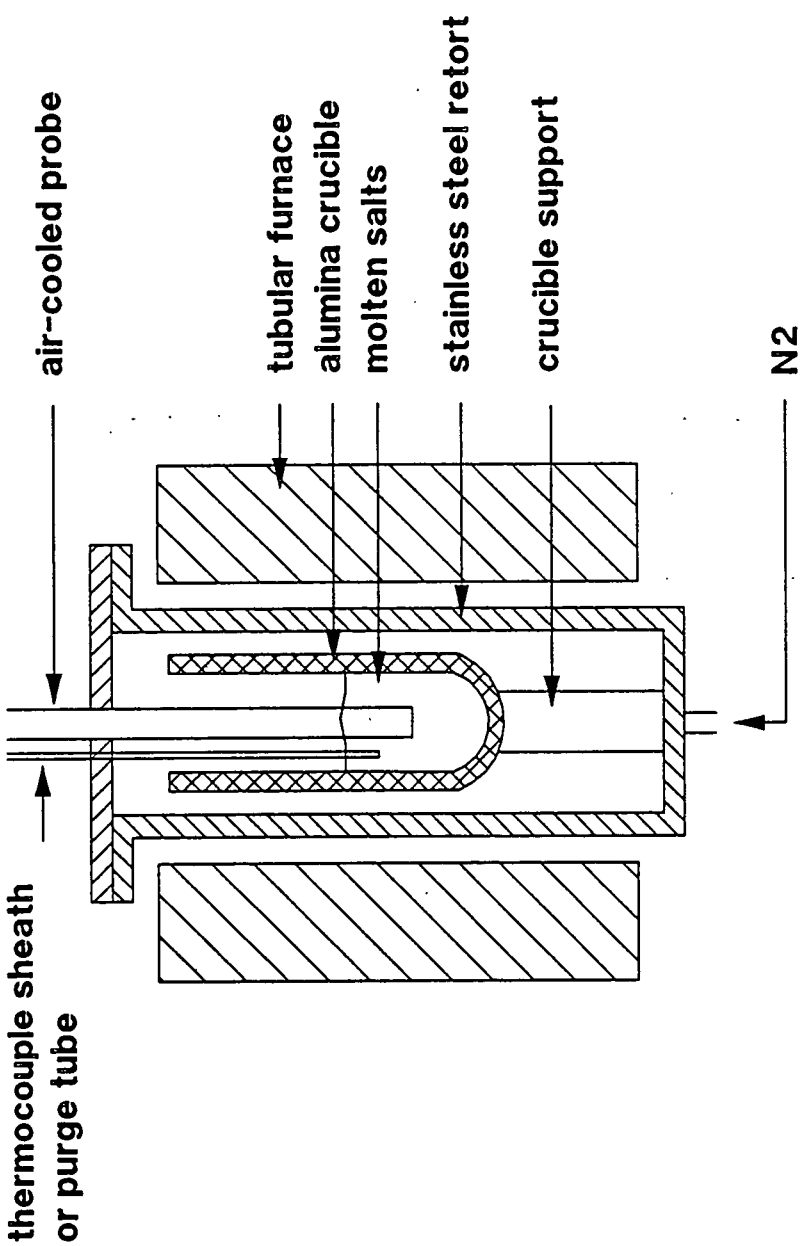

Figure 1. Experimental system for studying the corrosion of metal samples by a frozen smelt layer

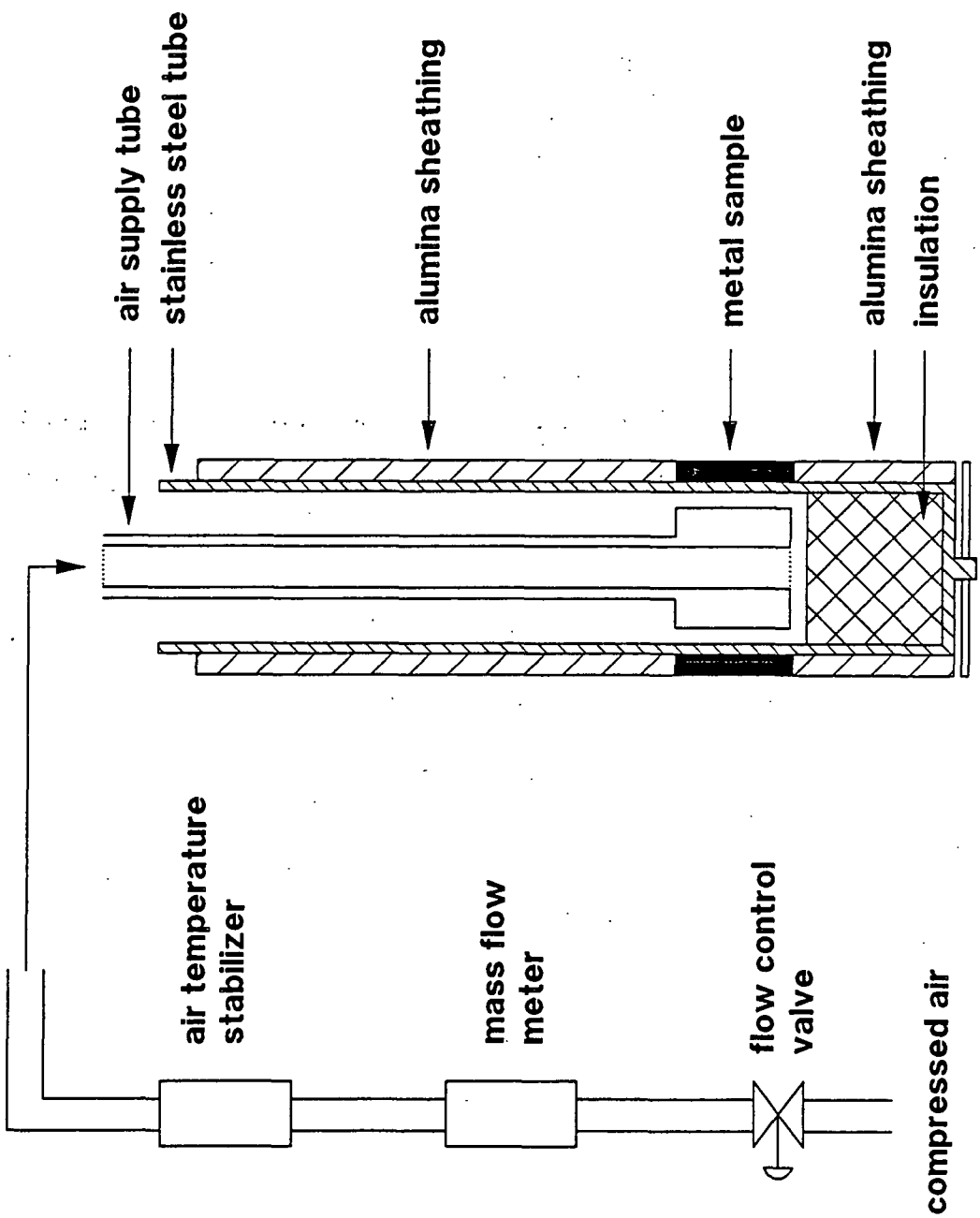

Figure 2. Air-cooled probe used for establishing a frozen smelt layer on a metal sample

valve, and was measured using a Hastings mass flow meter. The compressed air temperature varied with the ambient temperature, so a small heater with a controller was used to stabilize the inlet air temperature at a constant level.

The corrosion coupons were 2.54 cm long tubes, with an outside diameter of 2.80 cm and an inside diameter of 2.184 cm. The corrosion coupons were made from SA210 carbon steel boiler tube material. The composition of the material is shown in Table 13.

Table 13. Composition of SA210 boiler tube material

Element	wt%
C	0.18
Mn	0.60
S	0.014
P	0.011
Si	0.13
Fe	balance

The temperature of the corrosion coupon was measured directly using a 1.02 mm diameter stainless steel sheathed thermocouple. A 1.07 mm diameter hole was drilled in the sample, and the thermocouple was placed in the hole, such that the thermocouple junction was at the midpoint of the sample, just below the surface of the sample (Fig. 3). This is similar to the measurement of boiler tube temperatures using chordal thermocouples.[13] The sheathed thermocouple wire was placed in a groove cut in the probe, behind the alumina sheathing, so that it was protected from the molten smelt. The metal temperature was monitored continuously with a data acquisition system.

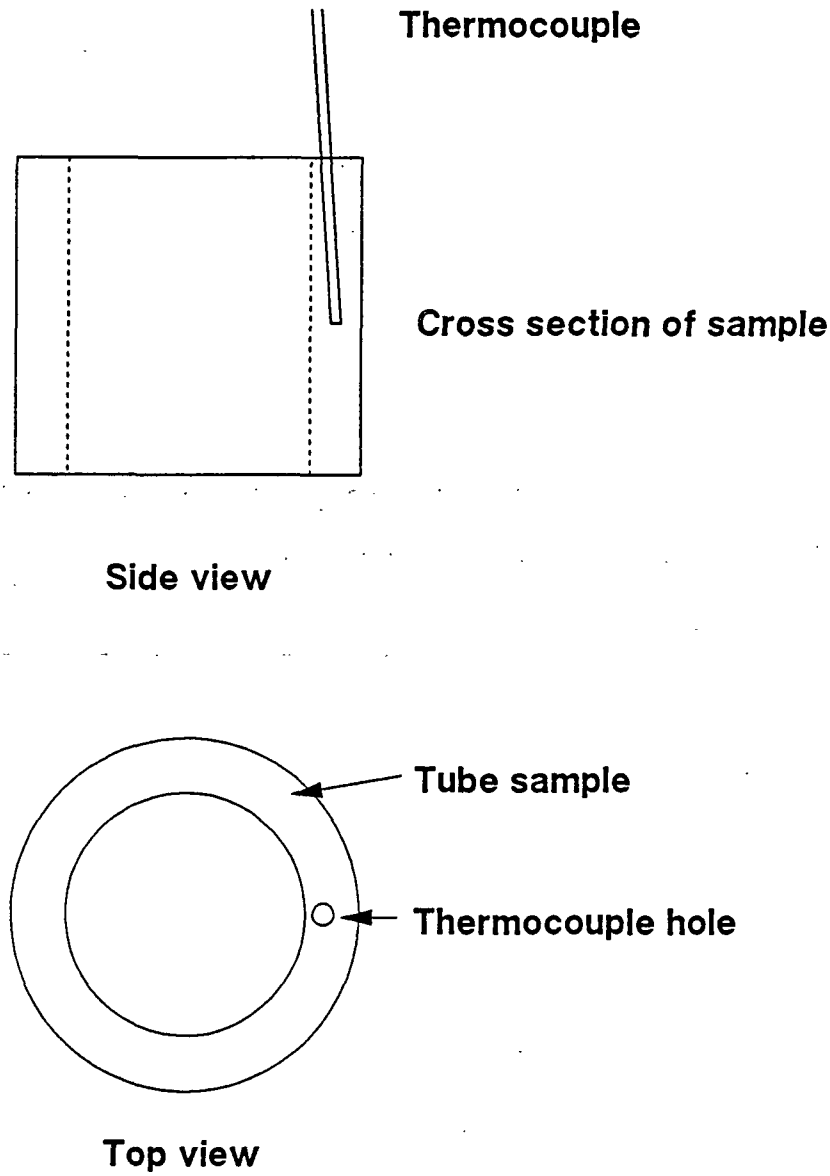

Figure 3. Location of thermocouple for measuring the temperature of the metal sample

Design of Air-Cooled Probe

The cooling medium flowing through recovery boiler waterwall tubes is boiling water, which has a relatively high boiling heat transfer coefficient. Water was not used as the cooling medium in the experimental system because of the possibility of a smelt-water explosion, should a leak develop in the probe and water contact the molten smelt pool.

Previous corrosion studies have been conducted using air-cooled probes inserted into the lower furnace of recovery boilers.[4,13] Other studies have been conducted with air-cooled probes inserted into recovery boiler superheaters.[28,29] Air-cooled probes also have been used in laboratory corrosion studies.[4,25] The advantages of using air as the cooling medium are that compressed air is readily available and is inexpensive, and there is no explosion concern if a leak develops in the probe. The primary disadvantage of using air as a cooling medium is that it has a low convective heat transfer coefficient in comparison to boiling water.

The convective heat transfer coefficient for a gas, such as air, flowing through a pipe is dependent on the gas velocity and the properties of the gas, as expressed by the Dittus-Boelter equation[30]:

$$hd/k = 0.023\ (du\rho/\mu)^{0.8}(C_p\mu/k)^{0.4} \qquad (1)$$

where:

h = convective heat transfer coefficient, W/m^2-K

d = diameter, m

k = thermal conductivity of the gas, W/m-K

u = gas velocity, m/sec

ρ = gas density, kg/m^3

μ = gas viscosity, kg/m-sec

C_p = gas heat capacity, J/kg-K

Equation 1 can also be applied to flow through an annulus, with d defined as the difference between the inner and outer diameter of the annulus. The heat transfer coefficient obtained from this equation must be modified when the pipe or annulus is short ($L/d < 60$) to account for entrance effects. The expression which accounts for entrance effects is[30]:

$$h_m = h \left(1 + K/(L/d) \right) \qquad (2)$$

where:

h_m = average heat transfer coefficient, W/m^2-K

K = constant, with value of 7 for a 90° turn entering the annulus

L = length of the annulus or pipe

d = diameter of the annulus or pipe

The correction factor, $(1 + K/(L/d))$ has a value of 1.42 for the air-cooled probe.

Equations 1 and 2 can be combined to give the following expression:

$$h_m = 0.023 \frac{u^{0.8}}{d^{0.2}} \frac{\rho^{0.8} C_p^{0.4} k^{0.6}}{\mu^{0.4}} (1 + 7d/L) \qquad (3)$$

In designing the probe, it was necessary to determine an appropriate annulus dimension and air flow, such that the heat transfer coefficient be large enough to obtain a heat flux through the metal sample similar to the heat flux through waterwall tubes. The average heat flux through waterwall tubes is 126 kW/m^2 (40,000 $Btu/hr-ft^2$).[4] The heat flux through the sample can be calculated using:

$$Q/A = h_m (T_m - T_a) \qquad (4)$$

where T_m is the measured metal temperature and T_a is the average temperature of the air contacting the metal.

For the design calculations, it was assumed that the average air temperature would be 38°C, since air would be at room temperature initially. Therefore, with a metal temperature of 343°C, h_m must be 410 W/m^2-K to get a heat flux of 126 kW/m^2. Equation 3 was used to determine an appropriate annulus dimension and air flow which would result in such an h_m, with the following air properties[31]:

$T = 38°C$ (100°F)

$k = 0.027$ W/m-K (0.0156 Btu/ft-hr-°F)

$\rho = 1.137$ kg/m^3 (0.071 lb/ft^3)

$\mu = 1.85 \times 10^{-5}$ kg/m-sec (0.0448 lb/hr-ft)

$C_p = 1005$ J/kg-K (0.24 Btu/lb-°F)

Substituting these values into Equation 3 gives:

$$h_m = 3.62 \frac{u^{0.8}}{d^{0.2}} (1 + 7\ d/L) \qquad (5)$$

Figure 4 shows values of the heat transfer coefficient, calculated from Equation 5, plotted for different air velocities and different annulus openings. This figure shows that an air velocity of 50 m/sec will result in a convective heat transfer coefficient of 420-470 W/m^2-K for each of the annulus openings shown. The annulus opening was selected to be 1.5 mm. The air flow rate required for an air velocity of 50 m/sec through an annulus of this dimension is 110 standard liter per minute (slpm).

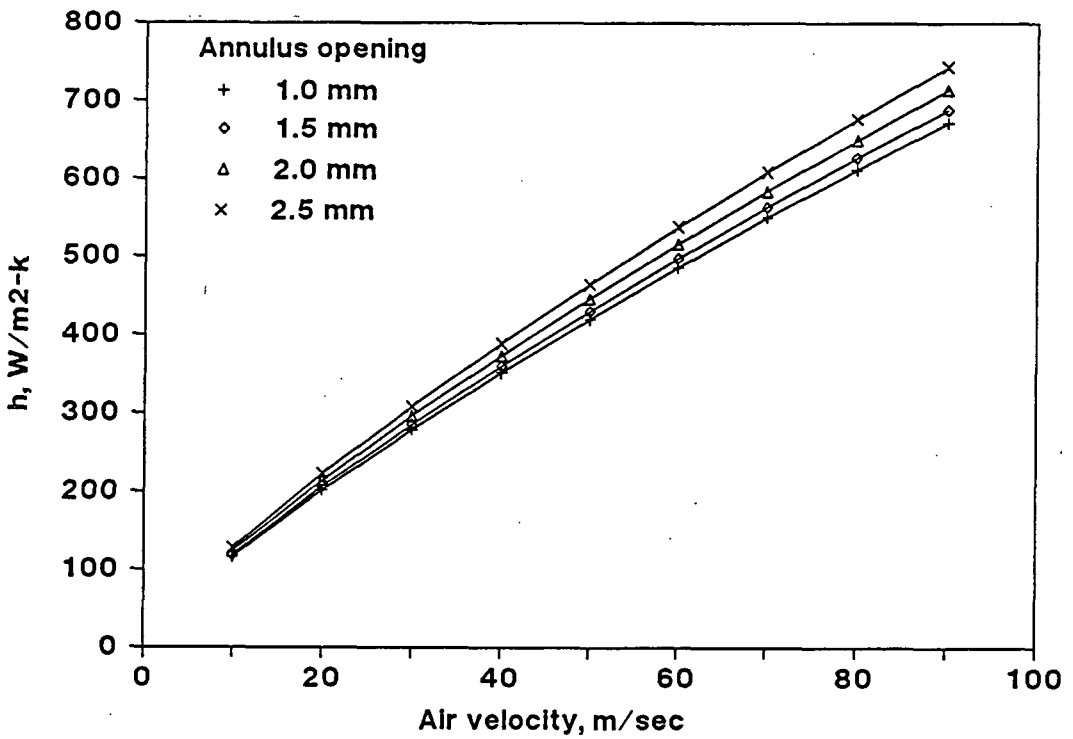

Figure 4. Calculated convective heat transfer coefficient vs. air velocity for annulus opening of 1-2.5 mm

Experimental Verification of Calculated Heat Fluxes

An experimental estimate of the heat flux through the metal sample was determined by measuring the temperature increase of the air flowing past the sample. Thermocouples were placed so that they measured the temperature of the air entering and exiting the annulus, as shown in Fig. 5.

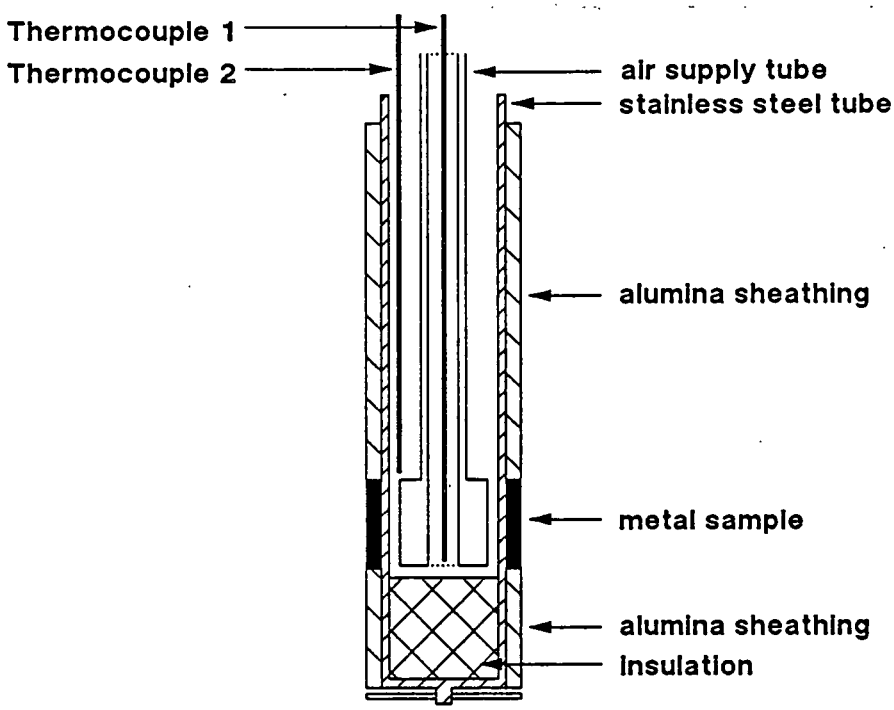

Figure 5. Location of thermocouples for measuring the temperature of the air before and after cooling the metal sample. Thermocouple 1 measures the air temperature before it cools the metal sample and Thermocouple 2 measures the air temperature just after it cools the metal sample.

From these measured air temperatures, it was discovered that the initial estimate of the average air temperature, 38°C, was much too low. This is because the air temperature increased from 25°C to about 90°C as the air flowed through the air supply tube. The air temperature entering the annulus was about 90°C, and the air leaving the annulus was about 150°C, so that the average air temperature was 120°C. Therefore, the heat transfer coefficient must be calculated using the properties of air at 120°C[31]:

$k = 0.0327$ W/m-K (0.0189 Btu/ft-hr-°F)

$\rho = 0.897$ kg/m^3 (0.056 lb/ft^3)

$\mu = 2.2 \times 10^{-5}$ kg/m-sec (0.0532 lb/hr-ft)

$C_p = 1005$ J/kg-K (0.24 Btu/lb-°F)

Equation 3 then becomes:

$$h_m = 3.14 \frac{u^{0.8}}{d^{0.2}} (1 + 7\ d/L) \qquad (6)$$

The heat flux through the probe is calculated using the convective heat transfer coefficient calculated by Equation 6 and the measured difference between the average temperature of the air and the metal temperature. The heat flux can also be estimated using the temperature rise of the air and the air flow rate. A comparison of these two estimates of the heat flux is shown in Table 14. The heat flux estimated using the calculated convective heat transfer coefficient is called the 'calculated heat flux', and the flux estimated from the temperature rise of the cooling air is called the 'measured heat flux'. The calculations used to determine these heat fluxes are shown in

Appendix I. Typically, the measured and calculated heat flux differ by less than 20%. There were some exceptions, such as Experiments 63 and 68, where the measured heat flux was only about 60% of the calculated heat flux. The likely reason for the poor agreement in Experiments 63 and 68 was a low measured air temperature rise, due to one or both of the thermocouples being improperly placed, since the measured air temperatures were sensitive to thermocouple placement. Slight adjustments of the thermocouple location could result in the measured temperature changing by 5-10°C.

There are two sources of error in the 'calculated heat flux'. First, there is some error in the convective heat transfer coefficient calculated by Equation 3, since this equation was developed empirically. The second source of error is in the determination of the difference between the average temperature of the air and the temperature of the surface it contacts. For these calculations, it was assumed that the temperature of the probe surface in contact with the air was the same as the measured temperature of the metal coupon. There actually is a temperature drop between the metal coupon and the probe, due to heat transfer resistance across the interface between the two metals. This difference may be as much as 28-56°C, as is discussed later.

Table 14. Comparison of Measured and Calculated Heat Fluxes Through Air-cooled Probe

Experiment	Air flow (slpm)	Air velocity (m/sec)	Calculated Heat flux (kW/m^2)	Measured Heat flux (kW/m^2)
41	207	105	143.3	128.3
42	226	115	179.1	163.8
43	226	115	177.5	173.7
50	193	98	148.6	134.6
53	190	97	140.2	139.6
60	170	86	129.6	131.6
63	215	109	172.8	102.2
68	193	98	150.3	85.8

Thus, the delta T used in the calculations ranges from 195-220°C, but may actually only be 140-195°C. As a result, the calculated flux may be as much as 40% more than the actual flux.

The 'measured heat flux' is not reliable, due to the fact that the measured air temperatures, especially for the air coming out of the annulus, are very dependent on the thermocouple placement. The measured air temperatures are only accurate to within 5-10°C at best, and the difference between the two air temperatures is small (30-55°C) in comparison to the measurement error. Thus, the measured heat flux can differ significantly from the calculated heat flux.

In summary, although both the 'calculated' and the 'measured' heat flux can differ from the actual heat flux due to measurement errors, the values (shown in Table 14) for the two estimates of the flux are in most cases within 10% of each other. These estimates demonstrate that the heat fluxes through the metal samples on the air-cooled probe are similar to the heat fluxes through waterwall tubes. These heat flux estimates were used only for comparison with waterwall tube heat fluxes, and were not used in the determination of the metal temperature or in the data analysis. Thus, more precise estimates were not necessary.

Heat Flux Through Sample Surface

Because the probe is cylindrical, the heat flux across any surface is a function of the distance of that surface from the center of the probe. The total heat transfer through the probe is constant, but the flux varies with the radius. The outer surface area of the metal sample is 22.3 cm^2, and the

surface area of the probe in contact with cooling air is 15.1 cm^2. Therefore, the flux at the outer surface of the sample is only 67% of the flux across the probe surface in contact with the cooling air. For example, in Experiment 53, the calculated heat flux is 140.2 kW/m^2. The heat flux across the surface of the metal sample is therefore 93.9 kW/m^2. This is somewhat lower than the average heat flux of 126.2 kW/m^2 through recovery boiler waterwall tubes.

Heat Transfer Between Sample and Probe

There is heat transfer resistance across the interface between the metal sample and the stainless steel probe. Because the two metal pieces do not fit perfectly together, there is a thin layer of stagnant air between the two pieces of metal. This resistance has been ignored in the above calculations.

The thermal conductivity of this stagnant air layer between the probe and the coupon is quite low, 0.035 W/m-K, compared to 51.9 W/m-K for carbon steel and 17.3 W/m-K for stainless steel.[31] Thus, even a very thin gap can result in a significant temperature difference between the two metals.

When the metal samples were prepared, the inside surface of the sample was polished with 120 grit silicon carbide paper until the sample fit snugly onto the probe. The polishing removed very little metal - considerably less than 0.0015 cm. The difference between the measured inner diameter of the metal sample and the measured outer diameter of the probe was less than 0.003 cm, so the gap dimension was less than 0.0015 cm. A gap of 0.0015 cm can result in a temperature difference of 54°C if the flux is 126 kW/m^2, as shown below:

$$Q/A = k\, dT/dx \qquad (7)$$

$$dT = (126\ kW/m^2)(0.0015\ cm)(m/100\ cm)/(0.035\ W/m\text{-}K)$$

$$dT = 54\ K$$

In addition, the thermal expansion of the sample and the probe when the probe was placed in the molten smelt tended to close any gap which existed, as the thermal expansion coefficient of the stainless steel is 1.73×10^{-5} cm/cm-K, and the thermal expansion coefficient of the carbon steel sample is 1.21×10^{-5} cm/cm-K.[31] Thus, the inner piece, the probe, will expand more than the outer piece, making for a tighter fit when the probe is inserted into the smelt. Therefore, the temperature difference between the metal and the probe will be less than 47°C, probably about 20-30°C.

Although it was important to carefully fit the sample to the probe, it was not necessary to know the temperature difference between the probe and the metal sample, since the metal temperature was measured directly, as was shown in Fig. 3. The reason it was important to carefully fit the sample to the probe is that as the gap between the sample and the probe increased, the temperature difference between them also increased, resulting in a higher metal temperature. If the gap between the sample and the probe was 0.005 cm, it was not possible to get the metal temperature down below 400°C.

Frozen Smelt Layer Thickness

The thickness of the frozen smelt layer which formed on the metal sample during each experiment was measured after the probe was removed from the furnace and allowed to cool. The thicknesses for several experiments are shown in Table 15.

The smelt thickness when the smelt contained sulfide, sulfate, and carbonate was 0.9-1.0 cm, and when the smelt also contained polysulfide the thickness was 1.65 to >2.4 cm. These are the two smelt compositions which were used in the experiments, as is discussed later in the Experimental section. When the smelt thickness is reported as >2.4 cm, this means that the smelt layer was too thick to remove the probe from the furnace, and some of the smelt layer was melted off by turning down the cooling air flow rate in order to remove the probe. Thus, a measurement of the smelt thickness was not possible, but it was at least 2.4 cm, since the hole in the retort cover was 7.6 cm, and the metal sample diameter was 2.8 cm.

Summary of Probe Conditions

The use of this air-cooled probe resulted in metal temperatures of about 320-350°C, which is the range of metal temperature at which corrosion of waterwall tubes is reported to occur. The thickness of the frozen smelt layer was 0.9-2.4 cm, with heat fluxes of 80-125 kW/m^2 through the surface of the corroding coupon. These conditions are representative of lower furnace waterwall conditions. Table 15 shows the measured metal temperature and the measured smelt thickness, along with the air flow and the calculated heat flux through the surface of the coupon, for several experiments.

Table 15. Summary of Probe Conditions for Several Experiments

Experiment	Air Flow (slpm)	Heat Flux at Sample Surface (kW/m^2)	Metal Temperature (°C)	Smelt Thickness (cm)
Smelt Composition - 15% Na_2S, 15% Na_2SO_4, 70% Na_2CO_3				
41	207	96.0	329	1.02
42	226	120.0	351	0.89
43	226	118.9	349	1.02
Smelt containing polysulfide generated by CO_2 bubbling				
50	192	99.6	342	2.03
53	190	94.0	341	2.03
60	173	86.8	341	1.65
63	215	115.8	343	>2.40
68	192	100.7	343	>2.40

Smelt Composition

The experimental apparatus was designed to simulate the frozen smelt layer covering the waterwall tubes in the lower portion of the furnace. Limited information is available regarding frozen smelt layer composition in the furnace, because it is very difficult to obtain a sample.

Plumley, et al.[4] obtained frozen smelt layer compositions by mounting an air-cooled probe in the plane of the furnace wall, near the smelt bed. The probe was exposed for 2.5, 24 and 168 hours. The frozen deposits which formed on the probe were removed and analyzed. The results are shown in Table 16.

Table 16. Composition of deposits formed on Air-cooled Probe in Lower Furnace Area (Probe temperature = 340°C)[4]

Component	Composition (wt%) 2.5 hr test	24 hr test	168 hr test
Na_2S	13.0	11.6	11.0
Na_2SO_4	13.5	12.2	20.2
Na_2CO_3	68.8	70.2	60.3
Na_2SO_3	1.8	0.9	1.3
$Na_2S_2O_3$	1.4	1.3	2.3
Na_2S_x	0.1	0.1	0.1
Other	0.9	1.1	1.7

Plumley, et al.[4] also collected smelt samples from the lower furnace of operating recovery boilers using a specially designed sampling cup. The cup was situated on the end of a long rod, and was inserted through a furnace port. The cup was placed against the waterwall tube, and a sample of the molten smelt running down the wall was collected. Samples were taken from two recovery boilers over a period of several months. It was not reported whether either of these boilers was the same boiler from which the data in Table 16 were obtained. The average smelt compositions are shown in Table 17.

Table 17. Average Smelt Composition Obtained by Sampling Cup Method in Lower Furnace[4]

Component	Unit A wt %	Unit B wt %
Na_2S	10.9	16.8
Na_2SO_4	14.5	14.3
Na_2CO_3	69.4	65.0
Na_2SO_3	1.3	0.4
$Na_2S_2O_3$	1.6	2.7
Other	1.8	0.1

Based on the information presented in these two tables, a smelt composed of 15% Na_2S, 15% Na_2SO_4, and 70% Na_2CO_3 is representative of the frozen smelt layer composition in the lower furnace. Small amounts of Na_2SO_3 and $Na_2S_2O_3$ were found in the frozen smelt on recovery boiler tubes. However, Na_2SO_3 and $Na_2S_2O_3$ are unstable in high temperature molten smelt.[26] Therefore, they were not added to the smelt, since they would simply decompose. The chosen smelt composition has a melting point of about 800°C (1470°F).[6]

Smelt Preparation

The salts used in smelt preparation were technical grade anhydrous sodium carbonate and sodium sulfate, reagent grade anhydrous sodium thiosulfate, anhydrous sodium sulfide prepared from reagent grade Na_2S-$9H_2O$, and sodium polysulfide (Na_2S_2).

Anhydrous sodium sulfide was prepared by drying Na_2S-$9H_2O$ in a vacuum oven at 200°C for 12 hours, with nitrogen (industrial grade-may contain as much as 0.1% O_2) purged through the vacuum oven. The dried sulfide was then ground into a powder in a nitrogen atmosphere and was stored in glass bottles. Weight loss measurements were made to test the drying procedure. The Na_2S-$9H_2O$ was weighed prior to drying, and the dried Na_2S also was weighed. The weight loss during drying showed that the sulfide was completely dried by this procedure.

Experiments were performed to test the stability of thiosulfate, polysulfide, and elemental sulfur in molten smelt containing carbonate. For each of these experiments, a smelt containing the species being investigated was prepared, and was heated up to 800°C. The smelt was sampled and analyzed to determine how much of the species being investigated remained in the melt.

To test the stability of thiosulfate in molten carbonate, a smelt was prepared with 30% sodium thiosulfate and 70% sodium carbonate. A smelt was prepared with 5% sulfur, 10% sodium sulfide, 15% sodium sulfate, and 70% sodium carbonate to test the stability of elemental sulfur in molten smelt containing sulfide, sulfate, and carbonate.

In the experiments to test the stability of polysulfide in molten smelt containing sulfide, sulfate, and carbonate, polysulfide was prepared and mixed with the other smelt components prior to heating up the smelt. This polysulfide was prepared from anhydrous sodium sulfide and reagent grade elemental sulfur according to the procedure of Rosen and Tegman.[23] An equimolar mixture of sodium sulfide powder and elemental sulfur was heated to 200°C for 12 hours in a sealed container to form polysulfide (Na_2S_2). Rosen and Tegman[23] reported that 80-90% conversion to polysulfide occurred under these conditions. The resulting material was ground to a powder in a nitrogen filled glove bag.

For the initial corrosion experiments, the smelt was prepared from 15% anhydrous sodium sulfide powder, 15% anhydrous sodium sulfate, and 70% anhydrous sodium carbonate. The sodium sulfide was placed at the bottom of an alumina crucible. Sodium sulfate was placed on top of the sulfide, and sodium carbonate was placed on top of the sulfate. The reactor was then sealed, and small nitrogen flow through the system was started. The smelt mixture was slowly brought up to 840°C over an 18 hour period. The nitrogen purge was continued throughout the heatup and the experiment to prevent oxidation of the smelt.

For the corrosion experiments with smelt containing polysulfide, the polysulfide was generated by bubbling CO_2 through a smelt prepared from 15% sodium sulfide, 15% sodium sulfate, and 70% sodium carbonate. This smelt was prepared in exactly the manner described above. The carbon dioxide bubbling through the molten smelt reacted with the sodium sulfide, oxidizing some of it to polysulfide. This reaction is discussed in the Results and Discussion section.

Sample Preparation

The corrosion coupons were 2.5 cm long tubes made from SA210 carbon steel boiler tube material. Each corrosion coupon had an inside diameter of 2.184 cm, and the inside surface was polished with 120 grit silicon carbide paper until the coupon fit snugly onto the probe. The thermocouple hole was then drilled in the wall of the coupon. The drilling of this hole had no effect on either the inner or the outer surface of the sample, since it was drilled in the end of the coupon.

Several hours before the coupon was placed in the smelt, the exposed surface was prepared. It was first polished with 80 grit silicon carbide paper to remove any surface irregularities. This was followed by polishing with 120 grit paper, to give the surface its final finish. The sample was polished by rotating the specimen with an electric motor, and abrading the rotating surface. Water was used as a polishing lubricant, to prevent heating of the surface, which could result in metallurgical changes in the sample.

After polishing, the sample was rinsed with distilled water, and then degreased with acetone. The sample was then blasted with purified bottled air to dry the surface, and to remove any water or acetone from the thermocouple hole. An analytical balance was used to obtain the initial weight of the coupon.

Corrosion Exposures

There were two types of corrosion exposures performed in this work. The first were exposures of metal samples to a smelt, with no smelt-gas interactions. The only gas flow into the system was the nitrogen purge. The second type of exposure involved smelt-gas interactions. In these experiments, carbon dioxide was bubbled through a smelt containing sodium sulfide, sodium sulfate, and sodium carbonate to generate polysulfide prior to placing the sample in the smelt.

Smelt Containing Sulfide, Sulfate, and Carbonate

These experiments were performed with smelt prepared from 15% sodium sulfide, 15% sodium sulfate, and 70% sodium carbonate, as described previously. The smelt was heated to 840°C over 18 hours, and then allowed to sit at 840°C for several hours, to insure that it was completely molten.

Prior to initiation of the corrosion exposure, a sample of the molten smelt was taken for analysis. The sample was taken by removing the cover from the probe opening in the retort cover, and dipping a steel sampling cup into the smelt pool. The sample was allowed to cool for about 30 minutes, and then was removed from the sampler and stored under nitrogen.

The exposure was started by inserting the probe, with cooling air flowing through it, into the furnace. The lower 7.6 cm of the probe were exposed to the molten smelt pool. The metal temperature initially overshot the desired temperature by 60-80°C, as is shown in Fig. 6 and 7. A maximum metal temperature was reached within 10 minutes, and then the sample cooled

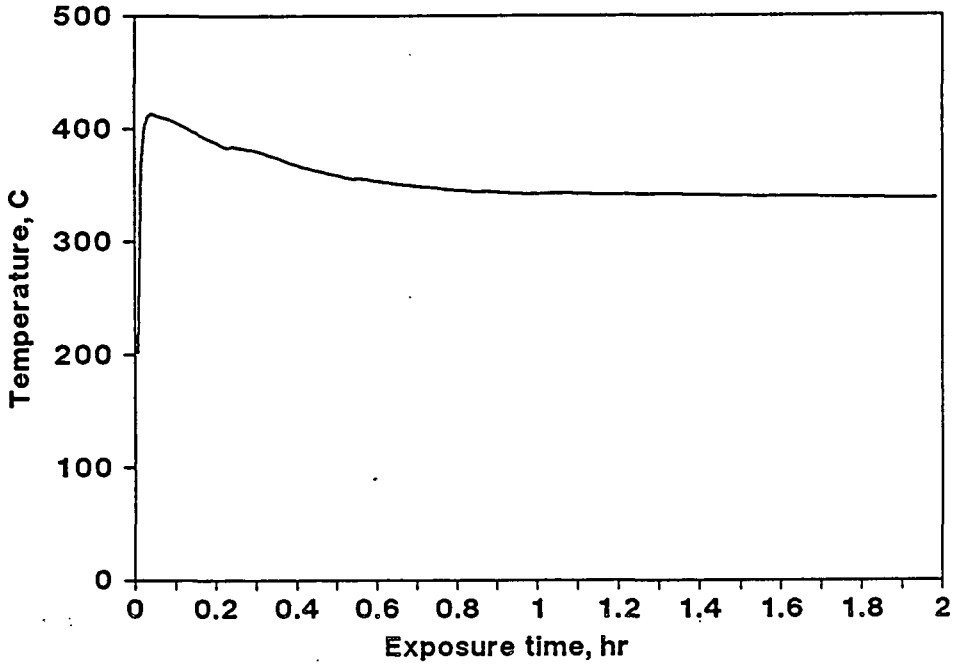

Figure 6. Temperature of metal sample throughout the first 2 hours of a 48 hour exposure (Exp. 62)

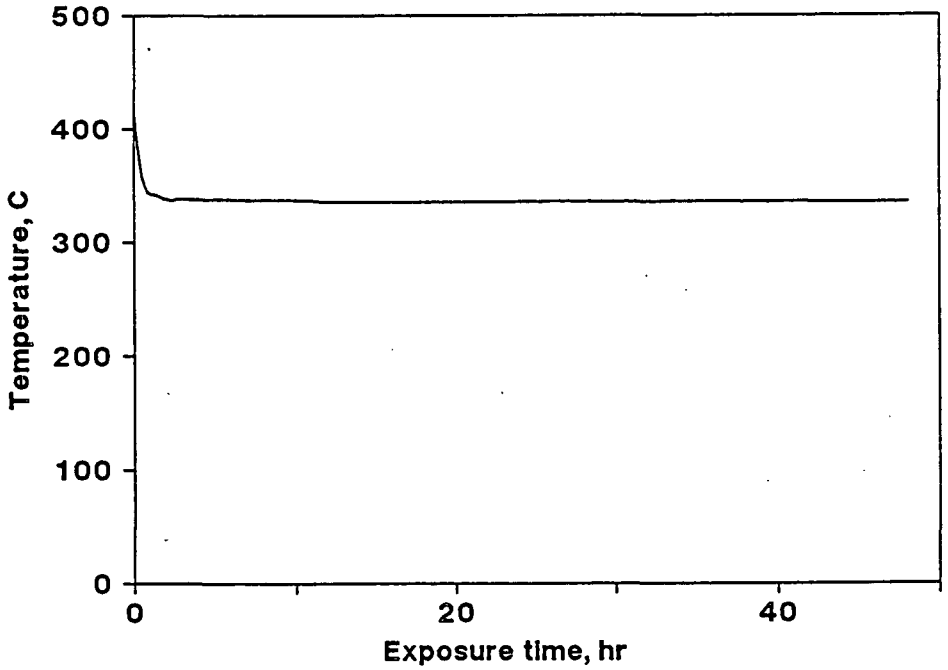

Figure 7. Temperature of metal sample throughout a 48 hour exposure (Exp. 62)

off as the frozen smelt layer thickened. Within about 1 hour, a stable temperature was reached. This suggests that it took about 1 hour to fully establish the frozen smelt layer.

The cooling air flow rate was initially set at 200 slpm for the experiments with a desired metal temperature of 340°C. The temperature did not always stabilize at 340°C, but ranged from 325-360°C. The air flow rate usually had to be manually adjusted to insure that the temperature stabilized in the desired range of 335-345°C.

Figure 6 shows a temperature profile over the first two hours of an exposure, with a desired temperature of 340°C. The temperature profile over the entire course of the same exposure is shown in Fig. 7. It can be seen that over the course of a long term exposure, the metal temperature was subject to some minor fluctuation. Generally, this stayed within a range of plus or minus 3°C.

After the desired exposure time, the probe was removed from the furnace. It was allowed to cool for about one hour, by maintaining the air flow, before it could be handled. The frozen smelt layer developed cracks as it cooled, making it quite easy to break the frozen layer off of the probe. The cooled frozen layer was not strongly adherent to either the metal sample or the alumina sheathing. A sample of the frozen layer was taken, and immediately stored in a bottle under nitrogen.

When another exposure was to be made in the same molten smelt pool, the molten smelt pool was replenished. To make up for the smelt which had been removed from the pool through sampling and removal of the frozen smelt

layer, 400-500 g of smelt powder of the same composition as the original smelt was added to the smelt pool.

Samples taken from the molten smelt were analyzed to determine the smelt composition prior to exposure of a corrosion coupon. This was to insure that the smelt pool composition was not being changed by the preparation procedure. Table 18 shows the composition of molten smelts prepared with 15% Na_2S, 15% Na_2SO_4, and 70% Na_2CO_3. Molten smelts A and B are different smelts. If these smelts are compared to the nominal composition of 15% Na_2S, 15% Na_2SO_4, 70% Na_2CO_3, it can be seen that there was a slight oxidation of sulfide to sulfate, and a very small amount of sulfite was generated.

When the air-cooled probe was exposed to the molten smelt, a layer of frozen smelt formed on the probe. The portion of the frozen smelt layer which formed in contact with the probe was similar in composition to the molten smelt, as shown in Table 18. The frozen smelt layer compositions shown in Table 18 were obtained by exposing the probe to the molten smelt for 2 hours, and then analyzing a sample of the innermost portion of the frozen smelt layer, the portion which had been in contact with the metal surface. The sample was obtained by scraping the innermost portion of the frozen layer with a razor blade. Frozen layer A was formed when the probe was inserted into molten smelt A, and frozen layer B was formed from molten smelt B.

Table 18. Composition of smelt samples from sulfide/sulfate/carbonate smelts (Nominal composition: 15% Na_2S/15% Na_2SO_4/70% Na_2CO_3)

Sample	Composition (wt%) Na_2S	Na_2SO_4	Na_2SO_3
Molten smelt A	13.5	16.2	1.3
Frozen layer A	12.6	16.1	1.2
Molten smelt B	12.2	14.8	2.4
Frozen smelt B	10.1	16.5	3.7

Andersson[6] has published a phase diagram for the sodium sulfide-sodium sulfate-sodium carbonate system. This system does not have a ternary eutectic. Rather, two solid phases, Na_2S and a solid solution of Na_2CO_3 and Na_2SO_4, exist in equilibrium with the ternary liquid phase. The minimum melting composition is 20 mole% Na_2CO_3, 35 mole% Na_2S, and 45 mole% Na_2SO_4.

The smelt composition used in this work does not correspond to a eutectic composition. The frozen smelt layer and the molten smelt are similar in composition because the frozen smelt is formed by non-equilibrium rapid cooling. The outer portion of the frozen smelt layer, which is discussed in the Results and Discussion section, forms more slowly. Thus, this portion of the frozen layer would be expected to be closer to the equilibrium composition predicted by the phase diagram. The outer portion of the frozen layer does have a lower Na_2S concentration than the molten smelt, as is predicted by the phase diagram.

Smelt Containing Polysulfide Sulfur

The procedure was modified slightly for the experiments with smelt containing polysulfide sulfur. Polysulfide was formed in the molten smelt by bubbling CO_2 through the smelt.

A molten smelt containing sulfide, sulfate, and carbonate was prepared as described above. Prior to the exposure, a CO_2 flow of 0.5 slpm was bubbled through the smelt for two hours. A nitrogen purge of 0.5 slpm flowed through the retort, but not the smelt, during the smelt heatup period, and this flow was continued during the CO_2 bubbling period, and during the corrosion exposure.

If the CO_2 purge tube was left in the smelt during the exposure of the probe, a bridge of frozen smelt formed on the smelt surface between the probe and the purge tube, connecting them. This made it difficult to remove the probe from the furnace at the end of the exposure without breaking the purge tube. So instead, the CO_2 purge was lifted out of the smelt prior to placing the probe in the smelt. The CO_2 flow was maintained, so that CO_2 was purged over the surface of the melt. This maintained a polysulfide content in the molten smelt. If the CO_2 was turned off, the polysulfide quickly decomposed, and the polysulfide content of the melt went to 0.

Table 19 shows the smelt composition for smelt prepared with 15% Na_2S, 15% Na_2SO_4, and 70% Na_2CO_3, through which 0.5 slpm CO_2 was bubbled for 2 hours. The composition of the frozen layer which formed on the probe in a very short exposure (1 hr) to the molten smelt is also shown. The frozen smelt which freezes in contact with the metal has a composition similar to the molten smelt pool.

Table 19. Composition of smelt samples from polysulfide smelt

	Composition (wt%)			
Sample	Na_2S	Na_2SO_4	Na_2SO_3	Polysulfide Sulfur
Molten smelt	10.0	17.5	2.3	0.5
Frozen smelt	9.3	17.7	2.0	0.4

POWDERED SMELT TESTS

These experiments were performed using the experimental system shown in Fig. 8. The experiments were performed using powdered smelt containing polysulfide. The smelt composition was similar to the composition of the frozen layer which initially formed on the metal sample during the tests with the air-cooled probe, as shown in Table 20.

To prepare the smelt powder, molten smelt composed of 15% Na_2S, 15% Na_2SO_4, and 70% Na_2CO_3 was prepared. Carbon dioxide was bubbled through the melt, at a rate of 0.5 slpm for 2 hours, to generate a stable quantity of polysulfide in the melt. This procedure was identical to the polysulfide smelt generation procedure used in the probe tests.

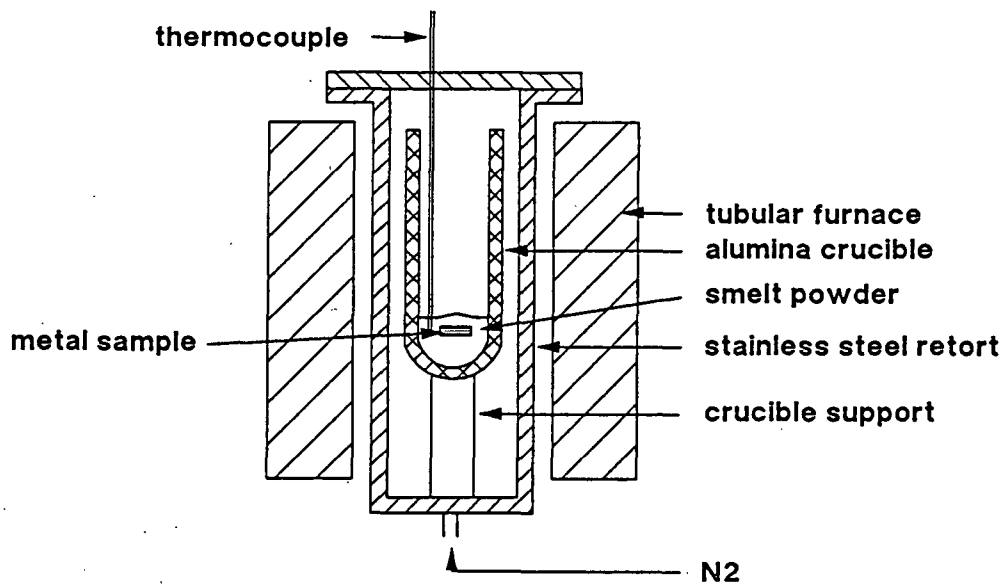

Figure 8. Experimental system for studying the corrosion of metal samples by smelt powder

Table 20. Composition of smelt powder in comparison to frozen smelt layer

	Composition (wt%)			
	Na_2S	Na_2SO_4	Na_2SO_3	Polysulfide sulfur
Frozen smelt layer	9.3	17.7	2.0	0.4
Smelt powder before exposure	8.3	19.2	2.0	0.4
	8.8	16.3	1.9	0.7
Smelt powder after exposure	7.3	20.1	1.9	0.4

A steel cup, which had been used to take samples of the molten smelt for analysis during the probe tests, was used to remove smelt containing polysulfide from the furnace. The smelt was allowed to cool for 15 minutes, and then was knocked out of the cup and stored in a nitrogen filled glass bottle. This procedure was repeated until a satisfactory quantity of smelt had been removed from the furnace. The CO_2 bubbling was continued throughout the procedure. The frozen smelt was then ground to a powder using a mortar and pestle in a nitrogen glove bag.

The corrosion tests were performed using SA210 carbon steel coupons. These coupons were flat bars, 7.6 x 1.3 x 0.32 cm. The coupons were given a 120 grit finish, and cleaned and preweighed. The coupons were placed on a bed of the smelt powder about 2.5 cm deep, in an alumina crucible. The coupon was then covered with about 0.6 cm of additional smelt powder. A thermocouple was placed in the smelt, near the corrosion coupon.

The crucible was placed in a stainless steel retort inside a tubular furnace. The system was rapidly heated up to 343°C. The temperature of the metal sample and the smelt powder was held at 343°C for the desired

exposure period. A nitrogen purge of 0.5 slpm flowed into the retort throughout the experiment.

CORROSION PRODUCT REMOVAL AND ANALYSIS

In order to determine the weight loss due to corrosion, the corrosion products were removed from the corrosion coupon. In the experiments with the air-cooled probe, it was possible to obtain a sample of corrosion product after the frozen smelt layer was removed from the sample. The product was removed from the sample by gently scraping the corroded surface with a small spatula. This corrosion product was analyzed using x-ray diffraction to identify the crystalline components. The cross section of some of the corrosion products were looked at with the scanning electron microscope to determine the corrosion product thickness.

The remainder of the corrosion product was removed using a cyclo-blaster with very small glass beads. The specimen was hand held and blasted at a blast velocity which removed the visible corrosion products from the surface of the specimen without removing uncorroded metal. The fact that the blasting did not remove a significant quantity of uncorroded metal was established by blasting uncorroded samples, and determining the weight loss.

A number of blanks were cleaned by this procedure to determine the weight loss due to this cleaning procedure. The corrosion samples were prepared and weighed just as the other samples. The samples were colored with magic marker, and then cycloblasted to remove the magic marker coloring. The samples were cleaned using the same technique as was used for corroded specimens. The weight loss due to the cleaning procedure was found to average

0.056 mg/cm^2, with a range of 0.036-0.072 mg/cm^2, as is shown in Table 21. This weight loss is considered satisfactorily small in comparison to the weight losses due to corrosion, which range from 1-4 mg/cm^2. The weight loss due to the cleaning procedure was less than 5% of the total weight loss.

Following blasting, the specimen was rinsed in distilled water, and then in acetone. The sample was then blown dry with air, and the final weight was determined.

Table 21. Weight loss during corrosion product removal procedure

Initial wt (g)	Final wt (g)	Wt. loss (mg/cm^2)
49.0134	49.0120	0.063
48.9357	48.9341	0.072
46.9568	46.9555	0.058
46.4792	46.4784	0.036
46.5537	46.5525	0.054
	Average	0.056

SMELT ANALYSIS

Samples of smelt taken from molten smelt pools were analyzed for sulfide, sulfate, sulfite, and polysulfide. The samples were obtained by dipping a portion out of the molten smelt pool with a stainless steel cup. The samples were ground to a powder in a nitrogen-filled glove bag.

The sulfide content of the smelt was determined by titration with mercuric chloride, and the sulfate and sulfite contents were determined by ion chromatography. The polysulfide content was determined using a gas chromatographic method[32]. The polysulfide sulfur was reacted with triphenylphosphine to form triphenylphosphine sulfide, which was detected using flame ionization gas chromatography. The procedures used for these analyses are described in Appendix II. Smelt samples taken from frozen smelt layers were analyzed in the same manner.

The ranges of accuracy for the reported concentrations in the smelt are discussed in Appendix II. The ranges of accuracy, reported as percent of the total weight of the smelt, are ±1% Na_2S, ±2% Na_2SO_4, ±1% Na_2SO_3, and ±0.2% S_x.

RESULTS AND DISCUSSION

SULFIDE/SULFATE/CARBONATE EXPOSURES

Frozen Smelt Layer Composition

The initial experiments were performed using smelt prepared with 15% sodium sulfide, 15% sodium sulfate, and 70% sodium carbonate. These are the three major species which exist in the lower waterwall region of the kraft recovery boiler. This composition was chosen as a representative simulation of the frozen smelt layer in the lower waterwall region.

In Table 18 in the experimental section, it was shown that the composition of the frozen smelt which initially formed in contact with the metal was similar in composition to the molten smelt pool from which the frozen smelt layer was formed. The frozen smelt layer after short term tests, less than 24 hours, was uniform in appearance. When the probe was exposed for 24 hours or longer, the frozen smelt layer was composed of two distinct layers. The layer closest to the metal was pink in color, and very similar in composition to the molten smelt from which the frozen layer was formed, as shown in Table 22. The outer portion of the frozen layer, which was closest to the molten smelt, was white, and was quite different in composition from the molten smelt. This outer layer had a sulfate content similar to the inner layer, but contained less sulfide, 4-4.8%, compared to 9.6-11.8% in the inner portion of frozen layer.

Table 22. Smelt compositions from sulfide/sulfate/carbonate exposures

Sample	Exposure time (hr)	wt% Na_2S	wt% Na_2SO_4	wt% Na_2SO_3
Molten smelt	0	12.2	14.8	2.4
Frozen layer, inner portion	72	9.6	14.6	2.2
Frozen layer, inner portion	94	11.8	14.2	-
Frozen layer, outer portion	72	4.8	14.4	3.3
Frozen layer, outer portion	94	4.0	17.1	1.4
Molten smelt	48	9.1	20.4	1.7
Molten smelt	48	10.3	22.7	2.6
Molten smelt	94	8.0	22.4	1.7

For comparison, the compositions of the molten smelt pool after 48 and 94 hour exposures are also shown. It can be seen that some of the sulfide in the molten smelt was oxidized to sulfate over the course of a long term test. Less than 5% of the oxidation of sulfide to sulfate can be explained by oxygen in the nitrogen which was purged through the retort. Industrial grade nitrogen, which contained less than 0.1% O_2, was purged through the retort at a rate of 0.5 slpm. Oxidation of the smelt apparently occurred because air entered the system, possibly when the retort was opened to insert the probe.

The sulfate content of the outer portion of the frozen layer was closer to the composition of the initial molten smelt than the final molten smelt, suggesting that the frozen layer did not grow throughout the experiment, but was formed early in the exposure, before significant oxidation of the smelt had occurred.

The phase diagram published by Andersson[32] for the sodium sulfide-

sodium sulfate-sodium carbonate system predicts that frozen smelt formed by equilibrium cooling from molten smelt composed of 15% Na_2S, 15% Na_2SO_4, and 70% Na_2CO_3 will contain less than 15% sulfide. After long term exposure of the probe to molten smelt, the outer portion of the frozen smelt layer on the probe contained less sulfide than the molten smelt at the end of the exposure. This suggests that the outer portion of the frozen smelt layer was in equilibrium with the molten smelt. The inner portion of the frozen smelt layer had a sulfide content similar to the initial molten smelt, suggesting that it was formed by non-equilibrium rapid cooling.

The composition of the inner portion of the frozen smelt layer was closer to the composition of the initial molten smelt than the final molten smelt. This proves that the frozen layer was permanent, and did not fall off and reform. If periodic removal and reformation of the frozen layer had occurred, the composition of the inner portion of the frozen layer would have more closely resembled the final smelt composition.

Corrosion Rates

A series of corrosion coupons were exposed to frozen smelt layers containing sulfide, sulfate, and carbonate for different exposure periods. Since it was not possible to monitor the corrosion rate continuously, it was necessary to run a number of exposures for different lengths of time in order to determine the kinetics of the corrosion process. The metal temperature for these experiments was 321-349°C (610-660°F). The results of these tests are shown in Fig. 9.

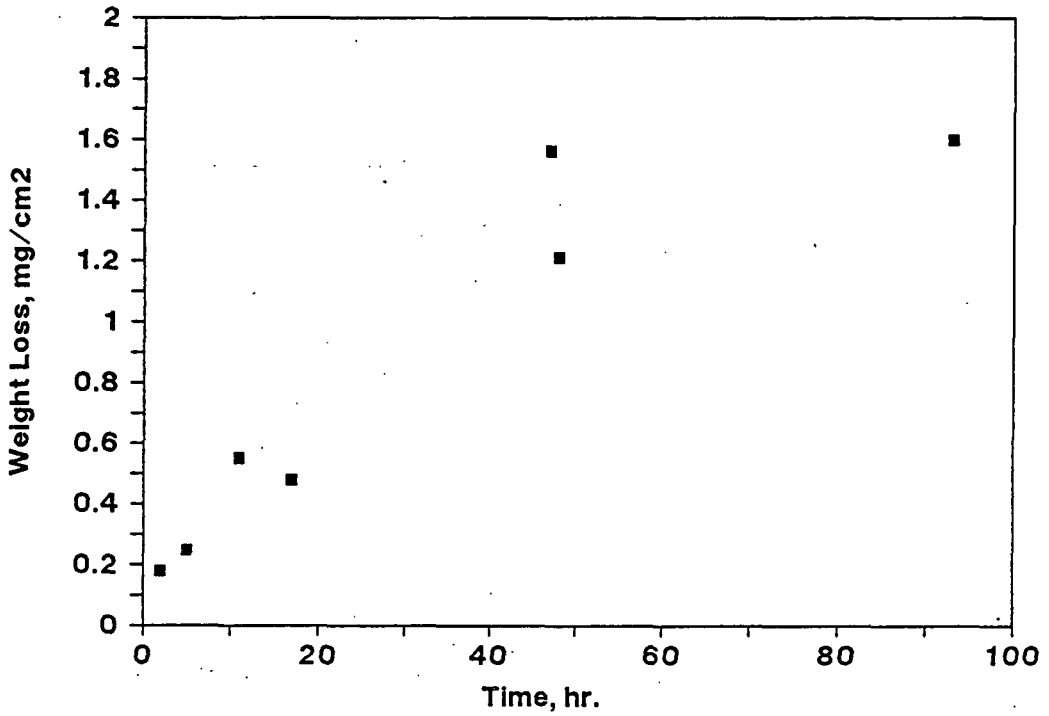

Figure 9. Corrosion rate data obtained in exposure of carbon steel to 15% Na_2S, 15% Na_2SO_4, and 70% Na_2CO_3 (Metal Temperature - 320-350°C)

After exposure to the smelt, the corrosion coupons were covered with a uniform layer of corrosion product, which was quite adherent to the corrosion coupon. In order to remove the corrosion product, the surface of the coupon had to be scraped with a spatula. The only experiment which resulted in enough removable corrosion product (10 mg) to perform x-ray diffraction was the 94 hour exposure. The corrosion product from this test was identified as a mixture of Fe_2O_3 and Fe_3O_4.

The corrosion of metal is an electrochemical process. The metal is oxidized, and the oxidant is reduced. The reduction reaction and the oxidation reaction must occur at the same time and to the same extent. Thus, the reduction reaction is quite important, since if this reaction can be prevented, the oxidation of the metal is stopped.

The oxidant in this corrosion process might be one of the smelt components, either sulfate, sulfite, or carbonate. Sulfide can not be further reduced. Possible reduction reactions include:

$$CO_3^{2-} + 2\ e^- \Longrightarrow CO + 2\ O^{2-} \qquad \text{(rxn. 8)}$$

$$SO_4^{2-} + 2\ e^- \Longrightarrow SO_3^{2-} + O^{2-} \qquad \text{(rxn. 9)}$$

In addition, it is possible that CO_3^{2-} or SO_4^{2-} dissociated to form CO_2 or SO_3, according to:

$$CO_3^{2-} \Longleftrightarrow CO_2 + O^{2-} \qquad \text{(rxn. 10)}$$

$$SO_4^{2-} \Longleftrightarrow SO_3 + O^{2-} \qquad \text{(rxn. 11)}$$

and the CO_2 or SO_3 was reduced at the metal surface:

$$CO_2 + 2\ e^- \Longrightarrow CO + O^{2-} \qquad \text{(rxn. 12)}$$

$$SO_3 + 2\ e^- \Longrightarrow SO_2 + O^{2-} \qquad \text{(rxn. 13)}$$

The oxidation reactions were:

$$Fe \Longrightarrow Fe^{2+} + 2\ e^- \qquad \text{(rxn. 14)}$$

and

$$Fe \Longrightarrow Fe^{3+} + 3\ e^- \qquad \text{(rxn. 15)}$$

The oxide ions generated in the reduction reaction combined with the oxidized iron to form the iron oxide corrosion product.

It is not critical to know which of these possible reduction reactions is occurring. However, the fact that iron oxides, and not iron sulfides, are generated as the corrosion products is quite important. This suggests that frozen smelt containing just carbonate, sulfide, sulfate, and a small amount of sulfite is not responsible for the accelerated corrosion which occurs near the primary airports of recovery boilers, since iron sulfide corrosion products have been observed there.[13,14] If frozen smelt is responsible for the formation of iron sulfides, other sulfur species than sulfide, sulfate, and a small amount of sulfite must be involved.

The extent of the corrosion reaction as a function of exposure time is shown in Fig. 9. This figure shows that 0.5 mg/cm^2 (0.5 mm/yr) of weight loss occurred in the first 12 hours of exposure. This weight loss includes the 0.06 mg/cm^2 which can be attributed to the corrosion product removal procedure. The reaction slows down after 12 hours, with only another 1.0 mg/cm^2 of weight loss occurring in the next 80 hours. This type of behavior is commonly observed in the oxidation of metals.

Two rate laws have been developed to describe this type of corrosion behavior, the parabolic rate law and the logarithmic rate law. These models describe corrosion processes in which the corrosion product layer which forms on the metal surface provides protection against continued corrosion by acting as a barrier between the metal and the oxidant. The two rate laws are based on different mechanisms of transport of the metal or the oxidant through the corrosion product layer.

The parabolic and logarithmic rate laws were fitted to the experimental data to determine if they describe the results. This will be discussed, but first each law will be described briefly.

The parabolic rate law describes corrosion which is limited by the diffusion of either metal ions or oxide ions through a growing oxide film.[33-35] This law is only applicable at temperatures high enough to allow the diffusion of ions through the corrosion product layer. It has been experimentally determined that Fe_3O_4 grows by the outward passage of cations, and Fe_2O_3 grows by the inward passage of anions[34], so this rate law can be applied to the high temperature oxidation of iron.

When the corrosion is limited by diffusion of ions through the corrosion product layer, the rate of growth of the corrosion product layer thickness is inversely proportional to the corrosion product thickness:

$$\frac{dy}{dt} = \frac{k_p}{y} \qquad (8)$$

where y is the corrosion product thickness, t is time, and k_p is a diffusion constant. The rate of growth of the corrosion product layer is proportional to the rate of corrosion. Equation 8 can be integrated to obtain the parabolic rate law:

$$y^2 = k_p t/2 + C \qquad (9)$$

The parabolic rate law has been experimentally verified for most metals over some range of temperature.[34] It has been reported, however, that in most cases the parabolic corrosion rate law is not followed during the initial stages of corrosion. The corrosion is not limited by diffusion of ions through the oxide layer until the oxide reaches a thickness on the order of several thousand angstroms.[35] The corrosion rate is observed to be a linear function of time prior to the establishment of this continuous corrosion product layer.

The oxidation of metals at low temperature, where the movement of ions through the oxide lattice by diffusion is negligible, is often described by a logarithmic rate law.[33,34] When ionic diffusion through the corrosion product layer is negligible, the only way the oxidant can reach the metal is by migration through pores in the corrosion product layer. These pores can be very small, such as occur at the lines where three grains meet. The oxidant reacts with the metal surface at the base of the pore, forming corrosion product which blocks the pore and prevents further oxidation. In addition, the compressive stresses associated with the formation of the oxide inside the pore may lead to the blocking of neighboring pores. The mathematical development of this type of model has been presented by Evans.[34] It results in a logarithmic rate law:

$$w = k_1 \ln(at + 1) \qquad (10)$$

Equation 10 describes the oxidation of iron in dry oxygen at temperatures below 200-300°C.

The temperature at which iron oxidation changes from logarithmic to parabolic behavior has not been well defined[34], but has been reported to be between 200 and 300°C. Since it was not clear which model was best applied to the experimental conditions used in this work, both types of model, Eq. 9 and 10, were fitted to the experimental data. This resulted in the following rate equations:

Parabolic: $w^2 = 0.0314t - 0.0118$ $r^2 = 0.85$ (11)

or

$$w = (0.0314t - 0.0118)^{0.5} \quad (12)$$

Logarithmic: $w = 0.857 \ln(0.069t + 1)$ $r^2 = 0.93$ (13)

where w is the weight loss due to corrosion in mg/cm^2, and t is the time in hours.

The best fit of each of these models to the experimental data, determined by regression analysis, is shown in Fig. 10 and 11. Both models fit the data well, indicating that the iron oxide layer provided protection against continued corrosion. Since both models fit the data equally well, it is not possible to determine whether the limiting step in the corrosion process is ionic diffusion through the iron oxide or transport of oxidant through pores in the iron oxide layer.

The instantaneous corrosion rate can be obtained by differentiation of the parabolic and logarithmic equations with respect to time:

Parabolic: $$\frac{dw}{dt} = \frac{0.016}{(0.0314t - 0.0118)^{0.5}} \quad (14)$$

Logarithmic: $$\frac{dw}{dt} = \frac{0.059}{(0.069t + 1)} \quad (15)$$

Using Eq. 14 and 15, the rate of corrosion at any time can be determined. Eq. 14 and 15 can be extrapolated to times greater than 100 hours to estimate corrosion rates after long exposure times. A table of estimated corrosion rates is shown in Table 23. This table shows that during

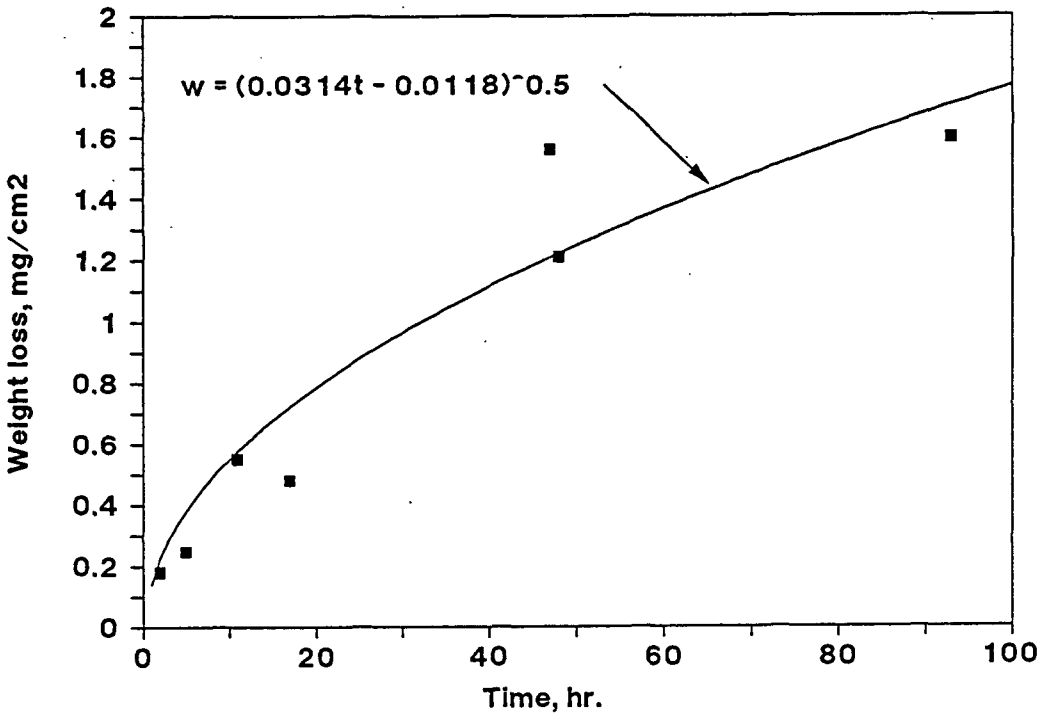

Figure 10. Parabolic Model fitted to corrosion rate data from exposure to frozen smelt containing 15% Na_2S, 15% Na_2SO_4, and 70% Na_2CO_3 (Metal Temperature - 320-350°C)

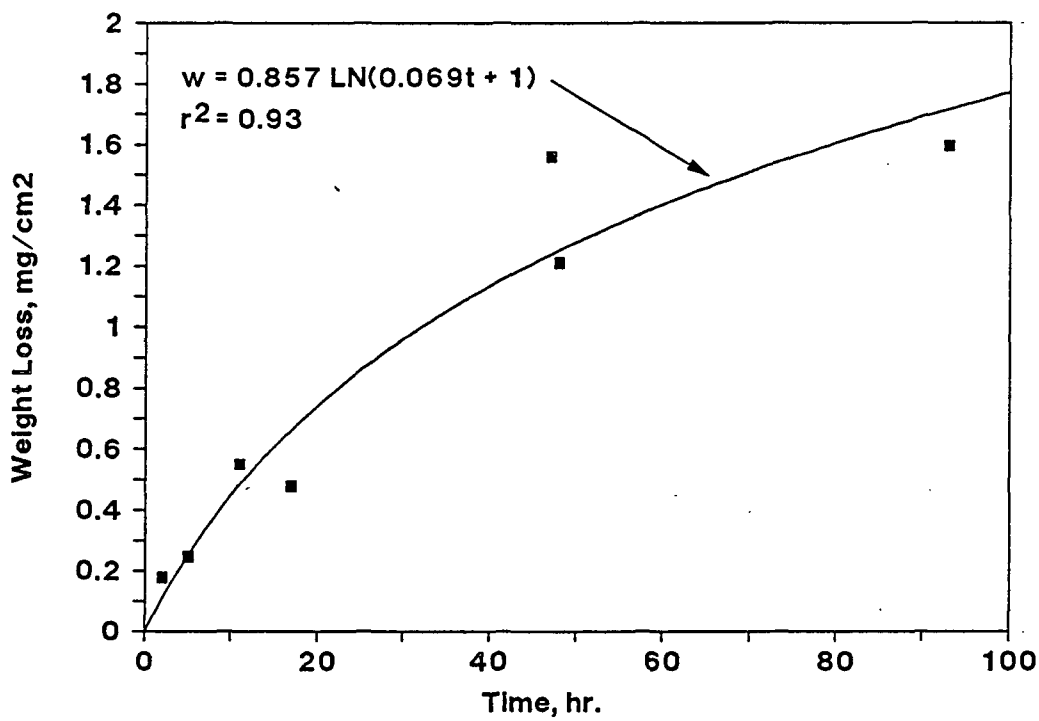

Figure 11. Logarithmic Model fitted to corrosion rate data from exposure to frozen smelt containing 15% Na_2S, 15% Na_2SO_4, and 70% Na_2CO_3 (Metal Temperature - 320-350°C)

Table 23. Long term instantaneous corrosion rates extrapolated from parabolic and logarithmic rate laws for corrosion of carbon steel by frozen smelt containing sulfide, sulfate, and carbonate at 340°C.

Time (days)	Instantaneous Corrosion Rate (mm/yr) Parabolic	Logarithmic
30	0.036	0.013
90	0.021	0.004
180	0.015	0.002

long exposures, if the corrosion product layer remains on the metal surface, the corrosion rate is predicted to be less than 0.1 mm/yr using either model.

The corrosion rates measured in recovery boilers are average corrosion rates over the exposure period, obtained by dividing the measured weight loss by the exposure time. If the parabolic and logarithmic models are extrapolated to times longer than 100 hours, estimates of average long term corrosion rates can be obtained by predicting the weight loss for an exposure period using Eq. 11 and 13, and then dividing the weight loss by the exposure time. Table 24 shows average long term corrosion rates predicted from the two models.

Table 24. Long term average corrosion rates extrapolated from parabolic and logarithmic rate laws.

Time (days)	Average Corrosion Rate (mm/y) Parabolic law	Logarithmic law
30	0.08	0.05
90	0.05	0.02
180	0.03	0.01

These average corrosion rates indicate that the corrosion due to frozen smelt containing sulfide, sulfate, and carbonate is quite low in comparison to recovery boiler corrosion rates. These long term corrosion rates are lower than the maximum allowable recovery boiler corrosion rate of 0.2 mm/yr[1], and are an order of magnitude lower than the accelerated corrosion rates of 0.5-1.5 mm/yr observed in recovery boilers. This low corrosion rate, combined with the fact that the experimental corrosion products are iron oxides, while corrosion products in areas of severe corrosion in boilers are iron sulfides, indicates that this type of corrosion is not related to accelerated waterwall corrosion in recovery boilers.

MINOR SMELT COMPONENTS

One of the characteristics of accelerated lower furnace corrosion is the formation of iron sulfide corrosion products.[13] The corrosion experiments performed with smelt composed of sulfide, sulfate, carbonate, and a small amount of sulfite resulted in the formation of protective iron oxides. No iron sulfides were identified by x-ray diffraction. This shows that neither the sulfide nor the sulfate in the frozen smelt layer is directly responsible for the formation of iron sulfide corrosion products.

Sulfur can exist in a number of oxidation states: S^{2-}, S_2^{2-} and other polysulfides up to S_5^{2-}, S, $S_2O_3^{2-}$, SO_3^{2-}, and SO_4^{2-}, as well as other compounds. The major sulfur species in the frozen smelt in the first experiments were sulfide, sulfate, and a small amount of sulfite. These species did not result in the formation of iron sulfide corrosion products. This suggests that if frozen smelt corrosion is the cause of iron sulfide

formation, one of the minor sulfur species which can exist in smelt - thiosulfate, polysulfides, or elemental sulfur - is the oxidant.

Previous experimental studies have suggested that elemental sulfur or polysulfide is the cause of high rates of corrosion of carbon steel. The results of Stelling and Vegeby[3] suggested that the corrosion occurring in H_2S-O_2 mixtures was the result of gas reactions which formed sulfur vapor. In smelt powder tests performed by Plumley, et al.[4], gas-smelt powder combinations which caused high corrosion rates also resulted in the formation of elemental sulfur, suggesting that elemental sulfur was responsible for the corrosion. In addition, when a frozen smelt layer containing sulfide, sulfate, and carbonate was exposed to gas containing H_2S and O_2, the frozen smelt layer reacted with the gas, forming 6% polysulfide sulfur in the frozen smelt.[9,18] The corrosion rate was low for the first four hours of the test, but then was accelerated, suggesting that the polysulfide caused the increased corrosion. Since these studies suggest that polysulfide or elemental sulfur caused accelerated corrosion of carbon steel, the effect of elemental sulfur and polysulfide on the corrosion of carbon steel by a frozen smelt layer was investigated.

When a frozen smelt layer is formed from molten smelt using an air-cooled probe, the frozen smelt in contact with the metal is similar in composition to the molten smelt. In order for a smelt component to exist at the frozen smelt/metal interface, it could have been captured in the frozen layer when it was formed from molten smelt, it could have been formed in the smelt pool and diffused through the frozen layer, or it could have been formed during the freezing process, which seems unlikely. For this reason, the stabilities of thiosulfate, elemental sulfur, and polysulfide in molten smelt

were investigated.

Thiosulfate

Grace, et. al.[24] report that the addition of thiosulfate to molten carbonate results in the formation of sulfide and sulfate, and the release of carbon dioxide, according to

$$Na_2S_2O_3 + Na_2CO_3 \Longrightarrow Na_2S + Na_2SO_4 + CO_2 \qquad \text{(rxn. 16)}$$

This decomposition reaction was verified in this work. Thiosulfate and carbonate were premixed, and then melted. Sampling and analysis of the molten smelt showed that the thiosulfate decomposed according to the stoichiometry shown above.

Elemental Sulfur

Dahl and Falk[18] and Cleaver and Davies[36] report that when elemental sulfur is added to molten smelt containing sulfide, polysulfide is formed. The reaction is complete, with no elemental sulfur being stable in the molten smelt.[36] Therefore, elemental sulfur can be considered equivalent to polysulfide Na_2S_x in molten smelt containing sodium sulfide.

Polysulfide

Sodium polysulfide was formed from elemental sulfur and sulfide according to the procedure of Rosen and Tegman[23] (see Experimental section). Sodium polysulfide with a stoichiometric ratio of Na_2S_2 was premixed with

sodium sulfide, sodium sulfate, and sodium carbonate. This mixture was melted, and the molten smelt was sampled and analyzed. Table 25 shows the results of a number of analyses.

Table 25. Compositions of molten smelts prepared with sodium polysulfide

	wt%			
Sample	Na_2S	Na_2SO_4	Na_2SO_3	Polysulfide Sulfur
Premixed smelt	13.5	15.0	0.0	1.5
Molten smelt	13.7	16.3	3.3	<1
Premixed smelt	12.1	15.0	0.0	2.9
Molten smelt A	15.1	14.1	3.6	1.3
Molten smelt B	15.0	15.3	2.2	0.7

Molten smelt A was taken immediately after the smelt became molten, and B was taken from the same smelt pool 4 hours later.

This table clearly shows that a large portion of the polysulfide which was mixed in the smelt had already decomposed by the time the smelt became molten. The polysulfide decomposition reaction appeared to produce sulfide, sulfate, and sulfite. It is likely that the polysulfide reacted with carbonate in the following reactions:

$$Na_2S_{x+1} + x\ Na_2CO_3 \Longrightarrow (1 + 0.75x)\ Na_2S + x/4\ Na_2SO_4 + x\ CO_2 \qquad \text{(rxn 17)}$$

$$Na_2S_{x+1} + x\ Na_2CO_3 \Longrightarrow (1 + 0.67x)\ Na_2S + x/3\ Na_2SO_3 + x\ CO_2 \qquad \text{(rxn 18)}$$

where x = 1 to 4.

These reactions appeared to continue over an extended period of time. Sample A, which was taken immediately after the smelt had reached the molten state, shows that over half of the polysulfide sulfur had reacted by the time

the smelt became molten. Sample B, taken 4 hours later from the same smelt, shows that the polysulfide sulfur continued to react slowly.

An additional experiment was performed to verify that sodium carbonate was involved in the decomposition of polysulfide. A molten smelt was prepared without carbonate. The carbonate was replaced by additional sodium sulfate. The smelt was premixed with 2.9% polysulfide sulfur, and a sample taken from the molten smelt contained 2.2% polysulfide sulfur. Only 25% of the polysulfide was consumed by smelt which did not contain carbonate, compared to 75% when the smelt contained carbonate. This shows that when the melt did not contain carbonate, less of the polysulfide reacted with the smelt. Some of the of sulfur which was lost may be the result of sulfur vaporization, since when the retort cover was removed, allowing air to enter the system, flaming was observed. The flames were similar to the flames observed in other experiments when elemental sulfur was poured into the retort. This suggests that there is a sulfur vapor pressure in equilibrium with the polysulfide in the melt.

Workers at the Swedish Corrosion Institute[18] premixed sulfur with sodium sulfide, sodium sulfate, and sodium carbonate. The mixture was then melted, and the molten smelt sampled and analyzed. The sulfur reportedly reacted with sulfide to form polysulfide. A portion of the polysulfide sulfur was then consumed, and sulfide and sulfate were generated. Almost all of the sodium carbonate in the melt reacted. These observations are consistent with Reaction 17.

The addition of sulfur to a molten smelt composed of sodium sulfide, sodium sulfate, and sodium carbonate was attempted in this work. Small sulfur pellets, each weighing about 2 g. were dropped into the smelt pool. The

pellets were less dense than the molten smelt, and floated on top of the melt. This resulted in vaporization and burning of the sulfur, making quantitative addition of sulfur to the melt difficult.

Sulfur was also premixed with sodium sulfide, sodium sulfate, and sodium carbonate in this work. The mixture was melted, and the molten smelt sampled and analyzed. The analyses, shown in Table 26, show that all of the sulfur reacted with the smelt, forming polysulfide, sulfide, sulfate, and a small amount of sulfite.

Table 26. Composition of molten smelts prepared with elemental sulfur

	wt%				
Sample	Na_2S	Na_2SO_4	Na_2SO_3	Elemental Sulfur	Polysulfide Sulfur
Premixed smelt	10.0	15.0	0.0	5.0	0
Molten smelt A	12.9	25.0	2.4	-	1.5
Molten smelt B	13.0	27.2	2.5	-	0.6

Smelt sample A was taken immediately after the smelt became molten, and smelt sample B was taken from the same smelt 4 hours later.

These results show that when elemental sulfur was added directly to smelt containing sulfide, sulfate, and carbonate, it formed polysulfide, which then reacted with carbonate to form sulfide, sulfate, and sulfite. Only 10% of the sulfur originally placed in the smelt remained as polysulfide sulfur 4 hours after the smelt became molten.

Because the polysulfide in the molten smelt reacted continuously with the carbonate, the amount of polysulfide captured in the frozen smelt layer was a function of when the probe was placed in the melt. This made it very difficult to perform reproducible experiments. Therefore, the interaction of

recovery furnace gases with molten smelt, which may generate stable quantities of sulfur species such as polysulfide in the melt, was considered.

SMELT/FURNACE GAS INTERACTIONS

In the kraft recovery furnace, the combustion gases are in contact with the molten smelt flowing down the lower waterwalls. In addition, there may be some direct contact between the furnace gases and the frozen smelt layer. Thus, corrosive species in the frozen smelt layer may be formed by frozen smelt/furnace gas interactions. Corrosive species also may be formed by the interaction of the furnace gases with molten smelt on the furnace walls, and be captured in the frozen layer when it forms. Additionally, the corrosive species in the frozen layer may be the result of molten smelt/gas interactions, followed by the transfer of the corrosive species from the molten smelt to the frozen layer.

In the experimental system, the frozen layer was surrounded by a molten salt pool at all times, so there was no opportunity for interaction between the frozen smelt layer and gases. Any interactions between the smelt and gas species must have occurred in the molten smelt.

Tallent and Plumley[13] reported that elemental sulfur was generated by reaction of CO_2 with Na_2S powder, according to the following reaction:

$$Na_2S + 2\ CO_2 \implies CO + S + Na_2CO_3 \qquad \text{(rxn. 19)}$$

In addition, Dahl and Falk[18] and Cleaver and Davies[36] reported that when elemental sulfur was added to molten smelt containing sulfide,

polysulfide was formed rapidly. The reaction was complete, and no elemental sulfur was stable in the molten smelt.[36] This suggests that bubbling CO_2 through molten smelt containing sulfide will result in the formation of elemental sulfur, which then combines with sulfide to form polysulfide.

When CO_2 was bubbled through a smelt prepared from 15% Na_2S, 15% Na_2SO_4, and 70% Na_2CO_3, a stable polysulfide content in the molten smelt was established. The polysulfide content of several smelts after CO_2 had been bubbled through them are shown in Table 27. These analyses show that the polysulfide content of the melt was not dependent on the duration of the CO_2 bubbling. This suggests that polysulfide was consumed in a reaction with sodium carbonate at the same rate that it was generated by Reaction 19, resulting in a stable quantity of polysulfide in the melt, as long as bubbling of CO_2 was continued.

Table 27. Polysulfide content of smelt prepared from 15% Na_2S, 15% Na_2SO_4, and 70% Na_2CO_3, through which 0.5 slpm CO_2 was bubbled

Time of bubbling (hr)	Polysulfide content (%)
2	0.6
2	0.9
4	0.6
4	1.1
5	0.6
8	0.8

POLYSULFIDE EXPOSURES

Frozen Smelt Layer Composition

In the experimental system, corrosive species generated through gas-molten smelt interactions could reach the metal surface by one of two means. If the gas was bubbled through the smelt prior to the establishment of a frozen smelt layer, the resulting species would be captured in the frozen smelt layer when it was formed. If the gas was bubbled through the smelt after the frozen layer was established, any resulting corrosive species would have to be transported through the frozen layer to reach the smelt-metal interface.

For these experiments, CO_2 was bubbled through the molten smelt prior to establishment of the frozen layer, so that the species generated by molten smelt-gas interaction were contained in the frozen smelt initially. In one experiment, the bubbling of CO_2 was not started until after the frozen smelt layer had been formed. After 48 hours, the yellow color indicative of polysulfide had penetrated partially (but not completely) through the frozen smelt to the metal surface. The rate of corrosion in this experiment was similar to that measured when the smelt contained just sulfide, sulfate, and carbonate. This shows that bubbling CO_2 through the molten smelt prior to the establishment of the frozen smelt layer is a more effective method of studying the effect of polysulfide on corrosion beneath a frozen smelt layer.

These experiments were performed using smelt composed of 15% sodium sulfide, 15% sodium sulfate, and 70% sodium carbonate. Carbon dioxide was

bubbled through the melt for two hours, at a rate of 0.5 slpm, prior to initiation of the corrosion test to establish a polysulfide content in the smelt. Carbon dioxide was purged over the surface of the melt during the remainder of the exposure.

In Table 19 of the Experimental section, the composition of the frozen smelt layer which initially formed on the metal was shown to be similar in composition to the molten smelt pool from which it was formed. The frozen smelt layer after short exposures had a uniform appearance and a yellow color, which was due to polysulfide.

After exposure of the probe to the molten smelt for 24 hours or longer, the frozen smelt was composed of two distinct layers. The outer layer, which was next to the molten smelt, was about one half the thickness of the frozen smelt layer, or 0.6 cm. The inner layer, which was next to the metal, could be subdivided further into two sections. The majority of the inner layer was pink, with a slight yellow tint. However, in some experiments, the portion which was closest to the metal surface was more strongly yellow. This yellow portion was called the innermost layer.

The outer layer was clear colored, and composed of large grains. The composition of this layer was quite different from the composition of either the molten smelt or the inner portion of the frozen layer, as shown in Table 28. The outer layer had only 3.0-5.2% Na_2S, compared to 10.0-11.5% Na_2S for the inner layer and the molten smelt. The polysulfide content was 0.3%, compared to 0.5-0.6% for the inner frozen smelt layer and the molten smelt.

The composition of the outer portion of the frozen smelt layer suggests that this portion of the frozen smelt layer was formed by equilibrium

Table 28. Analyses of frozen smelt layers from polysulfide experiments

Sample	Exposure time (hr)	wt% Na_2S	Na_2SO_4	Na_2SO_3	Polysulfide Sulfur
Molten smelt	0	10.0	17.5	2.3	0.5
"	0	11.2	15.4	2.6	0.6
Frozen layer-	48	11.0	15.0	1.8	0.5
inner portion	48	10.5	15.6	2.2	0.5
Frozen layer-	48	5.2	13.4	-	0.3
outer portion	48	3.0	14.5	1.1	NA
Frozen layer-	48	2.3	14.9	5.7	0.2
innermost portion	48	7.0	15.2	2.2	NA
Molten smelt	48	11.2	17.9	2.1	0.4
"	48	11.4	17.5	2.2	0.3

NA = not analyzed for

cooling. The phase diagram of the sodium sulfide-sodium sulfate-sodium carbonate system published by Andersson[32] predicts that frozen smelt formed by equilibrium cooling from molten smelt containing 15% sodium sulfide, 15% sodium sulfate, and 70% sodium carbonate will contain less sulfide than the molten smelt. The outer portion of the frozen smelt layer contained only 3.0-5.2% sodium sulfide, compared to 10.0-11.5% sodium sulfide in the molten smelt, which is consistent with the equilibrium composition predicted by the phase diagram.

The majority of the inner portion of the frozen layer was pink, with a slight yellow tint, indicating it contained polysulfide. It had a composition similar to the molten smelt from which it was formed. However, in some experiments the innermost portion, which was closest to the metal surface, was more strongly yellow. The thickness of this yellow-colored layer was about 0.16 cm. It had a much lower sulfide and a slightly lower

polysulfide content than the rest of the inner smelt layer. This suggests that the some of the sulfur originally in this layer was consumed by the corrosion reaction, which will be discussed later.

Corrosion Experiments

A series of corrosion tests were made with carbon steel coupons covered with a layer of frozen smelt containing polysulfide which had been generated by CO_2 bubbling. The exposure time ranged from 15 minutes to 100 hours. The metal temperature for these experiments was held between 330-350°C. The results of these experiments are shown in Fig. 12.

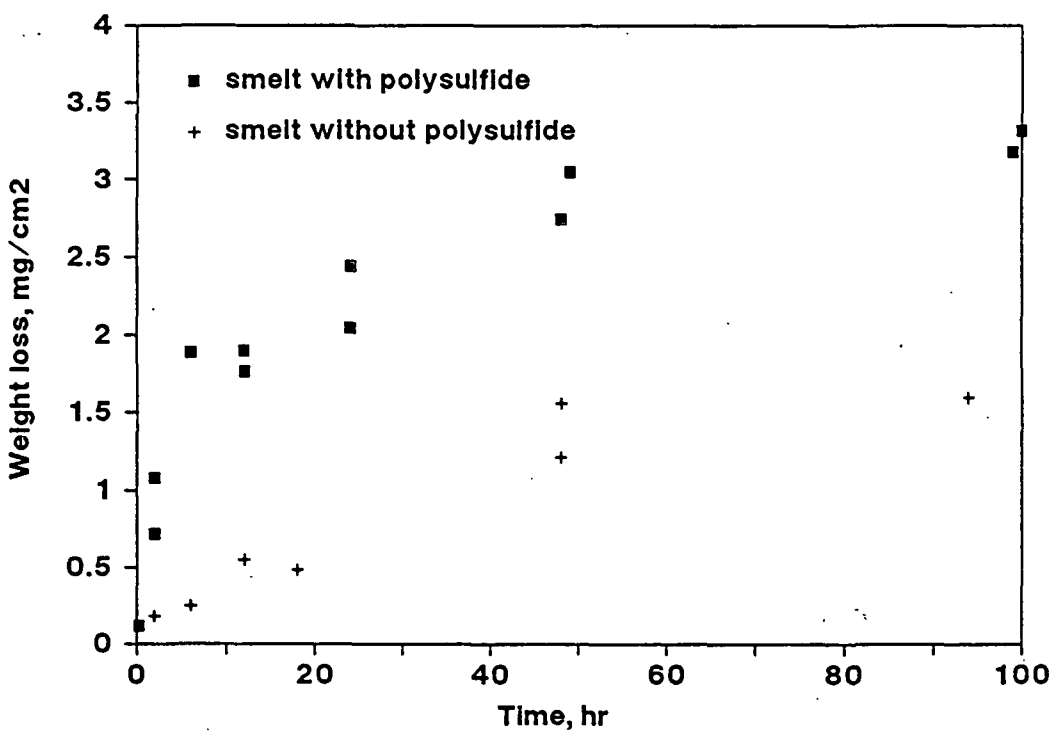

Figure 12. Comparison of experimental data obtained in corrosion tests with 15% Na_2S, 15% Na_2SO_4, 70% Na_2CO_3 smelt with and without polysulfide, with metal temperature of 320-350°C

Figure 12 shows that the corrosion rate was initially very high, and then after about 12 hours, the rate slowed down considerably. The weight loss due to corrosion was 1.8 mg/cm^2 in the first 12 hours, but only an additional 1.4 mg/cm^2 of weight loss occurred when the exposure was extended to 100 hours.

Figure 12 also shows that the weight loss due to corrosion in experiments with smelt containing polysulfide was significantly higher than that observed in the experiments without polysulfide. For example, in a 100 hour exposure, the weight loss with polysulfide in the smelt was 3.2 mg/cm^2, compared with 1.6 mg/cm^2 for the smelt containing no polysulfide. This difference in weight loss can be attributed to the initial high rate of corrosion which occurs when the smelt contains polysulfide. The rate of corrosion is the same for smelt with and without polysulfide for times longer than 48 hours.

The corrosion product in experiments with smelt containing polysulfide was identified as pyrrhotite, metal deficient iron sulfide ($Fe_{1-x}S$), by x-ray diffraction. The x-ray diffraction patterns of the corrosion products from these exposures are presented in Appendix III.

The iron sulfide corrosion product layer was considerably less adherent to the metal surface than the iron oxide layers described earlier. The iron oxides adhered tightly to the metal surface, and were only removed by scraping the surface with a metal spatula. The iron sulfide was loosely bound to the metal surface. Flakes of iron sulfide often fell off of the surface when the frozen smelt layer was removed, and flakes of iron sulfide could be removed simply by touching the surface of the metal coupon.

A scanning electron microscope (SEM) photograph of the cross section of an iron sulfide layer removed from the surface of a corroded coupon is shown in Fig. 13. The picture shows the cross section and a portion of the outer surface of an iron sulfide layer from Experiment 53. The thickness of the layer ranges from 5-8 microns. If the weight loss from this experiment is assumed to be uniform over the surface of the sample, the thickness of the iron sulfide layer can be calculated to be 8 microns, which is in good agreement with the observed thickness.

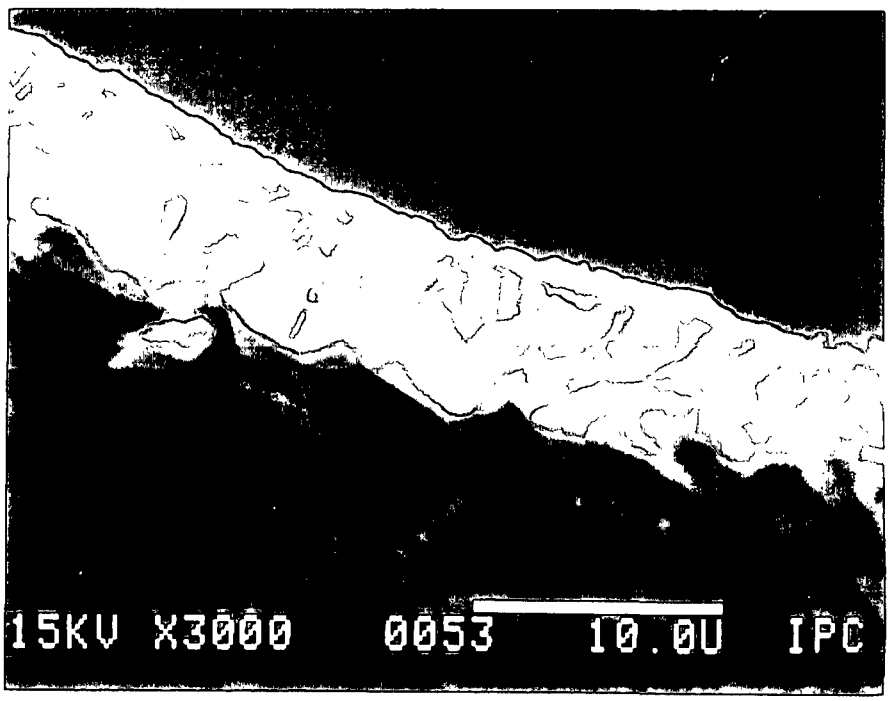

Figure 13. SEM micrograph of cross section of iron sulfide layer formed in 24 hour exposure of carbon steel sample to frozen smelt containing polysulfide

When the frozen smelt layer was carefully removed from the probe after exposure to a smelt containing polysulfide, the surface of the corroded coupon was covered with a uniform layer of iron sulfide, with the exception of a number of irregularly shaped and irregularly spaced areas in which there was no corrosion product. These areas comprised 10-20% of the surface area of the sample.

The inner surface of the frozen smelt layer was rough, with definite peaks and valleys. The depth of the valleys in the frozen smelt was greater than the thickness of the iron sulfide layer, which was less than 10 microns thick. There was corrosion product adherent to the areas of the frozen smelt layer which could be identified visually as peaks, or high points. This corrosion product was bluish-black, and was clearly visible on the yellow frozen smelt. These black spots on the frozen smelt corresponded with the areas of the sample surface on which there was no corrosion product, as can be seen in Fig. 14. This suggests that these dark spots are areas of smelt/metal contact, and that the corrosion product which formed in these areas was either dissolved in the frozen smelt layer, or adhered strongly to the frozen smelt when it was removed from the sample. The remainder of the sample was apparently not in direct contact with the frozen smelt layer, so the corrosion product remained on the metal surface when the frozen smelt layer was removed.

When the surface of a corroded coupon was viewed with the scanning electron microscope, after the corrosion product layer had been carefully removed with a small spatula, the area where there had been smelt-metal contact appeared slightly more corroded than the remainder of the surface. This is illustrated in Fig. 15 and 16, which are SEM micrographs of the corroded surface. In Fig. 15, the area which had been in direct contact with the metal surface is shown on the right. In the area on the left, the scratches from the surface polishing are still visible. There is a streak of

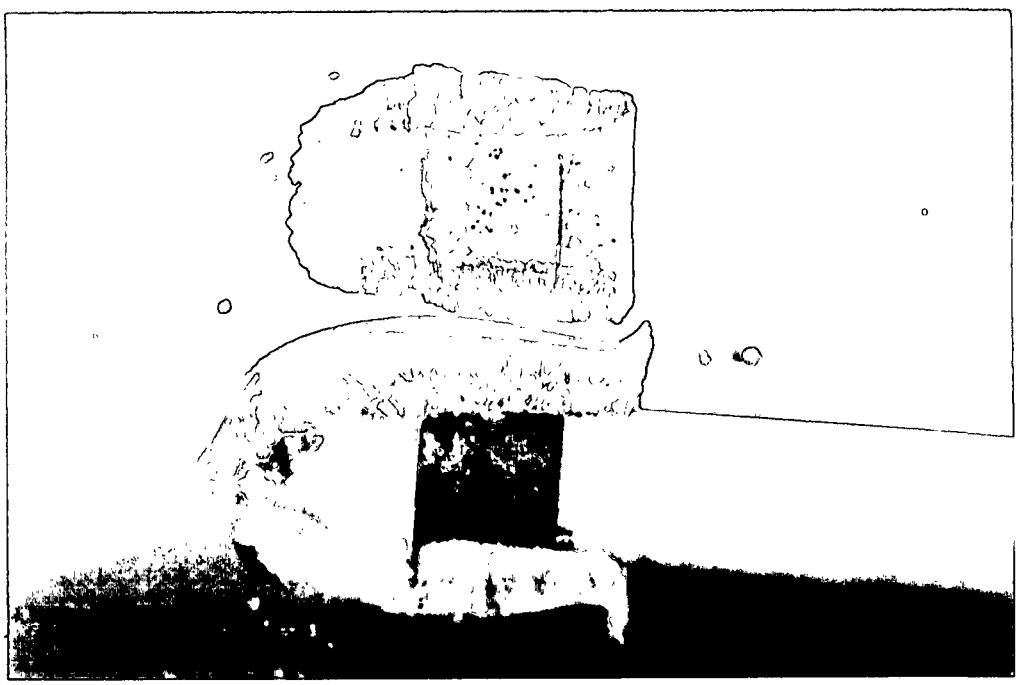

Figure 14. Photograph of surface of corroded coupon and inner surface of the frozen smelt layer, showing the areas where smelt-metal contact had occurred. Notice the one to one correspondence between the dark spots on the smelt and the areas on the metal surface which are not covered with iron sulfide

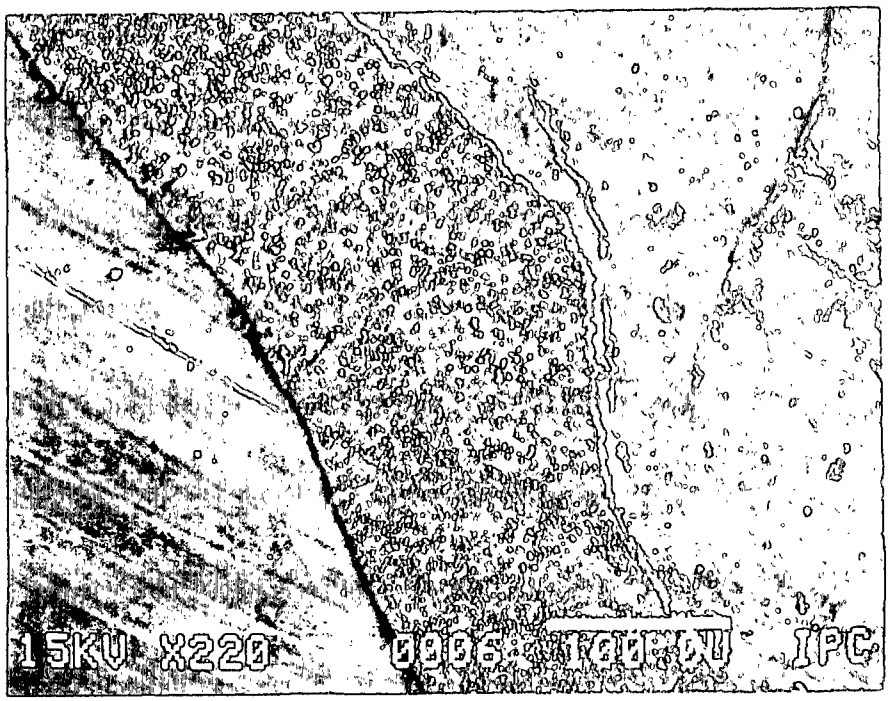

Figure 15. SEM micrograph of the edge of one of the areas where direct contact between the metal and the frozen smelt layer had occurred.

Figure 16. SEM micrograph of the edge of one of the areas where direct contact between the metal and the frozen smelt layer had occurred.

iron sulfide, still attached to the metal surface, running through the center of the picture. In the area on the right, the scratches are less distinct, and the surface appears to be rough. In Fig. 16, the area in the center of the picture was the area in direct contact with the metal. There is some iron sulfide remaining on the surface in the left portion of the figure. The characteristics of the sample in Fig. 16 are quite similar to those in Fig. 15. Both figures indicate that the metal is somewhat more attacked in the areas where smelt-metal contact had occurred.

In summary, the weight loss due to corrosion in the experiments with frozen smelt containing polysulfide was about twice the weight loss due to corrosion in the experiments with frozen smelt without polysulfide. In addition, the corrosion products in the experiments with polysulfide in the smelt were iron sulfides, as opposed to iron oxides in the experiments without polysulfide in the frozen layer. These two facts suggest that the corrosion mechanism occurring with polysulfide added to the frozen smelt involves polysulfide. This mechanism will be discussed later.

POWDERED SMELT TESTS

Powdered smelt tests were performed to provide further information regarding the corrosive sulfur species in the smelt containing polysulfide. The experimental procedure for these experiments was described in the Experimental section. A carbon steel coupon was buried in smelt powder of the same composition as the frozen smelt layer which is initially in contact with the metal in the air-cooled probe tests. The temperature of the metal sample was held at 340°C, which was the temperature of the sample in the probe tests. Nitrogen was purged through the retort during the smelt powder experiments.

The results of these smelt powder experiments are shown in Table 29. The weight losses are an order of magnitude lower than the corresponding weight losses with frozen smelt of the same composition covering the sample.

Table 29. Comparison of Powdered Smelt Tests to Air-cooled Probe Tests

Test	Exposure Time (hr)	Weight Loss (mg/cm^2)
Powder test	24	0.18
Powder test	24	0.28
Probe test	24	2.01
Probe test	24	2.40
Powder test	48	0.14
Powder test	48	0.82
Probe test	48	2.70

DISCUSSION

Corrosive Species

The results of the frozen smelt layer experiments showed that iron sulfide corrosion products were formed on the metal surface when the sample was exposed to a frozen smelt layer containing sulfide, sulfate, carbonate, and polysulfide. When metal was exposed to frozen smelt containing sulfide, sulfate, and carbonate, iron oxide corrosion products were formed. This suggests that the presence of polysulfide sulfur in the frozen smelt led to the formation of iron sulfide corrosion products.

After a very short (15 min) exposure of a coupon to a frozen smelt layer containing polysulfide, the entire metal surface was covered with a layer of iron sulfide. This iron sulfide layer appeared very uniform, with the exception of the areas of direct contact between the frozen smelt and the metal surface, where the corrosion product had been removed from the metal surface during removal of the frozen smelt layer. The formation of a continuous iron sulfide layer over the metal surface implies that sulfur sufficient to form this layer had reached the metal surface, even in areas where there was no direct contact between the smelt layer and the metal.

There are two possible mechanisms of transport of sulfur from the polysulfide in the frozen smelt layer to the reaction site in areas where the smelt did not contact the metal. First, sulfur in the form of polysulfide could diffuse through the frozen smelt to the reaction site at the points of contact between the smelt and the sample, followed by diffusion of sulfur

along the sample surface. The second mechanism by which sulfur might reach the sample surface is dissociation of polysulfide to sulfur vapor and sulfide, with the sulfur vapor attacking the metal:

$$Na_2S_x \Longrightarrow Na_2S + (x-1)\ S \qquad \text{(rxn. 20)}$$

$$S + 2\ e^- \Longrightarrow S^{2-} \qquad \text{(rxn. 21)}$$

Sulfur vapor is corrosive to carbon steel, even at very low partial pressures.[36,37] Both of these mechanisms would be expected to occur to some extent.

An estimate of the surface diffusion coefficient necessary to explain the complete coverage of the sample surface with iron sulfide in less than two hours by a surface diffusion mechanism can be obtained using the following equation:

$$X = (2Dt)^{0.5} \qquad (16)$$

where X = diffusion distance

D = diffusion coefficient

t = time

X is at least one half the distance between adjacent smelt-metal contact points. The average observed distance between contact points is about 2 mm, so X = 0.1 cm. The time to establish complete coverage of the metal sample with a FeS layer, t, is less than 15 min. This leads to an estimated D of 5.6×10^{-6} cm^2/sec needed to explain coverage of the metal surface with iron sulfide in 15 minutes.

The surface diffusion coefficient for sulfur on gold is 1.0×10^{-6} cm^2/sec at 420°C[38], and the surface diffusion coefficient of sulfur on

platinum is 3.0×10^{-7} cm^2/sec at 450°C.[39] A value for the surface diffusion of sulfur on steel was not found. If it is assumed that the sulfur surface diffusion coefficient on iron is within an order of magnitude of the surface diffusion coefficient on gold or platinum, iron surface diffusion could explain the formation of iron sulfide on the entire sample surface.

If surface diffusion were the major contributor of sulfur to the iron sulfide layer, it would be expected that the corrosion product would grow out from the areas of smelt-sample contact. This type of growth pattern would be visible in the surface structure of the iron sulfide layer. The iron sulfide layer was very uniform, and did not show any sign of growing out from the areas of smelt-sample contact, as shown in Fig. 17. This suggests that such a mechanism was not occurring to any significant extent.

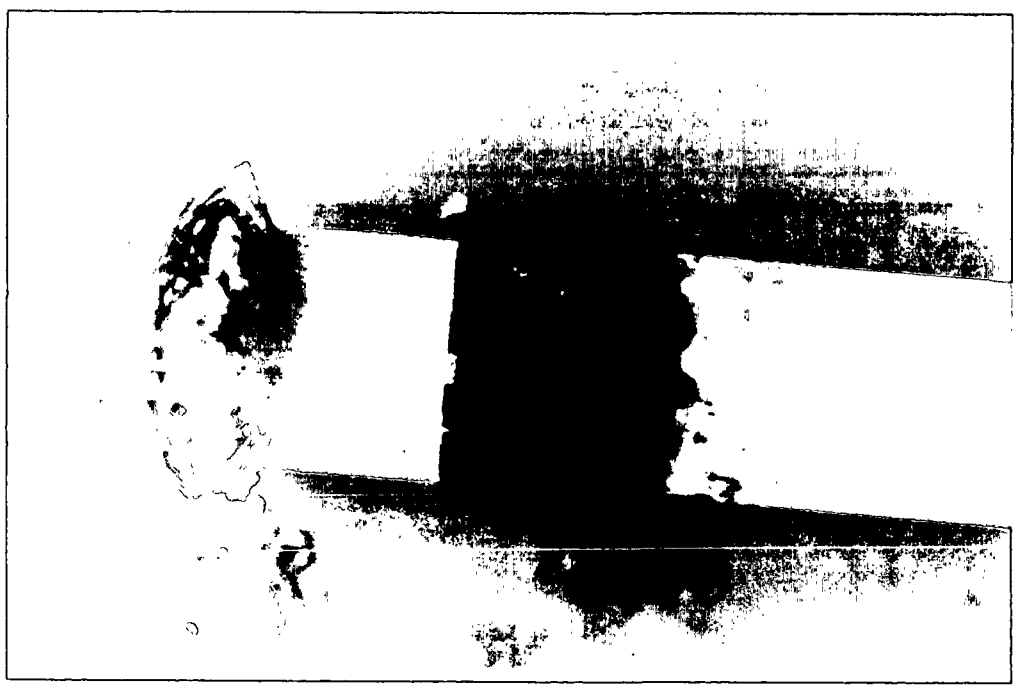

Figure 17. Photograph of the iron sulfide layer covering the metal surface after exposure to frozen smelt containing polysulfide

Although surface diffusion of sulfur might be rapid enough to account for the formation of iron sulfide in areas where there is no direct contact between the smelt and the sample, the appearance of the iron sulfide layer suggests that this was not occurring. Thus, the most likely mode of transport of sulfur to the reaction site is dissociation of polysulfide to form sulfur vapor, followed by vapor phase diffusion of sulfur to the sample surface.

Rate Limiting Step

The corrosion which occurred under a frozen smelt layer containing polysulfide did not proceed at a constant rate, but rather, the rate of corrosion slowed down as the time of exposure to the smelt was extended. The reason for this reduction in the corrosion rate as the exposure time was extended is discussed in this section. Transport of corrosive species within the frozen smelt layer to the reaction site, and transport processes within the corrosion product layer are considered as possible rate limiting steps. The shape of the corrosion curve which would result if diffusion of the corrosive species to the smelt-sample interface limited the corrosion process is compared to the experimental data. In addition, the logarithmic and parabolic laws, which describe corrosion limited by the formation of protective corrosion product layers, are fitted to the experimental data.

The shape of the corrosion curve can be qualitatively described by a mechanism in which the rate limiting step is diffusion of polysulfide to the smelt-sample interface. In the frozen layer experiments, the frozen smelt layer which formed on the air-cooled probe contained polysulfide. The polysulfide sulfur at the smelt-sample interface would be consumed in the

corrosion reaction. In order for the corrosion reaction to continue, more sulfur would have to diffuse to the smelt-sample interface. Thus, initially, the corrosion rate would be fast, since the polysulfide content at the interface would be high. After this polysulfide sulfur was consumed, the reaction would be limited by the rate of diffusion of polysulfide to the reaction site.

In order to determine whether the experimental corrosion rate curve can be described by such a mechanism, the shape of the curve showing the rate of diffusion of polysulfide sulfur to the interface between the frozen smelt and the metal as a function of time was determined. This was done by modeling the diffusion of sulfur from the cylindrical frozen smelt layer to the interface between the sample and the frozen smelt layer. The governing equation is

$$\frac{d[C]}{dt} = D \frac{1}{r} \frac{d}{dr} \left[r \frac{d[C]}{dr} \right] \qquad (17)$$

where:

C = the concentration of polysulfide in the frozen smelt, mg/cm^3

D = diffusion coefficient for polysulfide in frozen smelt, cm^2/sec

r = radial position in the frozen smelt, cm

This differential equation can be solved when an initial condition and two boundary conditions are specified. The initial condition is that the smelt has a uniform polysulfide content throughout its thickness. The first boundary condition is that at all time greater than 0, the polysulfide content at the inner surface of the frozen smelt layer is 0. This assumption is based on the polysulfide sulfur reacting with iron as soon as it reaches the sample

surface. It is important to note that it is assumed that there is no limitation of the reaction due to the corrosion product layer. The second boundary condition is that there is no flux across the interface between the inner and outer layers of the frozen smelt. This may not be entirely correct, but because the time for which the problem is being solved is short, the outer boundary condition has little effect on the solution of the problem.

Equation 17 was solved numerically with the program described in Appendix IV. In order to solve the equation, a value for D and a value for C_0, the initial polysulfide content of the melt, were specified. The computer program then calculated the concentration profile of polysulfide in the smelt at each time, and the total flux of polysulfide sulfur to the sample surface as a function of time. The total flux of polysulfide sulfur to the sample surface was converted to the amount of FeS formed.

The shape of the curve showing the rate of FeS formation which would occur if the limiting step was diffusion of polysulfide to the metal surface did not match the shape of the experimental corrosion rate curve. The experimental curve showed a sharper break in the corrosion rate at an exposure time of 24 hours. In Fig. 18, the experimental corrosion rate data is shown plotted along with the calculated corrosion rates for two different values of D. The curve with $D = 5.0 \times 10^{-7}$ cm^2/sec fits the data reasonably well at shorter times, but predicts much higher corrosion rates than are actually observed at longer times. This value of D was determined by plotting the predicted corrosion rate curve for different values of D vs the experimental data for the first 24 hours of exposure, and finding the value of D which resulted in the lowest sum of squares of the difference between the predicted and experimental data. The curve with $D = 1.0 \times 10^{-7}$ cm^2/sec underpredicts

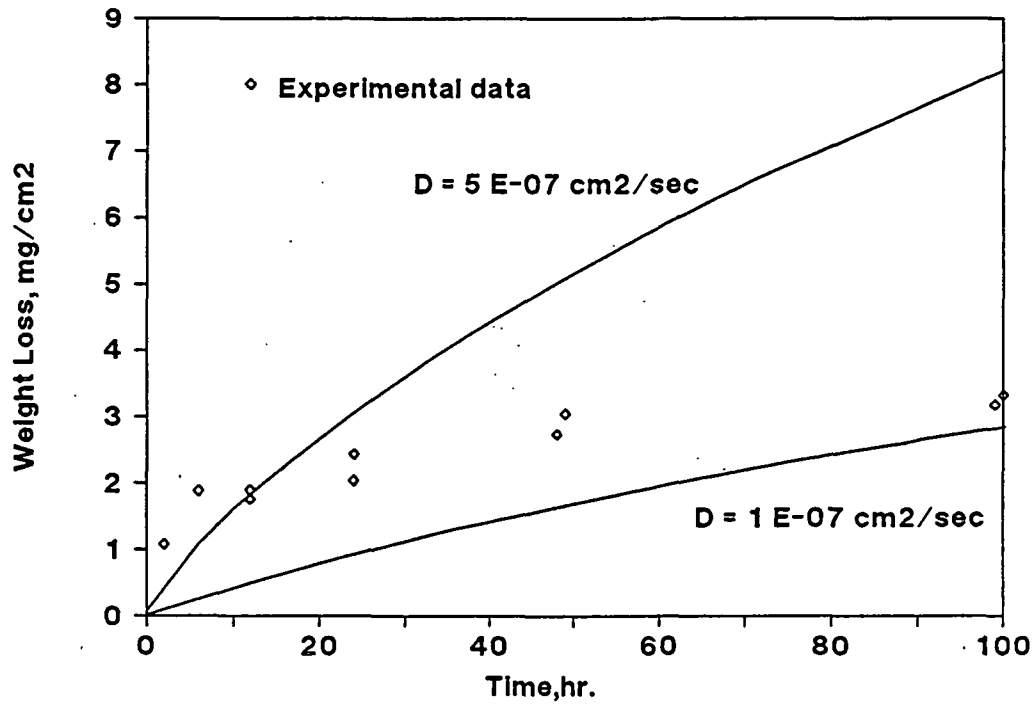

Figure 18. Weight loss which would occur if diffusion from frozen smelt to metal surface was limiting, plotted against experimental corrosion rate data

the corrosion rate at short times, and fits the data fairly well at longer times. The estimated value of D required to explain the initial high rate of iron sulfide formation is 5.0×10^{-7} cm^2/sec.

The results of these calculations suggest that diffusion of polysulfide sulfur to the sample surface could explain the observed corrosion curve, if the diffusion constant of sulfur through the smelt is dependent on the concentration of polysulfide sulfur in the smelt. If the mechanism of polysulfide sulfur diffusion is such that the diffusivity increases as the polysulfide concentration increases, the shape of the observed corrosion rate curve could be explained by a mechanism in which the limiting step is diffusion of polysulfide sulfur to the sample surface. Initially, the

polysulfide content near the smelt-sample interface would be high, and the diffusivity of polysulfide sulfur would be high. As the reaction proceeds, and the polysulfide sulfur concentration near the sample surface decreases, the sulfur diffusivity would decrease.

A corrosion reaction limited by transport processes in the corrosion product layer can be described by either a parabolic rate curve or a logarithmic rate curve. The development of these models was described previously.

The logarithmic model describes a corrosion mechanism where polysulfide sulfur reaches the metal surface by transport through pores, macroscopic holes, or cracks in the FeS layer. Figure 13 showed the cross section of an FeS layer, obtained with the SEM. This layer contained holes which could allow transport of polysulfide sulfur to the metal surface, providing physical evidence that the logarithmic model is applicable to this process.

The corrosion of iron by sulfur vapor has been reported to follow the parabolic rate law, as long as the corrosion product layer is free of cracks.[19,37,40] The limiting step in the corrosion process was the diffusion of iron ions through the iron sulfide layer. The reaction to form FeS occurred at the outer surface of the iron sulfide layer. This suggests that the parabolic law may be applicable to the corrosion under a frozen smelt layer containing polysulfide.

Best fits of the logarithmic and parabolic rate laws to the experimental data were determined by regression analysis, and are shown in Fig. 19 and 20, respectively. The following equations were obtained:

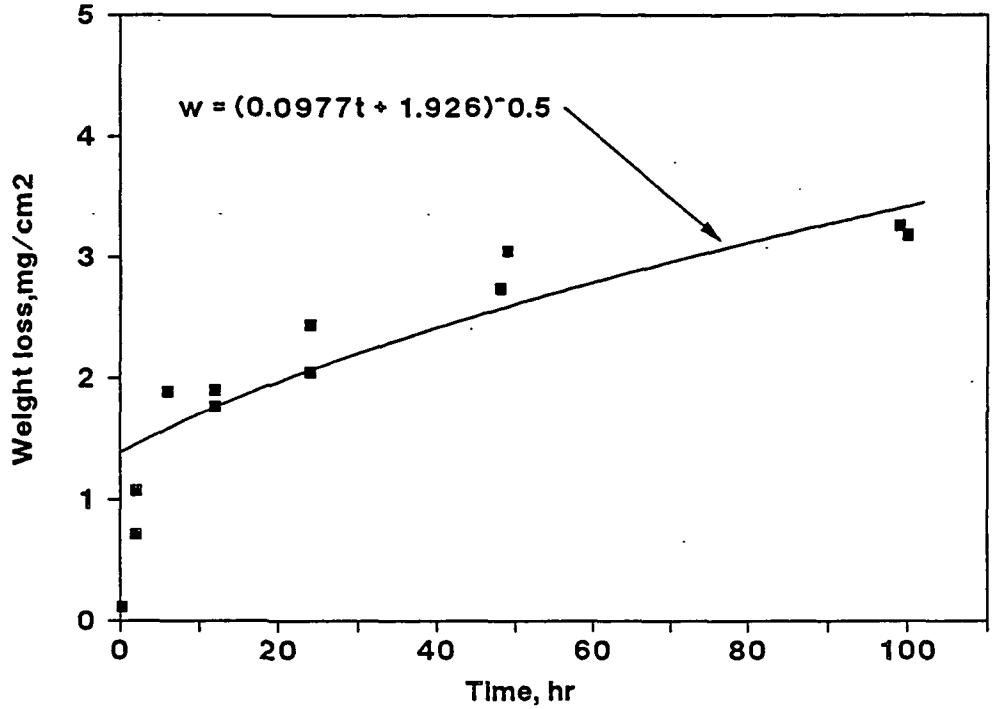

Figure 19. Parabolic Model fitted to the corrosion rate data from exposure to frozen smelt containing polysulfide (Metal Temperature - 340 C)

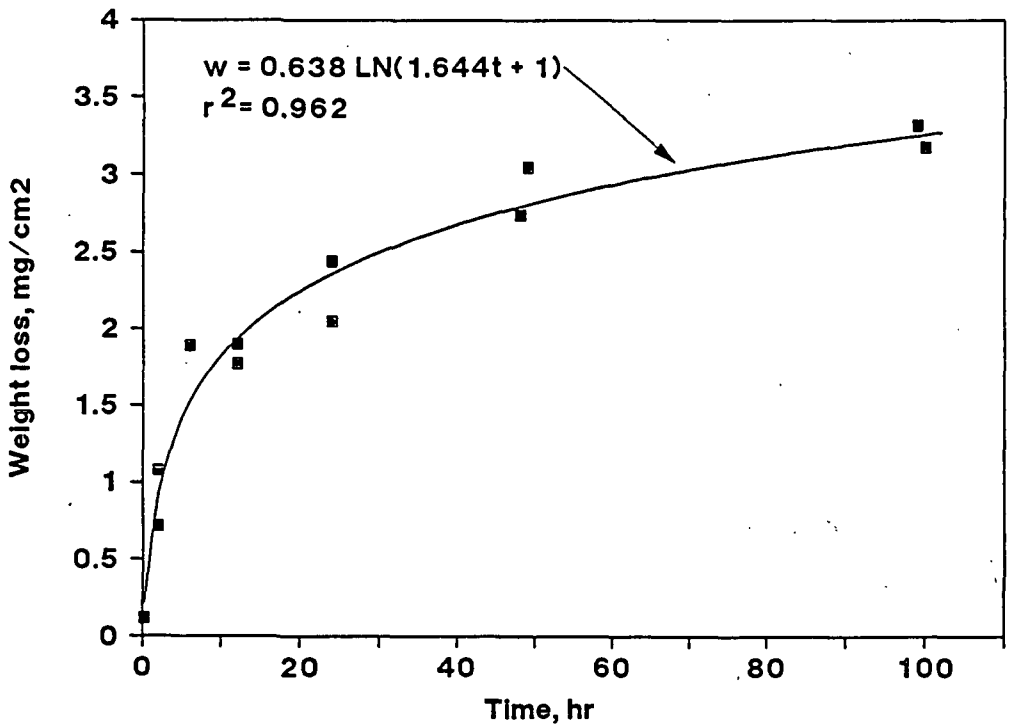

Figure 20. Logarithmic Model fitted to the corrosion rate data from exposure to frozen smelt containing polysulfide (Metal Temperature - 340 C)

Parabolic: $w^2 = 0.0977t + 1.926$ $r^2 = 0.86$ (18)

or

$w = (0.0977t + 1.926)^{0.5}$ (19)

Logarithmic: $w = 0.638 \ln(1.644t + 1)$ $r^2 = 0.96$ (20)

The best fit of the parabolic model to the data does not fit the data points from the short corrosion tests. However, the parabolic law describes the corrosion which occurred after the first two hours of exposure, although not as well as the logarithmic model. A possible explanation for the initial high rate of corrosion is that in the early stage of corrosion, the corrosion product layer did not prevent direct access of the corrosive species to the sample surface, so the corrosion occurred at a much faster rate than if diffusion through the corrosion product layer was required.

Fryt[37] has developed an equation which describes the parabolic rate constant for iron sulfide formation on carbon steel in sulfur vapor as a function of the temperature and sulfur partial pressure. He has experimentally verified this equation over the temperature range of 600-1000°C. Values of the parabolic rate constant calculated using this equation are shown in Table 30.

Table 30. Calculated values of the parabolic corrosion constant for corrosion of carbon steel in sulfur vapor, based on theoretical equation of Fryt[37] (T = 340°C)

Sulfur pressure(atm)	k_p (g^2/cm^4-sec)
10^{-16}	2.2×10^{-10}
10^{-18}	5.5×10^{-11}
10^{-20}	7.3×10^{-12}

The parabolic rate constant calculated from the experimental data is 0.0977 mg^2/cm^4-hr, which converts to 2.7×10^{-11} g^2/cm^4-sec, which is comparable to the rate constant for sulfur vapor corrosion at a sulfur vapor pressure of 10^{-18} atm. Thus, a very small sulfur pressure at the metal surface would account for the observed corrosion.

The logarithmic rate law describes the experimental data very well (Fig 20). The SEM photomicrograph of the structure of the iron sulfide layer (Fig 13), which showed holes and grain boundaries in the iron sulfide, also provides evidence that the logarithmic model is applicable.

These results show that the experimental data are best described by a logarithmic rate law. This suggests that the iron sulfide layer provides protection against continued corrosion by limiting the access of the corrosive species to the metal surface. The rate limiting step in the corrosion process is therefore transport within the iron sulfide layer.

The instantaneous corrosion rate at any time can be obtained by differentiating Equations 19 and 20 with respect to time:

$$\text{Parabolic:} \quad \frac{dw}{dt} = \frac{0.0489}{(0.0977t + 1.926)^{0.5}} \qquad (21)$$

$$\text{Logarithmic:} \quad \frac{dw}{dt} = \frac{1.05}{1.644t + 1} \qquad (22)$$

Using Equations 21 and 22, the instantaneous rate of corrosion at any time can be determined. If Equations 21 and 22 are extrapolated to times greater than 100 hours, corrosion rates after long exposure times can be

estimated. A table of estimated corrosion rates is shown in Table 31.

Table 31. Long term instantaneous corrosion rates extrapolated from parabolic and logarithmic rate laws for corrosion of carbon steel by frozen smelt containing sulfide, sulfate, carbonate, and polysulfide at 340°C.

Time (days)	Instantaneous Corrosion Rate (mm/yr) Parabolic	Logarithmic
30	0.063	0.010
90	0.036	0.003
180	0.026	0.002

From Table 31, it can be seen that the iron sulfide layer formed in these experiments provided as much protection against continued corrosion as the iron oxides which were formed in the exposures to smelt which did not contain polysulfide (Table 23). If the iron sulfide layer remained on the metal surface during long exposures, the corrosion rate is predicted to be less than 0.1 mm/yr by either the parabolic or the logarithmic model.

Smelt Powder Tests

Carbon steel coupons were exposed to smelt powder containing polysulfide, as described previously. These tests were originally intended to provide further information about the nature of the corrosive species in frozen smelt containing polysulfide. However, the results instead suggest that smelt powder experiments, which have been commonly performed in previous studies, may not accurately predict the corrosiveness of smelt components under recovery boiler conditions.

The results of the smelt powder experiments were shown in Table 29. The rate of corrosion observed in these experiments was an order of magnitude lower than the rate of corrosion in the frozen layer tests.

Similar tests were performed by Plumley et al.[4] In their experiments, carbon steel coupons were buried in polysulfide powder, and placed in a nitrogen atmosphere at 370°C. Plumley et al.[4] observed a corrosion rate of 0.22 mm/yr, which is very similar to the rate of corrosion observed in these experiments, 0.03-0.19 mm/yr at 340°C.

These results show that the corrosion of carbon steel due to smelt powder containing polysulfide at 340-370°C was an order of magnitude lower than the corrosion which occurred in the frozen smelt layer experiments. This result is consistent with previous experimental results discussed in the Literature Review section. In general, smelt powder tests result in corrosion rates an order of magnitude lower than frozen smelt layer experiments performed with the same smelt composition.

The principal difference between the two test methods is the initial exposure to molten smelt which occurs in the frozen smelt layer experiments. The corrosion coupons, which have been prepared in air, are covered with a thin oxide layer. When the coupon is exposed to the molten smelt, the molten smelt attacks this oxide layer, so that the frozen smelt layer contacts a bare metal surface. In the smelt powder experiments, the oxide layer is never removed, and it limits the corrosive attack by the smelt powder.

These experimental results suggest that smelt powder experiments, which have been commonly performed in previous studies, do not accurately

predict the corrosiveness of smelt components under recovery boiler conditions.

SUMMARY

The corrosion of carbon steel exposed to a frozen smelt layer containing sulfide, sulfate, and carbonate resulted in the formation of iron oxide corrosion products which were adherent to the metal surface and provided good protection against continued corrosion. The corrosion rate curve can be described by either a parabolic or a logarithmic corrosion rate model. The long term rate of corrosion predicted by either model was an order of magnitude lower than the accelerated corrosion rates seen in recovery boilers.

The corrosion of carbon steel by a frozen smelt layer containing polysulfide resulted in the formation of iron sulfide corrosion products. The corrosive species appeared to be sulfur vapor formed by the dissociation of polysulfide ions. The corrosion rate was initially high, but after approximately 12 hours of exposure, the rate of corrosion began to decrease. The corrosion rate curve can be described by a logarithmic corrosion rate model, which describes corrosion limited by the transport of the corrosive species through pores or flaws in a protective corrosion product film. Thus, the iron sulfide corrosion product layer was protective against continued corrosion, and the limiting step in the corrosion process was transport of sulfur through the iron sulfide layer to the metal surface. The long term rate of corrosion predicted by the model was an order of magnitude lower than recovery boiler corrosion rates.

Carbon steel coupons buried in smelt powder containing polysulfide were corroded at a rate an order of magnitude lower than coupons covered with a frozen smelt layer of the same composition. This suggested that smelt powder experiments do not accurately predict the corrosiveness of frozen smelt layer components under recovery boiler conditions.

IMPLICATIONS

The long term corrosion rate predicted by extrapolation of the logarithmic corrosion rate model for corrosion due to a frozen smelt layer containing polysulfide is less than 0.1 mm/yr, much less than the corrosion rates which are considered a problem in the lower furnace of recovery boilers. In the experimental system, the limitation on the corrosion reaction was access of the corrosive sulfur to the reaction site. The most likely limiting step was transport of sulfur through the iron sulfide layer which forms on the metal surface. Another possible limiting step was diffusion of sulfur from the frozen smelt to the reaction site.

There is evidence in the literature that the frozen smelt layer covering the waterwall tubes in recovery boilers will occasionally fall off and reform.[13-15] If this were to occur, it might significantly affect the rate of corrosion. If the corrosion product layer is protective, and is removed from the metal surface when the frozen smelt layer falls off, the metal would be exposed directly to the new frozen smelt layer, and the rate of corrosion would be high until the protective corrosion product layer was reestablished. If diffusion in the frozen smelt layer is limiting, removal and reformation of the frozen smelt layer would result in replenishment of sulfur at the interface between the smelt and the tube, leading to renewed corrosion.

The corrosion rate during the first 12 hours of exposure of carbon steel boiler tube material to a frozen smelt layer containing 0.5-1.0% polysulfide is about 1.6 mm/yr, but the rate of corrosion drops to 0.14 mm/yr after 48 hours of exposure, and to 0.07 mm/yr after 100 hours. The initial

rate of corrosion is similar to the corrosion rates considered to be dangerous in recovery boilers. This suggests that if the frozen smelt layer was to fall off occasionally, high corrosion rates could be sustained. For example, if the iron sulfide layer was removed every 12 hours, the corrosion rate could be sustained at about 1.6 mm/yr.

In the experiments, the iron sulfide layer which formed beneath a frozen smelt layer containing polysulfide was not very adherent to the metal surface. After each test, the frozen smelt layer had to be removed gently, or large pieces of iron sulfide flaked off. Thus, it seems likely that if the frozen smelt layer was to fall off of waterwall tubes covered with iron sulfide, at least a portion of the iron sulfide layer would be removed.

If the corrosion product is protective, two conditions must be met in order for accelerated corrosion to occur. The first is that gas-smelt interactions resulting in the formation of polysulfide must occur, so that the frozen smelt layer which forms on the metal surface contains polysulfide. The second is that the corrosion product layer must be removed from the tube surface, by the mechanical action of the frozen smelt layer falling off.

In the tests with smelt which did not contain polysulfide, iron oxides were formed as the corrosion products. The iron oxide layer which formed beneath the frozen smelt layer was very adherent to the metal surface. It required scraping with a spatula to remove it from the metal surface. This implies that in the areas of the boiler where the frozen smelt layer does not contain polysulfide, the corrosion products would be iron oxides. It also suggests that in the recovery furnace the removal of the frozen smelt layer from the waterwalls probably would not remove the iron oxide layer. However, if the iron oxide layer was removed every 12 hours, the rate of corrosion

could be 0.4 mm/yr, which is a significant corrosion rate.

In summary, the experimental results show that the exposure of carbon steel directly to a frozen smelt containing polysulfide caused rapid corrosion, with the formation of iron sulfide corrosion products. The iron sulfide corrosion products may provide some protection against continued corrosion. However, the iron sulfide corrosion products were not adherent to the metal surface, and it seems likely that in the recovery boiler, removal of the frozen smelt layer would result in the removal of the protective iron sulfide layer, exposing the metal directly to the newly formed frozen smelt layer, and leading to renewed high rates of corrosion.

This discussion suggests several areas for future research. First, it seems that the frequency at which the frozen smelt falls off the waterwalls and reforms may have a significant effect on the rate of waterwall tube corrosion. The frequency of this occurrence should be studied. The second area which should be studied is the effect of removal of the frozen smelt from the waterwalls on the corrosion product layer. The effect on both iron sulfide and iron oxide corrosion product layers should be studied.

CONCLUSIONS

The conclusions of this work are:

1. An experimental apparatus was constructed for studying the corrosion which occurs beneath a layer of frozen smelt under heat transfer conditions. The apparatus consisted of an air-cooled probe which was exposed to a molten smelt pool, forming a frozen smelt layer on the metal sample. The probe provided a good simulation of recovery furnace waterwall tube conditions. The heat flux through the probe was representative of recovery furnace waterwall heat fluxes, and the metal temperature was maintained at 320-350°C, which is at the high end of the range of waterwall tube temperatures. The probe was capable of maintaining a very stable corrosion sample temperature throughout a 100 hour exposure to the smelt. Metal temperatures as low as 320°C were obtained. Reproducible corrosion rate data were obtained.

2. The exposure of carbon steel to frozen smelt containing sulfide, sulfate, carbonate, and a small amount of sulfite resulted in the formation of iron oxide corrosion products. The corrosion data were described equally well by a logarithmic corrosion rate model and by a parabolic corrosion rate model. The limiting step in the corrosion reaction for each of these models is transport within the corrosion product layer. Thus, the iron oxide which formed between the metal and the frozen smelt layer protected the metal against continued corrosion. The long term corrosion rate extrapolated from this data was <0.1 mm/yr when the metal temperature was 320-350°C, which is well below accelerated recovery boiler corrosion rates of 0.5-1.5 mm/yr.

3. When the frozen smelt layer contained 0.5-1.0% polysulfide, iron sulfide corrosion product ($Fe_{1-x}S$) was formed on carbon steel. The polysulfide in the smelt caused sulfidation corrosion. With a metal temperature of 330-350°C, the corrosion rate in the first 12 hours of exposure to smelt containing polysulfide was three times the initial corrosion rate which occurred with smelt which did not contain polysulfide. The long term corrosion rate was about the same as for exposure to smelt without polysulfide, less than 0.1 mm/yr.

4. The corrosion rate data for smelt containing polysulfide can be described by two different models. The logarithmic corrosion rate model, which describes corrosion limited by a protective corrosion product layer, fits the experimental corrosion rate curve. The corrosion rate curve can also be described by a model in which diffusion of sulfur from the frozen smelt to the sample surface is the limiting step.

Thus, the reaction of smelt containing polysulfide with carbon steel to form $Fe_{1-x}S$ is limited by transport of sulfur to the reaction site. In the experimental system, this limitation could have been in either the frozen smelt layer or in the iron sulfide layer.

5. The corrosion rate during the first 12 hours of exposure to frozen smelt containing polysulfide was 1.6 mm/yr. Thus, the corrosion of recovery boiler waterwall tubes by frozen smelt could occur at a rate approaching 1.6 mm/yr if the frozen smelt layer contained polysulfide, and if the corrosion limitation was occasionally removed.

If the limiting step in the corrosion reaction is transport of sulfur through the iron sulfide layer, then repeated removal of this protective layer

by the mechanical action of the frozen smelt layer falling off of the tube would result in high corrosion rates.

If the limiting step in the corrosion process is transport of polysulfide sulfur from the frozen smelt to the metal surface, the repeated removal and reformation of the frozen smelt layer would result in replenishment of the polysulfide at the tube surface, and would lead to high corrosion rates.

Therefore, the frequency with which the frozen smelt falls off the waterwalls could be a significant factor affecting waterwall tube corrosion, and should be studied. The effect of the removal of the frozen smelt layer from the waterwalls on the corrosion product layer should also be studied.

LITERATURE CITED

1. Bowers, D.F. Current status of tube performance in recovery boilers for the pulp and paper industry. 1985 International Recovery Conference, :103-113 (1985).

2. Blackwell, B.; King, T. Chemical Reactions in Kraft Recovery Boilers. Sandwell and Company Ltd., Vancouver, B.C., 1985:8-28.

3. Stelling, O; Vegeby, A. Corrosion on tubes in black liquor recovery boilers. Pulp and Paper Magazine of Canada 70(8):51-77 (1969)

4. Plumley, A.L.; Lewis, E.C.; Tallent, R.G. External corrosion of waterwall tubes in kraft recovery furnaces. TAPPI 49(1):72A-81A (1966)

5. Borg, A.; Teder, A.; Warnqvist, B. Inside a kraft recovery furnace - studies on the origins of sulfur and sodium emission. TAPPI 57(1):126-129 (1974)

6. Andersson, S. Chemica Scripta 20(4):164-170 (1982)

7. Shivgulam, N.; Barham, D.; Rapson, H. Pulp and Paper Canada 80(9):89-92 (1979)

8. Plumley, A.L.; Roczniak, W.R. Recovery unit waterwall protection, a status report. TAPPI 58(9):118-121 (1975)

9. Moberg, O. Recovery Boiler Corrosion. NACE Pulp and Paper Industry Corrosion Problems - Volume 1, :125-136 (1974)

10. Dahl, L; Falk, I. Investigation of Alloyed Steels for use in Black Liquor Recovery Boilers - Report 3, Swedish Corrosion Institute, Stockholm, Sweden (1972)

11. Poturaj, S. The corrosion behavior of some types of steel in stagnant and flowing kraft smelts at 757°C. 1986 TAPPI Engineering Conference, :387-390 (1986)

12. Singbeil, D.; Garner, A. Test Methods for the Evaluation of Fireside Corrosion in Kraft Recovery Boilers, Report to the American Paper Institute (1988)

13. Tallent, R.G.; Plumley, A.L. Recent research on external corrosion of waterwall tubes in kraft recovery furnaces. TAPPI 52(10):1955-1959 (1969)

14. Moskal, M.D. Corrosion of high pressure kraft recovery boilers. 1988 TAPPI Kraft Recovery Operations Seminar,:285-291 (1988)

15. Pollak, P.; Oesterholm, R. Corrosion resistant, safe and economical composite tubes for black liquor recovery boilers. NACE Pulp and Paper Industry Corrosion Problems - Volume 2, :147-150 (1977)

16. Dahl, L.; Falk, I. Investigation of Alloyed Steels for use Black Liquor Recovery Boilers - Report 1, Swedish Corrosion Institute, Stockholm, Sweden (1971)

17. Dahl, L.; Falk, I. Investigation of Alloyed Steels for use Black Liquor Recovery Boilers - Report 2, Swedish Corrosion Institute, Stockholm, Sweden (1971)

18. Dahl, L.; Falk, I. Investigation of Alloyed Steels for use Black Liquor Recovery Boilers - Report 4, Swedish Corrosion Institute, Stockholm, Sweden (1972)

19. Fryt, E.M.; Smeltzer, W.W.; Kirkaldy, J.S. Chemical diffusion and point defect properties of iron sulfide ($Fe_{1-x}S$) at temperatures 600°-1000°C. Journal of the Electrochemical Society 126(4):673-683 (1979)

20. Conditt, F.H.; Hobbins, R.R.; Birchenall, C.E. Self-diffusion of iron and sulfur in ferrous sulfide. Oxidation of Metals 8(6):409-455 (1974)

21. Ahlers, P.E. Investigation of Alloyed Steels for use Black Liquor Recovery Boilers - Report 1, Swedish Corrosion Institute, Stockholm, Sweden (1971)

22. Ahlers, P.E. Recovery Boiler Fireside Corrosion, Project 3628 Status Report to the Engineering PAC, The Institute of Paper Chemistry (1989)

23. Rosen, E.; Tegman, R. A Preparative and X-ray Powder Diffraction Study of the Polysulfides Na_2S_2, Na_2S_4, and Na_2S_5. Acta Chemica Scandinavica 25(9):3329-3336 (1971)

24. Grace, T.M.; Cameron, J.H.; Clay, D.T. Char Burning. Summary Technical Report to the American Paper Institute Recovery Boiler Committee, prepared by the Institute of Paper Chemistry, Appleton, WI (Feb. 22, 1985)

25. Kaibara, T.; Yoshii, T.; Hayashi, T. On Smelt Corrosion Resisting Overlay-Weld for Furnace Tubes of Recovery Boilers. Proceedings of the 1st Symposium of Recovery of Pulping Chemicals :505-521 (1968)

26. Kubelka, V.; Votoupal, J. Chemical Recovery in kraft pulp mills. The Chemistry of the recovery process and the design of the recovery unit. Sbornik Vyzkum. Praci z Oboru Celulozy a Papiru 2:49-73 (1957)

27. Crowe, D.C. Recovery Boiler Fireside Corrosion, Project 3628. Status Report to the Engineering Project Advisory Committee, The Institute of Paper Chemistry. (March 29, 1988)

28. Tran, H.N.; Reeve, D.W.; Barham, D. Local Reducing Atmosphere - A Significant Cause of Superheater Corrosion in Kraft Recovery Units. 1984 TAPPI Engineering Conference Proceedings. :73-7 (1984)

29. Backman, R., Hupa, M., Uppstu, E. Fouling Mechanisms in Recovery Boiler Superheater Area. 5th International Symposium on Corrosion Problems in the Pulp and Paper Industry, :243-249 (1986)

30. Bennett, C.O.; Myers, J.E. Momentum, Heat, and Mass Transfer, 2nd ed., McGraw-Hill Book Co. (1974)

31. Perry, R.H.; Chilton, C.H. Chemical Engineers' Handbook, 5th ed. McGraw-Hill Book Company (1973)

32. Borchardt, L.G.; Easty, D.B. Gas chromatographic determination of elemental and polysulfide sulfur in kraft pulping liquors. Journal of Chromatography 299:471-476 (1984)

33. Kofstad, P. High Temperature Corrosion. Elsevier Applied Science (1988)

34. Evans, U.R. The Corrosion and Oxidation of Metals. Edward Arnold Publishers (1960).

35. Uhlig, H.H.; Revie, R.W. Corrosion and Corrosion Control, 3rd ed. John Wiley and Sons (1985).

36. Cleaver, B.; Davies, A.J. Properties of Fused Polysulfides - III. Electrochemica Acta 18(10):733-739 (1973)

37. Fryt, E.M.; Bhide, V.S.; Smeltzer, W.W.; Kirkaldy, J.S. Growth of the iron sulfide ($Fe_{1-x}S$) scale on iron at temperatures 600°-1000°C. Journal of the Electrochemical Society 126(4):683-688 (1979)

38. Narisawa, T. Kotai Butsuri 7(1):49-55 (1972) CA 78:151709

39. Bronzel, H.P., Ku, R., J. Chem. Phys. 59(4):1641-51 (1973) CA 79:129622

40. Foroulis, Z.A. Kinetics and mechanism of the reaction of iron with sulfur vapor in the temperature range of 250-500°C. Werkstoffe und Korrosion 29:385-393 (1978)

NOMENCLATURE

a = constant in logarithmic rate law, hr^{-1}

A = area, cm^2

C = constant of integration

[C] = polysulfide concentration, mg/cm^3

C_p = heat capacity, J/kg-K

d = diameter, m

D = diffusion coefficient, cm^2/sec

h = convective heat transfer coefficient, W/m^2-K

h_m = average convective heat transfer coefficient, W/m^2-K

k = thermal conductivity, W/m-K

K = constant in Equation 2

k_l = constant in logarithmic rate law, mg/cm^2

k_p = constant in parabolic rate law, mg/cm^2

L = length, m

Q = heat, W

r = radius, cm

t = time, hr

T = temperature, °C

T_a = average air temperature, °C

T_m = metal temperature, °C

u = gas velocity, m/sec

w = weight loss, mg/cm^2

x = length, m

X = diffusion distance, cm

y = corrosion product layer thickness, cm

Greek

μ = viscosity, kg/m-sec

π = density, kg/m^3

APPENDIX I

SAMPLE CALCULATIONS FOR EXPERIMENTAL DESIGN

In the Experimental section, several calculations were performed in describing the design of the air-cooled probe. Samples of these calculations are described here.

The 'calculated heat flux' was determined by multiplying the predicted convective heat transfer coefficient by the measured difference between the temperature of the metal sample and the average temperature of the air:

$$Q/A = h_m (T_m - T_a) \qquad (4)$$

The value of the convective heat transfer coefficient was predicted using the Dittus-Boelter equation, modified to account for entrance effects:

$$h_m = 0.023 \frac{u^{0.8}}{d^{0.2}} \frac{\rho^{0.8} C_p^{0.4} k^{0.6}}{\mu^{0.4}} (1 + Kd/L) \qquad (3)$$

where:

h_m = average convective heat transfer coefficient, W/m^2-K

u = gas velocity, m/sec

ρ = gas density, kg/m^3

C_p = gas heat capacity, J/kg-K

k = gas thermal conductivity, W/m-K

K = constant, with a value of 7 for a 90° turn entering the annulus

d = difference between inner and outer diameter of annulus, m

L = length of annulus, m

μ = gas viscosity, kg/m-sec

A sample calculation will be carried out with the data from Experiment 41. The following data are from Experiment 41:

Metal temperature - 330°C

Temperature of air into annulus - 93°C

Temperature of air out of annulus - 140°C

Air flow rate - 207 slpm

The average air temperature is the average between 93°C and 140°C, which is approximately 120°C. The air properties at the average air temperature are needed to compute the convective heat transfer coefficient:

$T = 120°C$

$\rho = 0.897$ kg/m^3

$C_p = 1005$ J/kg-K

$k = 0.0327$ W/m-K

$\mu = 2.2 \times 10^{-5}$ kg/m-sec

Substituting these values into Eq. 2 results in:

$$h_m = 3.14 \frac{u^{0.8}}{d^{0.2}} (1 + 7d/L) \qquad (6)$$

The air velocity, u, is calculated from the air flow rate and the cross sectional area across which the air flows in the annulus. Since the air flow rate is measured as standard cubic feet per minute, the actual volumetric flow rate must be determined, since the air is at 120°C, and not 25°C. This is accomplished by multiplying the flow rate by the density of air at 25°C,

and dividing by the density of air at 120°C. So u is calculated as follows:

$$u = x \text{ slpm} \frac{\rho(25°C)}{\rho(120°C)} \frac{1}{CSA}$$

$$u = 207 \text{ slpm} \frac{1.185 \text{ kg/m}^3}{0.897 \text{ kg/m}^3} \frac{1}{4.35 \times 10^{-5} \text{ m}^2} \frac{10^{-3} \text{ m}^3}{1} \frac{\text{min}}{60 \text{ sec}}$$

$$u = 104.8 \text{ m/sec}$$

The convective heat transfer coefficient is then calculated using Eq. 3:

$$h_m = 3.14 \frac{(104.8 \text{ m/sec})^{0.8}}{(0.00152 \text{ m})^{0.2}} \{1 + 7(0.00152 \text{ m}/0.0253 \text{ m})\}$$

$$h_m = 675 \text{ W/m}^2\text{-K}$$

The heat flux is then calculated from this heat transfer coefficient and th temperature, according to Eq. 1:

$$Q/A = (675 \text{ W/m}^2\text{-K}) \ (329°C - 117°C)$$

$$Q/A = 143.1 \text{ kW/m}^2$$

The measured heat flux is computed from the temperature rise of the air as it passes through the annulus, according to:

$$Q/A = M C_p \Delta T / A \qquad (23)$$

where:

M = mass flow rate of air, kg/sec

C_p = heat capacity of air, J/kg-K

Δ T = air temperature rise through the probe, °C

A = area across which heat is transferred in probe, m^2

The mass flow rate of the air is calculated from the volumetric flow rate by multiplying by the density of air at STP.

$$Q/A = (x \text{ slpm}) \ (\rho \text{ kg/m}^3 (@25^\circ C)) \ (60 \text{ min/hr}) \ C_p \Delta T \ / \ A \text{ ft}^2$$

$$Q/A = (207 \text{ slpm}) (1.185 \text{ kg/m}^3) \ (1005 \text{ J/kg-K}) \ (\text{min}/60 \text{ sec}) \ x$$
$$(140^\circ C - 93^\circ C) \ (10^{-3} \text{ m}^3/\text{l}) \ / \ 0.00151 \text{ m}^2$$

$$Q/A = 128.3 \text{ Kw/m}^2$$

APPENDIX II

SMELT ANALYSIS PROCEDURES

Smelt samples were ground in a nitrogen glove bag to obtain a smelt powder. When the smelt was a sample taken from molten smelt, the sample was broken open, and a portion from the inside of the sample was used. When frozen smelt layers were analyzed, the entire cross section of the sample was used, unless otherwise specified. The smelt powders were analyzed by the Institute of Paper Science and Technology analytical department for Na_2S, Na_2SO_4, Na_2SO_3, $Na_2S_2O_3$, and polysulfide sulfur. The procedures used in these analyses are discussed below.

SULFATE, SULFITE, THIOSULFATE

These ions were determined using ion chromatography, according to TAPPI Test Method T699 cm-87. 200 mg of the smelt powder was dissolved in 100 ml. of deoxygenated water, and then analyzed like green liquor.

The repeatability of these procedures for liquor analysis was reported in the procedure as a percentage of the mean value. The repeatability of the procedure for smelt was not reported. The repeatability values were:

Sulfate:	10-12%
Sulfite:	25-30%
Thiosulfate:	7-16%

If it is assumed that the repeatability values for the analysis of smelt are similar, the reported sulfate contents are ±2% sulfate, and

the reported sulfite contents are ±1% sulfite. Thiosulfate was not detected in the smelts.

POLYSULFIDE

Polysulfide was determined using a gas chromatographic method[32]. In this method, the polysulfide is decomposed to elemental sulfur in buffer at pH 5.5, and the elemental sulfur reacts with triphenylphosphine to form triphenylphosphine sulfide, which is determined by flame ionization gas chromatography.

The procedure described by Easty and Borchardt[32] was followed. It was modified slightly, since smelt was being analyzed. 5-10 mg smelt powder was placed directly in the reaction vessel containing 40 ml buffer and 10.0 ml toluene containing anthracene. The mixture was purged with nitrogen for a few seconds, and the reaction vessel sealed. Triphenylphosphine was then injected into the vessel. The remainder of the procedure was performed as described[32].

The repeatability of this procedure was not reported in the procedure. Duplicate analyses of the same sample differed by as much as 0.3%. The reported polysulfide contents are about ±0.2% polysulfide.

SULFIDE

The procedure used for determination of sulfide was a potentiometric titration with mercuric chloride. The procedure is described in either TAPPI

Test Method T-694 pm-82 or in the NCASI Atmospheric Quality Improvement Technical Bulletin No. 68, Oct, 1973.

This procedure is for analysis of liquor, so the procedure was modified slightly to analyze smelt. A sample of smelt powder, 0.2-0.3 g was weighed quantitatively, and dissolved in deoxygenated water. The dissolved smelt was then analyzed as a liquor. Duplicate analyses of the same sample differed by no more than 0.5% sulfide. However, since oxidation of the smelt may occur during the sample preparation, the range of variation on the reported sulfide contents may be ±1.0% sulfide.

APPENDIX III

X-RAY DIFFRACTION PATTERNS OF CORROSION PRODUCTS

X-ray diffraction patterns for two iron oxides, magnetite (Fe_3O_4) and hematite (Fe_2O_3) are shown on the first page. On the next page, x-ray diffraction patterns for two iron sulfides, pyrrhotite ($Fe_{1-x}S$) and pyrite (FeS_2) are shown. Then the x-ray diffraction patterns for corrosion products obtained in the experiments are shown.

Experiment 40 was a 94 hour exposure to a sulfide/sulfate/carbonate smelt. The corrosion product is iron oxide.

The rest of the diffraction patterns are for corrosion products formed during exposure to frozen smelt containing polysulfide. The length of each exposure is shown below:

Experiment	Exposure time (hr)
49	2
50	12
60	48
62	49
63	100

The corrosion product from each of these experiments is pyrrhotite.

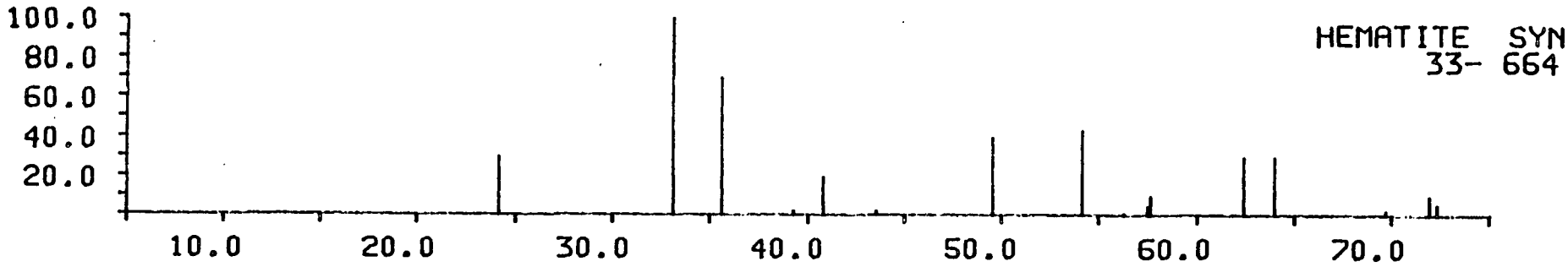
100.0
80.0
60.0
40.0
20.0
10.0
20.0
30.0
40.0
50.0
60.0
70.0
HEMATITE SYN
33- 664

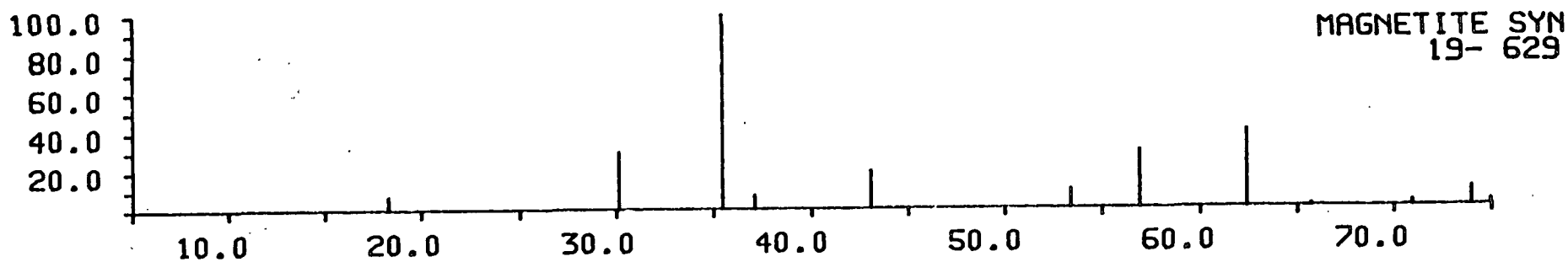
100.0
80.0
60.0
40.0
20.0
10.0
20.0
30.0
40.0
50.0
60.0
70.0
MAGNETITE SYN
19- 629

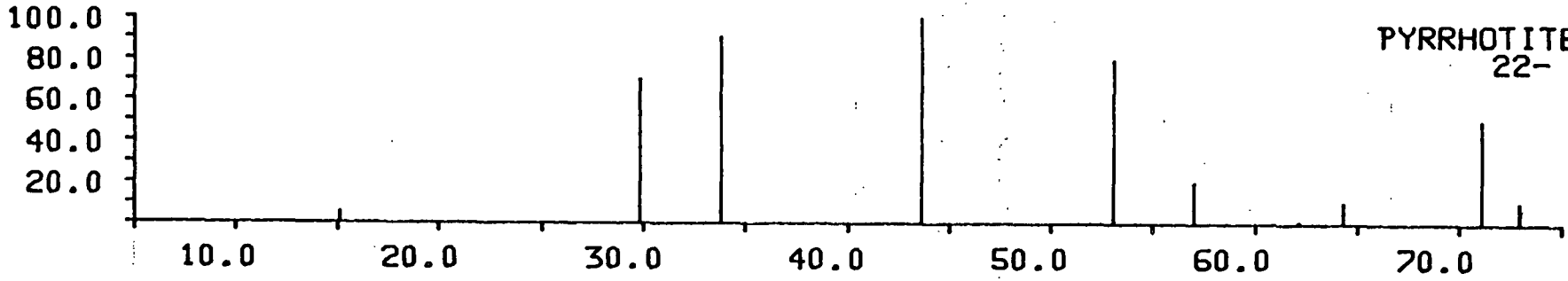
100.0
80.0
60.0
40.0
20.0
10.0
20.0
30.0
40.0
50.0
60.0
70.0
PYRRHOTITE 5C
22- 358

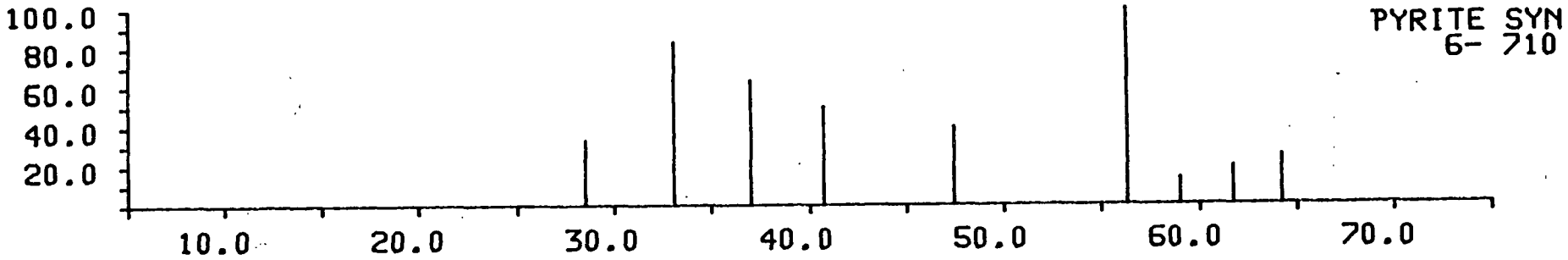
100.0
80.0
60.0
40.0
20.0
10.0
20.0
30.0
40.0
50.0
60.0
70.0
PYRITE SYN
6- 710

Experiment 40: 94 hour exposure to frozen smelt containing sulfide, sulfate, and carbonate

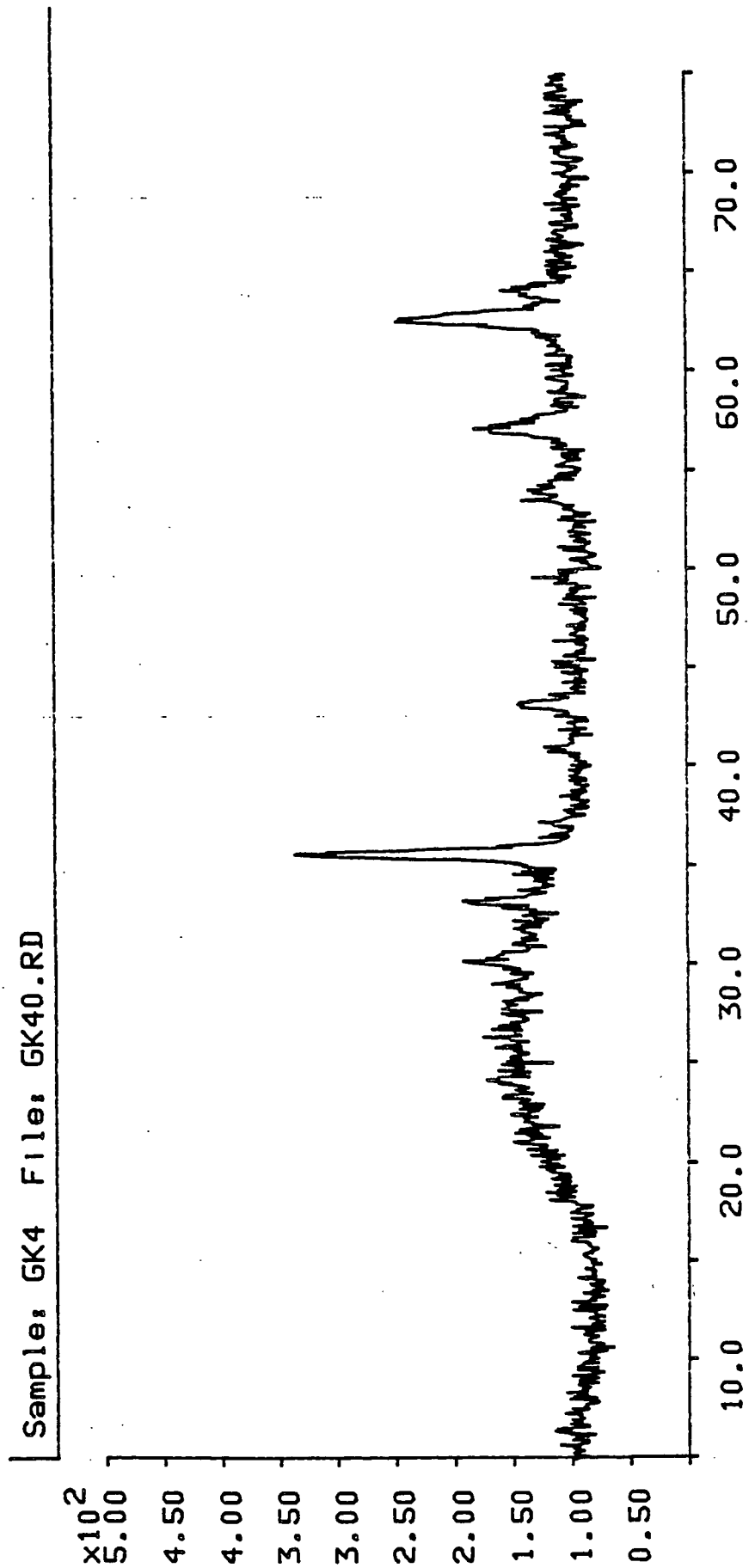

Experiment 49: 2 hour exposure to frozen smelt containing sulfide, sulfate, carbonate, and polysulfide

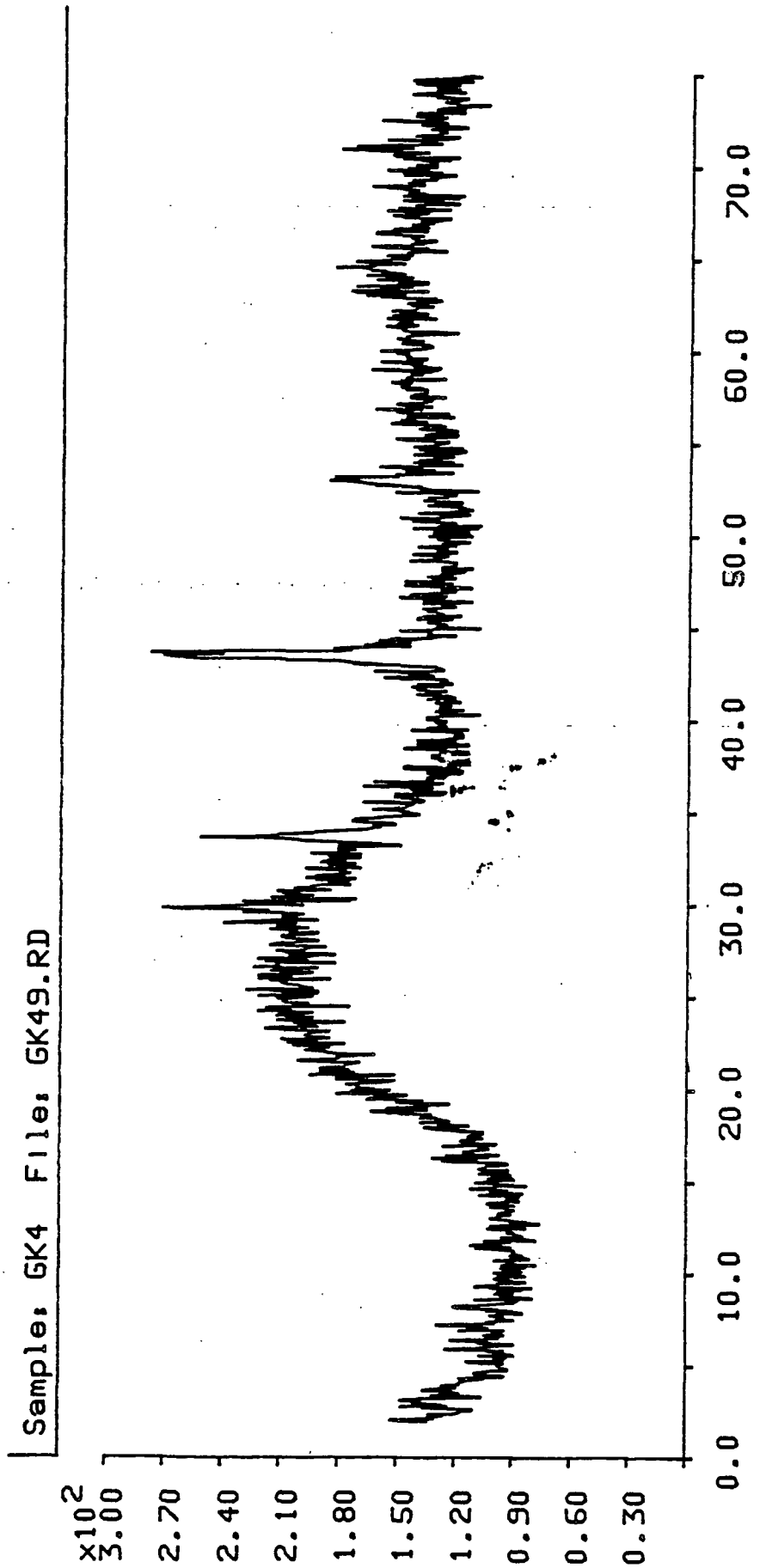

Experiment 50: 12 hour exposure to frozen smelt containing sulfide, sulfate, carbonate, and polysulfide

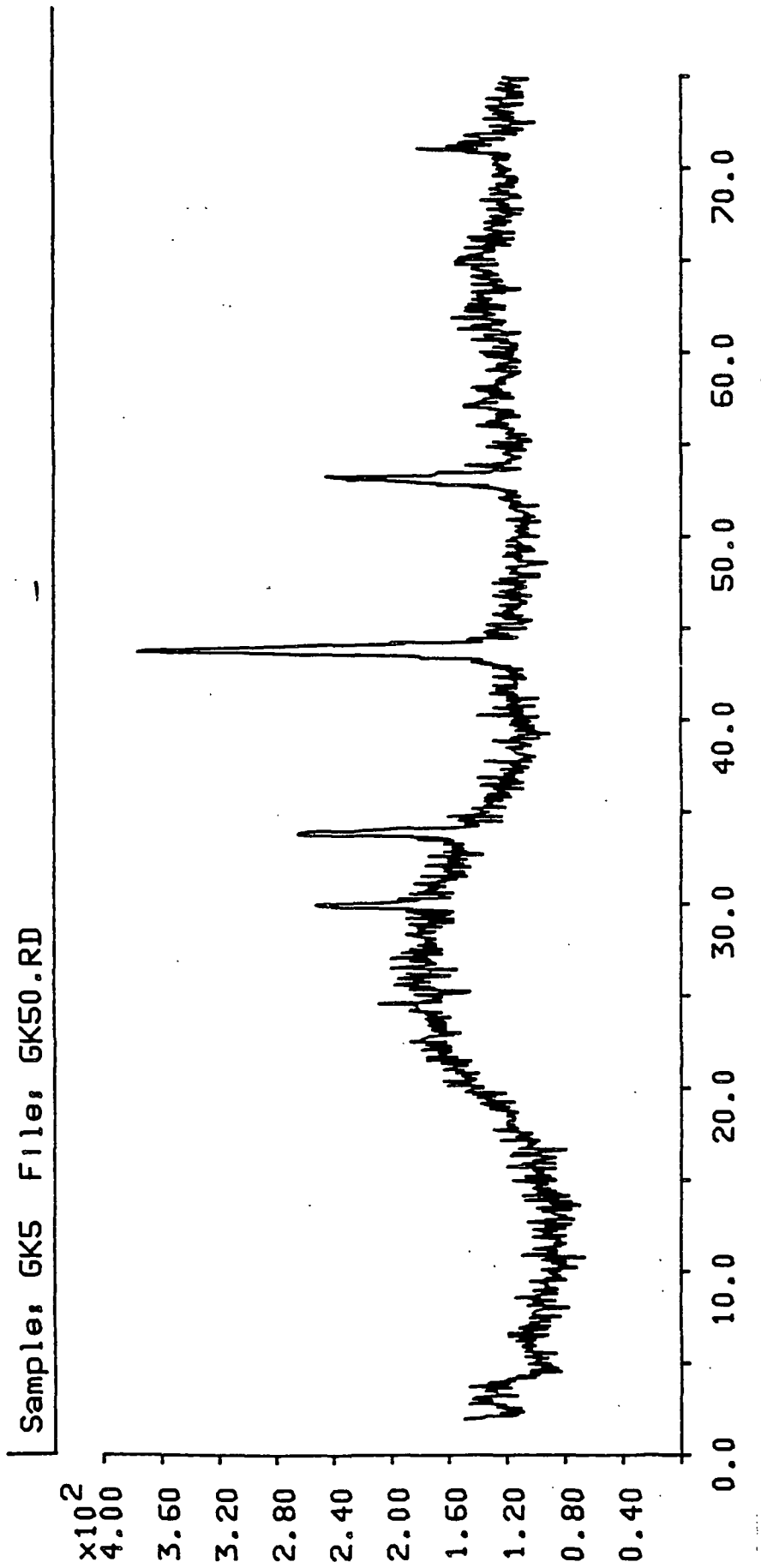

Experiment 60: 48 hour exposure to frozen smelt containing sulfide, sulfate, carbonate, and polysulfide

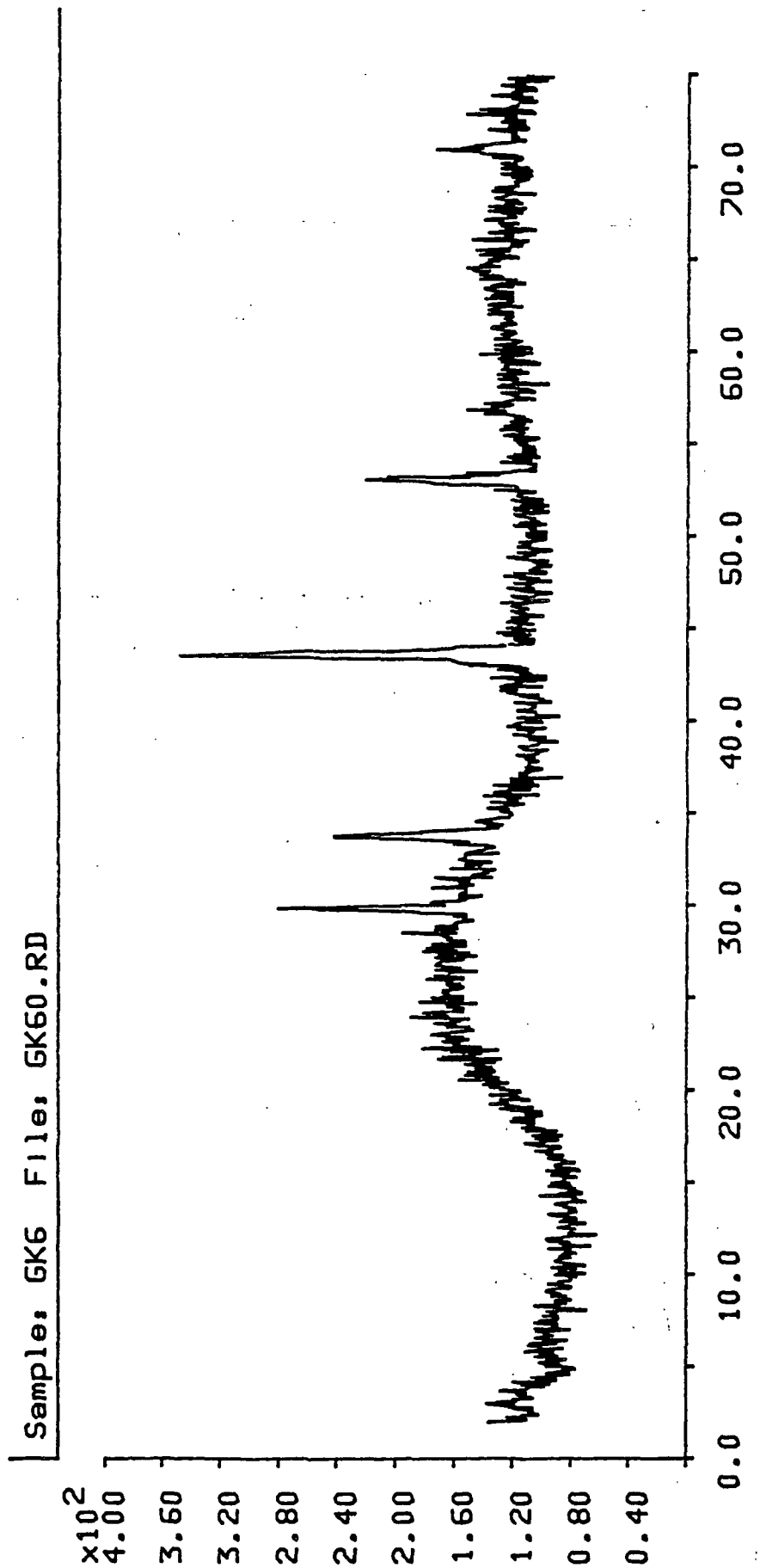

Experiment 62: 49 hour exposure to frozen smelt containing sulfide, sulfate, carbonate, and polysulfide

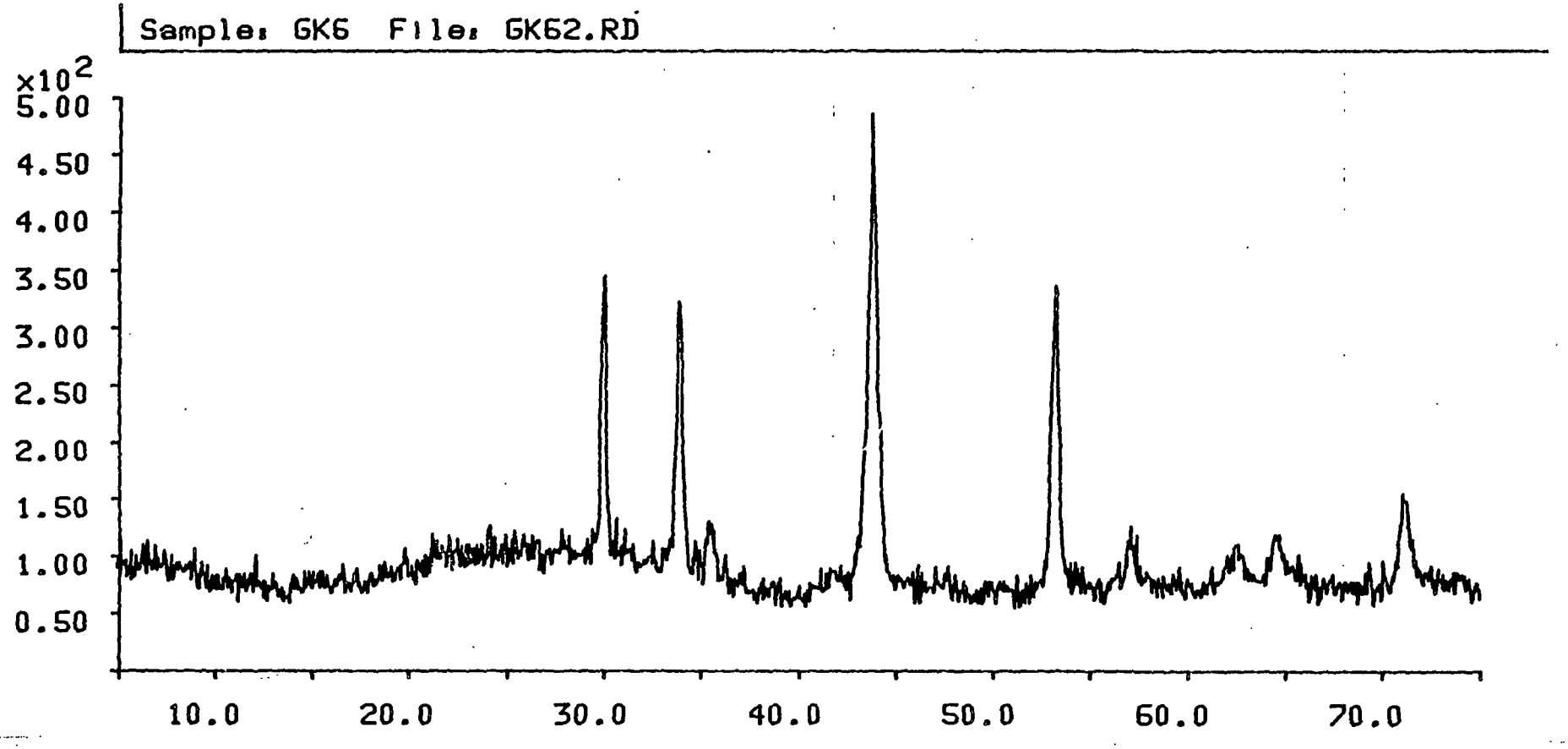

Experiment 63: 100 hour exposure to frozen smelt containing sulfide, sulfate, carbonate, and polysulfide

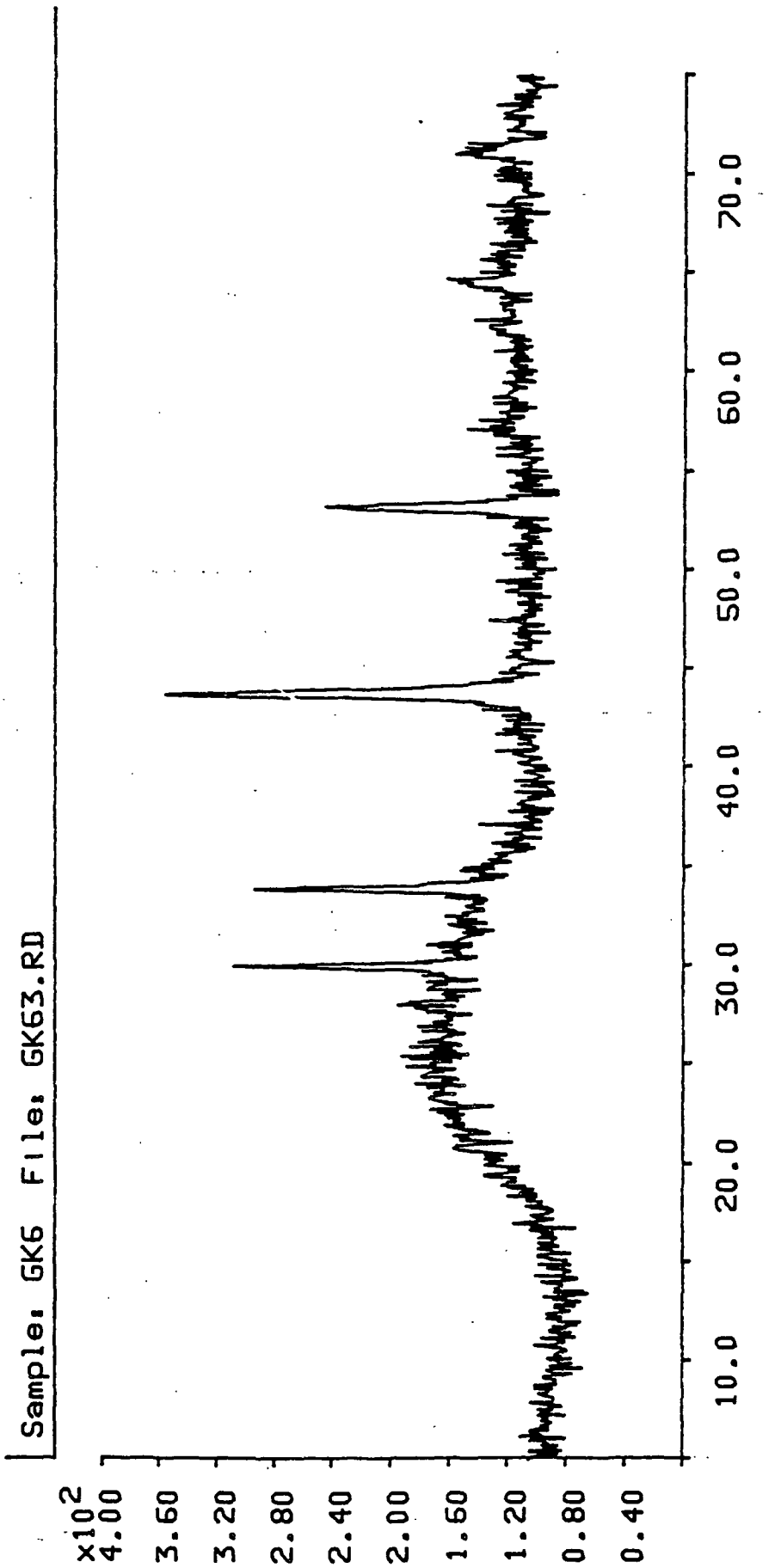

APPENDIX IV

DESCRIPTION OF PROGRAM FOR SOLVING DIFFUSION EQUATION

A program was written to solve the diffusion equation in cylindrical coordinates:

$$\frac{d[C]}{dt} = D \frac{1}{r} \left\{ \frac{d}{dr} \left[r \frac{d[C]}{dr} \right] \right\}$$

This equation was used to model the diffusion of polysulfide to the surface of a cylindrical metal sample through a frozen smelt layer. It was assumed that the corrosion reaction is limited by diffusion of polysulfide to the smelt-metal interface. It also was assumed that the frozen smelt layer initially has a uniform concentration of polysulfide. As polysulfide is consumed in the corrosion reaction at the smelt-metal interface, a concentration gradient is established in the smelt. This gradient drives diffusion of polysulfide from the frozen smelt to the metal surface.

This problem was solved by defining an initial condition and two boundary conditions. The initial condition is that the inner portion of the frozen smelt layer initially has a uniform concentration of polysulfide, called C_0. The boundary condition at the smelt-metal interface is that the polysulfide content at the interface is 0. This assumes that the polysulfide reacts with the metal as fast as it reaches the interface, which is a good assumption if the limiting step in the reaction is diffusion in the frozen smelt layer. The other boundary condition is that the flux of polysulfide across the interface between the inner and the outer portions of the frozen smelt layer is zero. This assumption may not be entirely correct. However, the calculated polysulfide concentration gradient shows that the polysulfide

at the interface between the inner and outer portions of the frozen smelt layer is not depleted. Thus, the outer boundary condition does not have a significant effect on the solution of the problem.

The problem was solved numerically using a finite difference approximation to the partial differential equation. The radius of the frozen smelt layer was broken into a number of increments, and a finite difference approximation to the differential equation was written at each node. This resulted in a series of algebraic equations, which were solved by Gauss elimination. This series of equations was solved for each increment of time. The results of the integration were a concentration profile of polysulfide within the frozen smelt layer for each time step, and the flux out of the frozen smelt to the metal surface at each time step. The total flux to the metal surface was obtained by summing the flux for each increment of time.

The inputs to this program are a value of the diffusion coefficient, in cm^2/hr, and the initial polysulfide content of the smelt, in mg/cm^3. The initial polysulfide content was 10 mg/cm^3, based on a weight % of 0.5%, and a smelt density of 2 g/cm^3. The result of the program is the flux of sulfur to the metal surface as a function of time. This must be converted to a corrosion weight loss to compare it to the experimental data. This is easily done, since the corrosion product is known to be FeS. The total flux of sulfur, in mg/cm^2 is multiplied by 56/32 to obtain the weight of iron consumed by the reaction with sulfur.

The calculated reaction vs. time curve was compared to the experimental data to determine the value of D which resulted in the best fit. The goodness of fit was evaluated by calculating the sum of squares of the difference between the calculated and experimental reaction rates. It was

found that the diffusion curve did not have the same shape as the experimental data, and therefore the diffusion curve only fit portions of the experimental curve. The sum of squares of the residuals was then calculated only for the region of the curve which was being investigated.

A listing of the program follows.

```
10 PRINT "*************************************************************"
20 PRINT "*                                                           *"
30 PRINT "*                    THESIS MODEL                           *"
40 PRINT "*                                                           *"
50 PRINT "*                                                           *"
60 PRINT "*************************************************************"
70 '
80 'input the number of increments in the r-direction, and the time of
    integration and time increment
90 '
100 PRINT : PRINT "INPUT THE NUMBER OF INCREMENTS IN THE DIRECTION OF
    THE RADIUS"; : INPUT M
110 PRINT : PRINT "INPUT THE LENGTH OF TIME TO INTEGRATE FOR"; : INPUT TIME
120 PRINT : PRINT "INPUT THE TIME INCREMENT"; : INPUT DK
130 PRINT : PRINT "INPUT THE DIFFUSION COEFFICIENT"; : INPUT DIFF
150 PRINT : PRINT "INPUT THE INITIAL POLYSULFIDE CONTENT"; : INPUT C0
170 '
180 H = 1.27 / M
190 N = TIME / DK
200 KH = DK / H ^ 2
210 '
220 'dimension the arrays
230 '
240 DIM U(M, M + 1)
250 DIM C(3, M)
260 DIM COL(M), Y(M)
270 DIM RXN(N)
280 RXN(0) = 0
281 NDATA = 10
282 DIM EXDATA(3, NDATA)
283 EXDATA(1, 1) = 2: EXDATA(1, 2) = 6: EXDATA(1, 3) = 12: EXDATA(1, 4) = 12:
284 EXDATA(1, 5) = 24: EXDATA(1, 6) = 24: EXDATA(1, 7) = 48: EXDATA(1, 8) = 49
285 EXDATA(1, 9) = 99: EXDATA(1, 10) = 100
286 EXDATA(2, 1) = 1.08: EXDATA(2, 2) = 1.89: EXDATA(2, 3) = 1.77:
    EXDATA(2, 4) = 1.9
287 EXDATA(2, 5) = 2.04: EXDATA(2, 6) = 2.44: EXDATA(2, 7) = 2.74:
    EXDATA(2, 8) = 3.05
288 EXDATA(2, 9) = 3.32: EXDATA(2, 10) = 3.18
299 '
300 'assign initial values to the array t
310 '
320 FOR I = 1 TO M
330 C(2, I) = C0
```

```
340 NEXT I
350 '
360 'set up array for Gauss elimination
370 '
380 'reset array to 0
390 '
400 FOR DT = 0 TO N - 1
410 FOR I = 1 TO M
420 FOR J = 1 TO M + 1
430 U(I, J) = 0
440 NEXT J
450 NEXT I
460 FOR I = 1 TO M
470 C(1, I) = C(2, I)
480 NEXT I
503 '
510 'set up array of coefficients
520 '
530 FOR I = 1 TO M
540 IF I = 1 THEN GOSUB 1430
550 IF I > 1 AND I < M THEN GOSUB 1580
560 IF I = M THEN GOSUB 1670
570 NEXT I
580 '
590 'perform Gauss elimination - complete pivoting
600 '
610 FOR I = 1 TO M: COL(I) = I: NEXT I
620 '
630 FOR I = 1 TO M - 1
640 PIVOT = U(I, I): NPIVOT = I: PIVROW = I: PIVCOL = I
650 FOR J = I TO M
660 FOR K = I TO M
670 IF ABS(U(J, K)) <= ABS(PIVOT) THEN 690
680 PIVOT = U(J, K): PIVCOL = K: PIVROW = J
690 NEXT K
700 NEXT J
710 '
720 '
730 'swap rows
740 '
750 IF PIVROW = NPIVOT GOTO 800
760 FOR J = 1 TO M + 1
770 SWAP U(PIVROW, J), U(NPIVOT, J)
780 NEXT J
790 '
800 ' swap columns
810 '
820 IF PIVCOL = NPIVOT GOTO 880
830 FOR J = 1 TO M
840 SWAP U(J, PIVCOL), U(J, NPIVOT)
845 NEXT J
850 NCOL = COL(I): COL(I) = COL(PIVCOL): COL(PIVCOL) = NCOL
870 '
880 'normalize the pivot row
890 '
```

```
900 FOR J = 1 TO M + 1
910 U(NPIVOT, J) = U(NPIVOT, J) / PIVOT
920 NEXT J
930 '
940 'perform the elimination
950 '
960 FOR J = NPIVOT + 1 TO M
970 IF U(J, I) = 0 THEN GOTO 1020
980 FACTOR = U(J, I) / U(I, I)
990 FOR K = NPIVOT + 1 TO M + 1
1000 U(J, K) = U(J, K) - FACTOR * U(I, K)
1010 NEXT K
1020 NEXT J
1030 FOR J = I + 1 TO M
1040 U(J, I) = 0
1050 NEXT J: NEXT I
1060 '
1070 'perform the back substitution
1080 '
1090 Y(M) = U(M, M + 1) / U(M, M)
1100 FOR NX = 1 TO M
1110 SUM = 0
1120 I = M - NX + 1
1130 FOR J = I + 1 TO M
1140 SUM = SUM + U(I, J) * Y(J)
1150 NEXT J
1160 Y(I) = (U(I, M + 1) - SUM) / U(I, I)
1170 NEXT NX
1180 '
1190 'sort the t's into the proper order
1200 '
1210 FOR I = 1 TO M
1220 NX = COL(I)
1230 C(2, NX) = Y(I): Y(I) = 0
1235 NEXT I
1236 '
1237 ' calculate amount of sulfur which has diffused out of system
1238 '
1241 REACT = DK * DIFF * C(1, 1) / H
1242 RXN(DT + 1) = RXN(DT) + REACT
1243 '
1244 ' store extent of reaction in array
1245 '
1246 FOR I = 1 TO NDATA
1247 IF (DT + 1) * DK = EXDATA(1, I) THEN EXDATA(3, I) = RXN(DT + 1) * 1.75
1248 NEXT I
1250 NEXT DT
1251 '
1252 ' compute the sum of squares
1253 '
1254 SSQ = 0
1255 FOR I = 1 TO 4
1256 SSQ = SSQ + (EXDATA(2, I) - EXDATA(3, I)) ^ 2
1257 NEXT I
1260 '
```

```
1270 'print the results
1280 '
1310 FOR J = 1 TO M
1320 PRINT USING " ##.###"; C(2, J);
1330 NEXT J
1360 PRINT : PRINT "HIT RETURN TO CONTINUE"; : INPUT JUNK
1370 PRINT
1395 PRINT RXN(N)
1411 FOR J = 0 TO NDATA
1412 PRINT USING " ###.###"; EXDATA(1, J), EXDATA(2, J), EXDATA(3, J)
1413 NEXT J
1415 PRINT KIN, DIFF, SSQ
1416 PRINT "HIT RETURN TO CONTINUE"; : INPUT JUNK
1417 FOR I = 1 TO 20
1418 J = I * 10
1419 PRINT J / 2, RXN(J) * 1.75
1420 NEXT I
1425 END
1430 '
1440 'subroutine to put R = 0 equation in array
1450 '
1460 U(I, I) = 1 + KH * DIFF * (1.27 + H) / (1.27 + H / 2) +
     KH * DIFF * 1.27 / (1.27 + H / 2)
1470 U(I, I + 1) = -KH * DIFF * (1.27 + H) / (1.27 + H / 2)
1480 U(I, M + 1) = C(1, I)
1570 RETURN
1580 '
1590 'subroutine to put R equation in array for  0<R<m
1600 '
1610 U(I, I) = 1 + KH * DIFF * (1.27 + I * H) / (1.27 + (I - .5) * H) +
     KH * DIFF * (1.27 + (I - 1) * H) / (1.27 + (I - .5) * H)
1620 U(I, I + 1) = -KH * DIFF * (1.27 + I * H) / (1.27 + (I - .5) * H)
1630 U(I, I - 1) = -KH * DIFF * (1.27 + (I - 1) * H) / (1.27 + (I - .5) * H)
1640 U(I, M + 1) = C(1, I)
1660 RETURN
1670 '
1680 'subroutine to put R = m equation in array
1690 '
1700 U(I, I) = 1 + KH * DIFF * (1.27 + (I - 1) * H) / (1.27 + (I - .5) * H)
1710 U(I, I - 1) = -KH * DIFF * (1.27 + (I - 1) * H) / (1.27 + (I - .5) * H)
1720 U(I, M + 1) = C(1, I)
1740 RETURN
```

APPENDIX V

EXPERIMENTAL DATA

This appendix presents in tabular form the corrosion rate data shown in the figures in the Results and Discussion section.

Table A1. Corrosion rate data for exposure to smelt composed of 15% Na_2S, 15% Na_2SO_4, and 70% Na_2CO_3 (Sample surface area 22.3 cm^2)

Experiment	Metal Temp. (°C)	Exposure Time (hr)	Weight Loss (mg)	Weight Loss (mg/cm^2)	Corrosion Rate(mm/yr)
64	335	2	4.0	0.18	1.00
41	329	6	5.5	0.25	0.46
42	349	12	12.3	0.55	0.51
43	349	18	10.7	0.48	0.30
27	338	48	34.8	1.56	0.36
39	335	48	27.0	1.21	0.28
40	321	94	35.6	1.60	0.19

Table A2. Corrosion rate data for exposure to smelts prepared with 15% Na_2S, 15% Na_2SO_4, and 70% Na_2CO_3, through which CO_2 was bubbled to generate 0.5% polysulfide (Sample surface area 22.3 cm^2)

Experiment	Metal Temp. (°C)	Exposure Time (hr)	Weight Loss (mg)	Weight Loss (mg/cm^2)	Corrosion Rate(mm/yr)
70	380	0.25	2.6	0.12	5.20
71	340	2	16.0	0.72	4.00
49	371	2	24.0	1.08	6.00
52	341	6	42.1	1.89	3.51
50	343	12	39.4	1.77	1.64
54	349	12	42.4	1.90	1.77
51	341	24	45.6	2.04	0.95
53	341	24	54.4	2.44	1.13
60	332	48	61.2	2.74	0.64
62	335	49	68.0	3.05	0.69
68	343	99	70.9	3.18	0.36
63	343	100	74.0	3.32	0.37

Table A3. Corrosion rate data for exposure to smelt powder containing 0.5% polysulfide. The smelt powder was prepared from 15% Na_2S, 15% Na_2SO_4, 70% Na_2CO_3 molten smelt through which CO_2 had been bubbled to generate polysulfide. (Sample surface area 25 cm^2)

Experiment	Metal Temp. (°C)	Exposure Time (hr)	Weight Loss (mg)	Weight Loss (mg/cm^2)	Corrosion Rate(mm/yr)
66	343	24	4.6	0.18	0.09
70	343	24	7.0	0.28	0.13
67	343	48	3.5	0.14	0.03
69	343	48	20.4	0.82	0.19